Mémoire

Auteur : Araceli, Salvatore
Promoteur(s) : Damanet, François
Faculté : Faculté des Sciences
Diplôme : Master en sciences physiques, à finalité approfondie
Année académique : 2023-2024
URI/URL : http://hdl.handle.net/2268.2/20483

Faculty of Sciences - Department of Physics

Third quantization in open quantum systems

Author: Salvatore ARACELI
Supervisor: Prof. François DAMANET

Master's thesis submitted in the partial fulfillment of the requirements for the Master's degree in Physical Science.

Academic Year 2023-2024

Acknowledgements

I would like to thank all the people that contributed directly or indirectly to this master's thesis. It was a long journey and I could not achieve it without their help. First of all, I would like to express my deepest gratitude to my promoter, Pr. François Damanet for his time, devotion, and support. He brought out the best in me. I would also like to thanks Mr. Baptiste Debecker for the pertinence of his advice and remarks.

I would like to extend my sincere thanks to Pr. Peter Schlagheck, Geoffroy Lumay and Ngoc Duy Nguyen to be part of my reading committee. I hope that they enjoy the reading as much as possible.

Finally, I would like to thank my family and friends for their emotional support, patience, and constant encouragement throughout these five years.

Contents

Introduction

The mathematical description of closed and isolated quantum systems has been established since the middle of the last century. It has a proven track record for multiples field of applications such as in the study of superconductor, with the BCS theory [1] and in atomic Physics [2]. However, closed systems are an idealization of real systems, just as in classical physics. When considering interactions between an open system and its environment, the Schrödinger equation becomes unsolvable on its own due to the large degree of freedom of the environment. Thus, a new formalism has been developed to generalize the Schrödinger equation to open quantum systems. Instead of a *ket vector* from the Hilbert space, the state of the (open) system is described by an operator, namely the *density operator*, acting on the Hilbert space. For open systems, the time evolution of its state is described by a *master equation*. The advantage of the master equation over the Schrödinger equation is that, under certain assumptions, the environment can be eliminated, resulting in a solvable equation of motion for the system only. The most common form of such a master equation is the *Lindblad master equation*. There are two main methods of resolution for the master equation. First, one could integrate the differential equation via numerical methods. However, for large systems, this method becomes impractical. Secondly, it is possible to adapt the formalism of Hilbert space for the linear space of density operators. Thus, solving the master equation is equivalent to diagonalize the generator of the dynamic, which is called the Liouvillian. As the Hamiltonian generates the dynamics of closed systems and is an operator acting on ket vectors, the Liouvillian is a *superoperator* acting as an operator on the level of density operators. In this master's thesis, we will be interested to solve master equations with the second method.

The first objective of this master thesis is to present an elegant and promising exact method of resolution for such master equations. This method is called the third quantization. It extends the idea of second quantization to the space of density operators, transforming the problem into one that can be addressed using techniques from many-body physics. Initially developed by Prosen for fermionic systems [3], the third quantization has since been adapted for bosonic systems [4] and other types of master equations [5, 6], providing a versatile framework for studying a wide range of open quantum systems. The elegance of this method lies in the fact that it can be used for an arbitrary number of bosonic modes and the obtained solution is in an analytical form. The interest of developing such resolution tools for open quantum systems stems from its current prominence as a highly active research area in quantum physics. Indeed, the study of the Lindblad master equation plays an important role in fields as *quantum cryptography* [7], *quantum information* [8], *quantum measurement* [9] and in condensed matter [10]. Among all the usages of the third quantization method, let us cite the study of phase transition for spin models [11, 12], applications in quantum transport [6].

The second objective of this master thesis is to apply this method to a concrete problem, namely quantum thermal transport. We will use the third quantization to study the transport of bosonic particles between two baths of different temperatures, mediated by a junction compounded of several bosonic sites. In the framework of this master thesis, we will limit our study to two sites. This quantum transport setup is the first step towards to the study of quantum thermodynamics problems such as quantum heat engines. Quantum thermodynamics is also an active and promising field of research, see [13, 14] for a complete review of the topic. Devices

such as quantum thermal engines could have a direct application in the industry field via the design of new thermal transistors [15, 16].

The structure of this master's thesis is the following. In the first part, we introduce the mathematical tools allowing to describe open quantum systems. In the first chapter, we describe the second quantization in closed systems. Following this, we present the Bogoliubov transformation and show its application within the BCS theory.
In chapter 2, we study open quantum systems in detail. We give the definition of the density operators and show its properties. Then, we present and derive the Lindblad master equation for a general case. Afterwards, we introduce the Fock-Liouville Hilbert space of density operators and show that a certain isomorphism makes it possible to find a matrix representation of the generator of the dynamics. We end this chapter by studying the properties of this generator.
In chapter 3, we introduce and derive the third quantization method in a general frame for two bosonic modes. We show the robustness of this method and what it allows us to know about the system of study.

The second part of this master thesis is dedicated to the application of the third quantization to quantum transport problems. To the best of our knowledge, this is the first time that the third quantization method is applied to quantum thermodynamics problems, and constitutes thus our original contribution to the field, which opens many perspectives for future research. In chapter 4, we show its usage in detail for a simple but non trivial system, namely the *single-site junction*. We are interested in its steady state, the spectrum of the Liouvillian and the particle current. In addition, we study the symmetries within this system. We also compare our result obtained via third quantization with a numerical method.
In chapter 5, we study the *two-site junction*. We compare two approaches of derivation for the Lindblad master equation throughout the result obtained via third quantization and we show how another more accurate master equation could be used, the Redfield one.

Part I

Theoretical tools

Chapter 1

Second Quantization

In this chapter we briefly present the formalism to describe quantum closed systems with N indistinguishable particles. We first introduce the Fock space and define creation and annihilation operators. The second part of this chapter is dedicated to the Bogoliubov transformation, which is a method used to diagonalize Hamiltonians and thus find their ground state. We focus our presentation around the BCS theory, one of the well-known application of this transformation.

1.1 Fock space

Considering N indistinguishable[1] particles, the Hilbert space associated is the tensor product of N Hilbert spaces $\mathcal{H}_1$

$$\mathcal{H}_N = \mathcal{H}_1 \otimes ... \otimes \mathcal{H}_1, \tag{1.1}$$

where $\mathcal{H}_1$ is the Hilbert space associated with a single particle. Via the symmetry postulate, we define two subspaces of $\mathcal{H}_N$: $\mathcal{H}_N^+$ and $\mathcal{H}_N^-$, depending if the wavefunction ψ of the system is entirely symmetrical or entirely antisymmetrical with respect to the exchange of spatial coordinates and spins within any pairs of two particles [17]. For such spaces, a basis is given by

$$\mathcal{B}^{\pm} = \bigcup_{N=0}^{\infty} \mathcal{B}_N^{\pm} = \mathcal{B}_0 \cup \mathcal{B}_1 \cup \mathcal{B}_2^{\pm} \cup ..., \tag{1.2}$$

where

$$\mathcal{B}_N^{\pm} = \left(|n_0, n_1, n_2, ...\rangle_{\pm} : \sum_{k=0}^{\infty} n_k = N \right). \tag{1.3}$$

Here, $|n_0, n_1, n_2, ...\rangle_{\pm}$ is a Fock state and n_k denotes the occupation number, i.e., the number of particles in each single particle state $|\phi_k\rangle$. The $+$ $(-)$ upper index refers to bosonic (fermionic) particles. For bosons, $n_k \in \mathbb{N}$ for all $k \in \mathbb{N}$ while for fermions, $n_k \in \{0, 1\}$ for all $k \in \mathbb{N}$ due to the Pauli exclusion principle. To be as complete as possible, we also specify the vacuum state, corresponding to an absence of particles in the system

$$|0\rangle \equiv |0, 0, 0, ...\rangle . \tag{1.4}$$

We now introduce the creation and annihilation operators, $a_k^{\dagger}, a_k$.[2] The application of a creation (annihilation) operator on a Fock state adds (removes) a particle on a given state k in

[1] Indistinguishable means here that all the particles have the same properties: same mass, same spin, same electric charge.

[2] The reader should note that the notation of operators here and throughout the master's thesis is without the usual hat.

the system. Considering the bosonic case, the application of these operators to a general Fock state is

$$a_k \left|n_0, n_1, ..., n_k, ..\right\rangle = \sqrt{n_k} \left|n_0, n_1, ..., n_k - 1, ..\right\rangle, \tag{1.5}$$

$$a_k^\dagger \left|n_0, n_1, ..., n_k, ..\right\rangle = \sqrt{n_k + 1} \left|n_0, n_1, ..., n_k + 1, ..\right\rangle. \tag{1.6}$$

If $n_k = 0$, $a_k \left|n_0, n_1, ..., n_k, ..\right\rangle = 0$, the null vector[3]. For fermionic particles, we have

$$a_k \left|n_0, n_1, ..., n_k, ..\right\rangle = (-1)^{n_0 + ... + n_{k-1}} n_k \left|n_0, n_1, ..., n_k - 1, ..\right\rangle, \tag{1.7}$$

$$a_k^\dagger \left|n_0, n_1, ..., n_k, ..\right\rangle = (-1)^{n_0 + ... + n_{k-1}} (1 - n_k) \left|n_0, n_1, ..., n_k + 1, ..\right\rangle. \tag{1.8}$$

The creation and annihilation operators admits the following properties:

- The application of $a_k^\dagger a_k$ to a (bosonic or fermionic) Fock state multiplies this state by the associated occupation number n_k

$$a_k^\dagger a_k \left|n_0, n_1, ..., n_k, ..\right\rangle = n_k \left|n_0, n_1, ..., n_k, ..\right\rangle. \tag{1.9}$$

- For bosonic particles, the *canonical commutation relations* (CCR) are

$$[a_k, a_{k'}^\dagger] = \delta_{kk'}, \quad [a_k, a_{k'}] = [a_k^\dagger, a_{k'}^\dagger] = 0, \tag{1.10}$$

  for $k, k' \in \mathbb{N}$. The notation $[A, B]$ is the commutator of the operators A and B, $[A, B] \equiv AB - BA$.

- For fermionic particles, the CCR are slightly different,

$$\{a_k, a_{k'}^\dagger\} = \delta_{kk'}, \quad \{a_k, a_{k'}\} = 0, \tag{1.11}$$

  where $\{A, B\}$ is the anticommutator of A and B, $\{A, B\} \equiv AB + BA$.

- In both cases, the creation operators can be used to generate any Fock state. We have

$$\left|n_0, n_1, n_2, ...\right\rangle = \frac{1}{\sqrt{n_0!}} \left(a_0^\dagger\right)^{n_0} \frac{1}{\sqrt{n_1!}} \left(a_1^\dagger\right)^{n_1} \frac{1}{\sqrt{n_2!}} \left(a_2^\dagger\right)^{n_2} ... \left|0\right\rangle. \tag{1.12}$$

An example of simple Hamiltonian with creation and annihilation operator is the quantum harmonic oscillator. Considering only one mode, we have

$$H = \hbar \omega a^\dagger a,$$

where ω is the frequency of the mode. Generalizing for multiples modes, this becomes

$$H = \sum_k \hbar \omega_k a_k^\dagger a_k.$$

1.2 Bogoliubov transformation

The aim of a Bogoliubov transformation is to find a new set of creation and annihilation operators such that any complicated Hamiltonian can be written in a diagonal form, like a harmonic oscillator so that to obtain directly the eigenstates and corresponding energies of the system of interest. To illustrate how this transformation works, we show its usage in the well-known BCS theory. Developed by Bardeen, Cooper and Schrieffer in 1957 [1], this theory describes the origin of superconductivity through the creation of bound pairs of electrons, known as Cooper pairs,

[3] Not to be confused with the vacuum state $\left|0\right\rangle$.

due to an attractive interaction between them. Bogoliubov himself applied this transformation for the BCS theory [18]. We briefly review the transformation, following the main steps of [19].

The Hamiltonian for BCS is

$$H_{\text{BCS}} = \sum_{k,\sigma} \xi_{k\sigma} c^\dagger_{k\sigma} c_{k\sigma} + \frac{1}{N} \sum_{k,k'} V_{kk'} c^\dagger_{k\uparrow} c^\dagger_{-k\downarrow} c_{-k'\downarrow} c_{k'\uparrow}, \tag{1.13}$$

where $c_{k\sigma}, c^\dagger_{k\sigma}$ are the annihilation and creation operators for electrons of mode k and spin σ, $\xi_{k\sigma}$ is the frequency of the corresponding mode in units where $\hbar = 1$. The first term of this Hamiltonian describes the single-particle energy of the electronic system while the second term corresponds to the interactions between the electrons. The latter is non-quadratic in $c_{k\sigma}$ or $, c^\dagger_{k\sigma}$ which makes impossible the BCS transformation. To bypass this issue, we use a *mean field approximation*: any product of operator A, B will be replaced by

$$AB \simeq \langle A \rangle B + A \langle B \rangle - \langle A \rangle \langle B \rangle,$$

where $\langle O \rangle$ is the mean value of the operator O. Applying this approximation to the interaction term, we obtain

$$H_{\text{BCS}} = \sum_{k,\sigma} \xi_{k\sigma} c^\dagger_{k\sigma} c_{k\sigma} - \sum_k \Delta^*_k c_{-k\downarrow} c_{k\uparrow} - \sum_k \Delta_k c^\dagger_{k\uparrow} c^\dagger_{-k\downarrow}, \tag{1.14}$$

with

$$\Delta_k = -\frac{1}{N} \sum_{k'} V_{kk'} \langle c_{-k'\downarrow} c_{k'\uparrow} \rangle,$$
$$\Delta^*_k = -\frac{1}{N} \sum_{k'} V_{kk'} \langle c^\dagger_{k'\uparrow} c^\dagger_{-k'\downarrow} \rangle.$$

The Hamiltonian is now quadratic in $c_{k\sigma}, c^\dagger_{k\sigma}$ but as it contains terms in $c_{k\sigma} c_{k\sigma}$ and $c^\dagger_{k\sigma} c^\dagger_{k\sigma}$, it is not yet diagonal. It is then difficult to identify to eigenstates and energies of the system. Thus, we introduce a new mapping for the fermionic creation and annihilation operators,

$$\begin{pmatrix} \gamma_{k\uparrow} \\ \gamma^\dagger_{k\downarrow} \end{pmatrix} = \begin{pmatrix} u^*_k & -v_k \\ v^*_k & u_k \end{pmatrix} \begin{pmatrix} c_{k\uparrow} \\ c^\dagger_{k\downarrow} \end{pmatrix}. \tag{1.15}$$

This mapping corresponds to the Bogoliubov transformation. The new set of operators have to satisfy the fermionic CCR, which requires the following conditions on the coefficient u_k, v_k

$$\{\gamma_{k\uparrow}, \gamma^\dagger_{k\downarrow}\} = 1$$
$$\Leftrightarrow |u_k|^2 + |v_k|^2 = 1.$$

Inverting the mapping, we find

$$c_{k\uparrow} = u_k \gamma_{k\uparrow} + v_k \gamma^\dagger_{k\downarrow}, \tag{1.16}$$
$$c^\dagger_{k\downarrow} = -v^*_k \gamma_{k\uparrow} + u^*_k \gamma^\dagger_{k\downarrow}. \tag{1.17}$$

Now, we inject the previous equation in (1.14) and we choose u_k, v_k such that the terms in $\gamma_{k\sigma} \gamma_{k\sigma}$, $\gamma^\dagger_{k\sigma} \gamma^\dagger_{k\sigma}$ vanish. We finally find

$$\boxed{H_{\text{BCS}} = \sum_{k,\sigma} E_k \gamma^\dagger_{k\sigma} \gamma_{k\sigma},} \tag{1.18}$$

with the dispersion $E_k = \sqrt{\xi_k^2 + |\Delta_k|^2}$. Here we effectively see that the Hamiltonian is diagonal and looks like a harmonic oscillator with multiples modes. We call these modes *normal modes* because they do not interact with each other. The coefficients E_k are the eigenvalues of the Hamiltonian. Hence, the diagonal form of the Hamiltonian shows that the electrons are no more the relevant particles in the presence of interactions. The stable particles of the system are the Bogoliubov particles created by $\gamma_{k\sigma}$ of energy $E_{k\sigma}$. With this diagonalization, we can write the state of the system at any time as

$$|\psi(t)\rangle = \sum_{k,\sigma,i} e^{iE_k t} b_{k,\sigma,i} \, |\phi_{k,\sigma,i}\rangle \,, \tag{1.19}$$

where the set $\{\phi_{k,\sigma,i}\}$ are the eigenvectors of H_{BCS} given by

$$\phi_{k,\sigma,i} = \frac{1}{\sqrt{i!}} \left(\gamma_{k\sigma}^\dagger\right)^i |0\rangle \tag{1.20}$$

and $b_{k,\sigma,i} = \langle \phi_{k,\sigma,i} | \psi(0) \rangle$.

To summarize the ideas of this section, we started with the BCS Hamiltonian (1.13) and defined a new set of fermionic creation and annihilation operators such that the Hamiltonian becomes diagonal, similar to the Hamiltonian of a harmonic oscillator. Applying the new creation operator $\gamma_{k\sigma}^\dagger$ does not directly add an electron of mode $k\sigma$. Instead, it corresponds to quasi-particle modes that do not interact with each other. Additionally, we obtain the spectrum of the Hamiltonian, which is necessary to study the energy dispersion of the system.

It is possible to define a Bogoliubov transformation for more general cases, such as in open quantum systems. Indeed, we will apply the same logic: finding new modes such that the generator of the dynamics, the Liouvillian (kind of equivalent of the Hamiltonian for open systems), has a diagonal representation. Thus, we will also obtain the associated spectrum, which is a central subject of study for open quantum systems, as it will give access to the steady states of the systems.

Chapter 2

Open quantum systems

The aim of this chapter is to present and develop mathematical tools that are necessary to study the dynamics of open quantum systems. We first give a definition for an open system and exhibit the differences with closed ones. We also introduce the density operator. Then, we develop the standard form of the time evolution equation for open systems, namely the Lindblad master equation. We continue by constructing a Hilbert space where the vectors are now the density operators. With this space and a specific isomorphism, we are able to give a matrix representation for the generator of the dynamics of the system. We end this section by studying the spectrum of this generator.

2.1 Introduction

An open quantum system is a system included in a larger system that interacts with his environment. As in thermodynamics, an open system can exchange particles and energy with its environment. A representation of the situation is sketched in Figure 2.1. The system, described by the Hilbert space $\mathcal{H}_S$, Hamiltonian H_S and density operator ρ_S is coupled with its environment, itself described by the Hilbert space $\mathcal{H}_E$, Hamiltonian H_E and density operator ρ_E. The total system (system of study + environment) has the same structure, with Hilbert space $\mathcal{H}_T = \mathcal{H}_S \otimes \mathcal{H}_E$, Hamiltonian $H_T = H_E + H_S + H_{\text{int}}$, where H_{int} contains the interactions between the system and the environment, and density operator ρ_T. Typically, we study systems where the dimension of $\mathcal{H}_E$ is much larger than of $\mathcal{H}_S$. In such cases, solving the Schrödinger equation for the entire system is infeasible. Throughout this chapter, we will demonstrate that, under certain assumptions and approximations, it is possible to derive an equation that describes the dynamics of the system alone. To achieve this, we first need to define the density operator and outline its properties.

2.2 Density operator

We shall define the density operator and study its properties. This operator is mainly used to describes open systems although it is defined for a general framework.

Consider a system whose state is unknown but we know that it has a probability p_1 to be in the state $|\psi_1\rangle$, p_2 to be in a state $|\psi_2\rangle$,... . If $\sum_k p_k = 1$, the set $\{p_k, |\psi_k\rangle\}$ defines a mixed state which contains all the physical information of the system. For a set $\{p_k, |\psi_k\rangle\}$, we can define the density operator ρ as

$$\rho = \sum_k p_k \left|\psi_k\right\rangle \left\langle\psi_k\right| . \tag{2.1}$$

A *density operator* ρ fulfills two mathematical conditions:

1. ρ has unit trace, $\text{Tr}[\rho] = 1$,

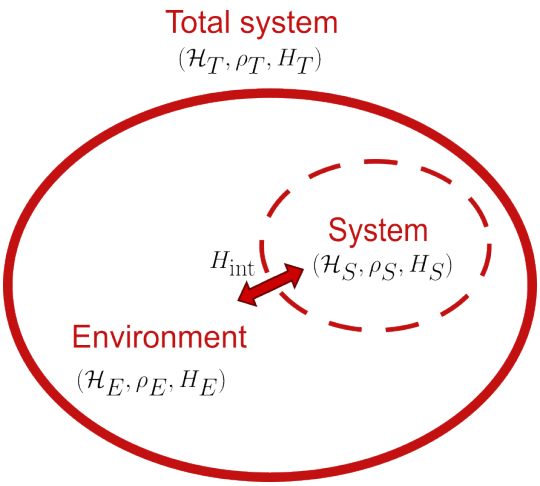

Figure 2.1: An open quantum system is a part of a larger system that includes the environment, which interacts with the open subsystem.

2. ρ is a positive operator.

Furthermore, any operator fulfilling these conditions is considered a density operator. One can show that for an arbitrary density operator ρ, there exists a set $\{p_k, |\psi_k\rangle\}$ of positive numbers p_k and $|\psi_k\rangle \in \mathcal{H}$ such that

$$\rho = \sum_k p_k |\psi_k\rangle \langle\psi_k| . \tag{2.2}$$

The density operator ρ admits the following properties

- ρ is an Hermitian operator.
- If the states $|\psi_k\rangle$ follow the Schrödinger equation, we have

$$\frac{d}{dt}\rho = -i[H, \rho], \tag{2.3}$$

  in units where the reduced Planck constant $\hbar = 1$. This equation is the Liouville-Von Neumann equation and it has a classical equivalent in mechanics.
- The expectation value of any observable A[1] is given by

$$\boxed{\langle A\rangle = \text{Tr}[A\rho].} \tag{2.4}$$

- $\frac{1}{N} \geq \text{Tr}[\rho^2] \geq 1$,$N$ being the dimension of $\mathcal{H}$ [20]. The equality is achieved when every p_k is equal to 0 except one. In this case, the system is said to be in a pure state.

If we fix an arbitrary basis $\{|k\rangle\}$ for $k \in \{1, .., N\}$ of $\mathcal{H}$, the density operator has a matrix representation given by

$$\boxed{\rho = \sum_{k,l=1}^{N} \rho_{kl} |k\rangle \langle l| ,} \tag{2.5}$$

where $\rho_{kl} = \langle k| \rho |l\rangle$. Equivalently, we can write

$$\boxed{\rho = \begin{pmatrix} \rho_{11} & \rho_{12} & \cdots & \rho_{1N} \\ \rho_{21} & \rho_{22} & \cdots & \rho_{2N} \\ \vdots & \vdots & \ddots & \vdots \\ \rho_{N1} & \rho_{N2} & \cdots & \rho_{NN} \end{pmatrix}.} \tag{2.6}$$

[1] An observable is hermitian operator. Unless otherwise specified, all operators will be assumed to be Hermitian throughout this thesis.

The diagonal elements of this matrix are called *populations*. Due to the properties of ρ, the populations are real number and $\sum_k \rho_{kk} = 1$. The off-diagonals elements are called *coherences* and $\rho_{ij} \in \mathbb{C}$, $\rho_{ij} = \rho_{ji}^*$. The notation $(\cdot)^*$ refer to the complex conjugate.

We shall recall that as ρ is an operator, $\rho \in \mathcal{B}(\mathcal{H})$ where $\mathcal{B}(\mathcal{H})$ denote the space of the operators acting on $\mathcal{H}$.

2.2.1 Reduced density matrix

In the case where the Hilbert space is composed of two subspaces, $\mathcal{H} = \mathcal{H} = \mathcal{H}_A \otimes \mathcal{H}_\mathcal{B}$ (for example a system and its environment), one could be interested in studying the physical properties of only one on the two subsystems corresponding to one of the subspaces. To do so, we define the *reduced density matrix*. If the state of the whole system is described by the density operator ρ, the definition of the reduced density matrix of the subsystem A is the operator

$$\rho_A = \mathrm{Tr}_B[\rho], \tag{2.7}$$

where $\mathrm{Tr}_B[\cdot] = \sum_k \langle k| \cdot |k\rangle$ and $\{|k\rangle\}, k \in \{1, ..., N\}$ an arbitrary basis of $\mathcal{H}_B$. Taking the partial trace over a subspace allows us to study the subsystem A without considering the degrees of freedom of the subsystem B. Indeed, if O_A is an operator acting on the subspace A, i.e., $O_A \in \mathcal{B}(\mathcal{H})$, we have

$$\langle O_A \rangle = \mathrm{Tr}_A[O_A \rho_A]. \tag{2.8}$$

Furthermore, tracing over the subspace B equation (2.3), we obtain the exact time evolution of the density operator associated with the subsystem A

$$\boxed{\frac{d}{dt}\rho_A = -i\,\mathrm{Tr}_B\left([H, \rho]\right).} \tag{2.9}$$

Therefore, if we consider subsystem A as our open system of interest and B as its environment, solving this equation will provide us with the time evolution of subsystem A. The next section is dedicated to presenting the approximations that enable us to solve this equation.

2.3 Lindblad master equation

In the second part of this master thesis, we will be interested in deriving an explicit master equation for several particular systems. It is thus insightful to discuss how master equations are derived in general.

In this section, we describe and derive the *Markovian master equation of Lindblad form* developed by Gorini, Kossakowski, Sudarshan and Lindblad in [21, 22, 23]. We shall recall that ρ_S indicate the density operator of the system, ρ_E the one of the environment and ρ_T the total density operator, corresponding to the state of the total system (system of study + environment). The standard form of the Lindblad master equation is

$$\boxed{\dot{\rho}_S(t) = -i\left[H_S + H_{\mathrm{Ls}}, \rho_S(t)\right] + \sum_\mu \left(L_\mu \rho_S(t) L_\mu^\dagger - \frac{1}{2}\left\{L_\mu^\dagger L_\mu, \rho_S(t)\right\}\right),} \tag{2.10}$$

where we can see that the only density operator that appears is the one of the open system. The first term of this equation is related to the unitary evolution of the system. The operator H_S is the Hamiltonian of the system and H_{Ls} is the Lamb shift Hamiltonian, its role is to renormalize the system energy levels due to interaction with the environment [20]. We cite it here to be as complete as possible but for the systems that we will study, we will neglect it. The second term contains the effects of the interaction with the environment, i.e., the dissipative evolution. The operators L_μ are usually refereed to as *jump operators*, where $\mu \in \{1, ..., d_S^2 - 1\}$ with d_S

the dimension of $\mathcal{H}_S$. Each term $L_\mu \rho_S L\mu^\dagger$ corresponds to one of the possible quantum jumps, while the anti-commutator term is needed to normalize properly the system if no jumps occur [24]. An recurrent example of jump for the systems that we will study is the creation operator $a^\dagger$. If the physical system contains a source that adds particles in the system, the corresponding master equation will contain a term that contains a creation operator. Similarly, an excited atom returning to its ground state will emit a photon, represented in the master equation by a term in a.

Any Markovian master equation can be expressed in this form, but not every equation in this form is a valid master equation. Specifically, it must preserve the properties of the density operator: the positivity and the unit trace for every time t.

2.3.1 Derivation of the Lindblad master equation

We show here how to derive the standard form of the Lindblad master equation in a general case, starting from equation (2.3), following the derivation presented in [20].

We first recall the Liouville-Von Neumann equation for the total system, which gives its time evolution

$$\dot{\rho}_T(t) = -i[H_T, \rho_T(t)]. \tag{2.11}$$

The total Hamiltonian H_T can be separated into the effect on the system H_S, the environment H_E and the interaction between them H_{int} such that $H_T = H_S \otimes \mathbb{1}_E + \mathbb{1}_S \otimes H_E + H_{\text{int}}$. Here, the operators $\mathbb{1}_S$ and $\mathbb{1}_E$ are the unitary operators on the Hilbert spaces $\mathcal{H}_S$ and $\mathcal{H}_E$. We now move from Schrödinger picture, where the operators are constant in time and the states dependent on the time[2], to interaction picture where both depend on the time.

The interaction picture

In this picture, the density matrix evolves with time due to the interaction Hamiltonian while the operators evolve due to the free Hamiltonian $H_0 = H_S + H_E$. Thus, we have the time evolution of any operator $O(t)$ defined in $\mathcal{B}(\mathcal{H}_T)$ given by

$$O_I(t) = e^{i(H_S+H_E)t} O e^{-i(H_S+H_E)t}, \tag{2.12}$$

where the subscript I indicate that we are in the interaction picture. For an operator defined in $\mathcal{B}(\mathcal{H}_X)$ where $X = S$ or E, we have

$$O_{X,I}(t) = e^{iH_X t} O_X e^{-iH_X t}. \tag{2.13}$$

To give a bit of context, changing from Schrödinger picture to interaction picture is the same transformation as entering a rotating frame of reference to solve a problem of rotating motion in classical mechanics.

This change of picture allows us to remove the effect of the Hamiltonians of the system and environment in the evolution of ρ_T and only keep the interaction term, which simplifies the problem. The equation (2.11) now reads

$$\dot{\rho}_T(t) = -i[H_{\text{int}}(t), \rho_T(t)]. \tag{2.14}$$

Integrating on both sides, equation (2.14) reads

$$\rho_{T,I}(t) = \rho_{T,I}(0) - i \int_0^t ds[H_{\text{int,I}}(s), \rho_{T,I}(s)]. \tag{2.15}$$

[2]Even though ρ is an operator, it depends on the state of the system and therefore evolves over time.

Injecting (2.15) into (2.14) and taking the trace over the environment, we have successively

$$\dot{\rho}_{T,I}(t) = -i\left[H_{\text{int},I}, \rho_{T,I}(0)\right] - \int_0^t ds\left[H_{\text{int},I}(t), \left[H_{\text{int}}(s), \rho_{T,I}(s)\right]\right], \tag{2.16}$$

$$\text{Tr}_E\left[\dot{\rho}_{T,I}(t)\right] = \dot{\rho}_{S,I}(t) = -i\text{Tr}_E\left[H_{\text{int},I}, \rho_{T,I}(0)\right] - \int_0^t ds\text{Tr}_E\left[H_{\text{int},I}(t), \left[H_{\text{int},I}(s), \rho_{T,I}(s)\right]\right]. \tag{2.17}$$

Note that for the following, we drop the I subscript to lighten the notations. In addition, we admit that the first term of the r.h.s of the last equation can be omitted without loss of generality. We will not show it here but this development is done in [20]. It relies on the following assumptions:

- Initially, the system and the environment are not correlated, $\rho_T(0) = \rho_S(0) \otimes \rho_E(0)$,
- the initial state of the environment is thermal, which means its density matrix is of the form

$$\rho_E = \frac{e^{-H_E/T}}{\text{Tr}_E[e^{-H_E/T}]}, \tag{2.18}$$

  where T is the temperature of the bath and we take the Boltzmann constant $k_B = 1$.

Equation (2.17) reads now

$$\dot{\rho}_S(t) = -\int_0^t ds\text{Tr}_E\left[H_{\text{int}}(t), \left[H_{\text{int}}(s), \rho_T(s)\right]\right]. \tag{2.19}$$

This equation is not yet usable for two reasons. First, the state of the system still depends on the state of the environment trough ρ_T. Furthermore, it is not local in time, as we have to integrate over the time to solve the equation. Bypass these issues requires two strong assumptions. The first one is the *Born approximation*. It states that the influence of the system over the environment is weak enough to consider that the environment is in a stationary state, i.e., we have $[H_E, \rho_E] = 0$. This means that the total state can be rewritten for all the time evolution as $\rho_T(t) = \rho_S(t) \otimes \rho_E$. Even under this assumption, the equation is still non local in time. To do so, we first do a changing on the integration variable $s \to t - s$. Equation (2.19) reads now

$$\dot{\rho}_S(t) = -\int_0^t ds\text{Tr}_E\left[H_{\text{int}}(t), \left[H_{\text{int}}(t-s), \rho_S(t-s) \otimes \rho_E\right]\right]. \tag{2.20}$$

Until now, we have not said anything about the coupling term. From now on, we consider that the coupling is weak, i.e., the system and the environment are non-correlated during all the time evolution. This will allow us to make the *Markov approximation*: $\rho_S(t-s) \simeq \rho_S(t)$. One way of explaining this approximation is that the state of the system at the current time does not depend on the state at previous times. We also have to extend the upper limit of the integral to ∞. This strong assumption is justified because we consider a weak interaction between the system and the environment.

Hierarchy of the typical timescale and validity of the Markov approximation

There is three typical timescales for master equations:

1. τ_{rel}, the relaxation time of the system. This timescale corresponds to the duration required for the system to reach its steady state due to interactions with the environment.
2. τ_{cor}, the correlation time of the bath. This timescale is the time it takes for the bath to lose information about the system.
3. τ_{s} is the typical time evolution of the system.

The Born-Markov approximation is valid for

$$\tau_{\text{cor}} \ll \tau_{\text{rel}}.$$

The Secular approximation for

$$\tau_{\text{cor}} \ll \tau_{\text{s}}.$$

We have the following hierarchy for our timescales,

$$\boxed{\tau_{\text{cor}} \ll \tau_{\text{s}} \ll \tau_{\text{rel}}.} \tag{2.21}$$

The proof of the validity of the Markovian approximation will not be discussed here, see for example [9] for more details.

After the Born-Markov approximations, the time evolution of ρ_S is

$$\dot{\rho}_S(t) = -\int_0^\infty ds \text{Tr}_E \left[H_{\text{int}}(t), [H_{\text{int}}(s), \rho_S(s) \otimes \rho_E]\right]. \tag{2.22}$$

This equation is called the *Redfield equation* [25]. It will be used at some point in the chapter 5. Still, for the Lindblad form of the master equation, we have to expand the double commutator and simplify some terms to finally get rid of the time integration. Regarding the remark at the beginning of this section, we also have to assure that our final equation preserve the positivity and the trace of the density matrix[3]. The interaction Hamiltonian H_{int} in the Schrödinger picture can always be written as

$$H_{\text{int}} = \sum_i S_i \otimes E_i, \tag{2.23}$$

with S_i and E_i acting on $\mathcal{H}_S$ and $\mathcal{H}_E$ respectively. Each S_i can be decomposed into a sum of eigenoperators of the superoperator[4] $[H_S, \cdot]$,

$$S_i = \sum_\omega S_i(\omega), \tag{2.24}$$

where

$$[H_S, S_i(\omega)] = -\omega S_i(\omega). \tag{2.25}$$

As an Hamiltonian is always hermitian, we also have

$$[H_S, S_i^\dagger(\omega)] = \omega S_i(\omega). \tag{2.26}$$

It is proven that this decomposition can always be made [26]. Applying this decomposition for the interaction Hamiltonian in the interaction picture, one finds

$$\begin{aligned} H_{\text{int}}(t) &= \sum_{j,\omega} e^{-i\omega t} S_j(\omega) \otimes E_j(t), \\ &= \sum_{j,\omega} e^{i\omega t} S_j^\dagger(\omega) \otimes E_j^\dagger(t). \end{aligned} \tag{2.27}$$

The reader must keep in mind that the operators $E_j(t)$ are taken here in the interaction picture. To combine this decomposition with the Redfield equation, we have to expand the double commutator:

$$\begin{aligned} \dot{\rho}_S(t) = -\text{Tr}_E \Bigg[&\int_0^\infty ds H_{\text{int}}(t) H_{\text{int}}(t-s) \rho_S(t) \otimes \rho_E(0) - \int_0^\infty ds H_{\text{int}}(t) \rho_S(t) \otimes \rho_E(0) H_{\text{int}}(t-s) \\ &- \int_0^\infty ds H_{\text{int}}(t-s) \rho(t) \otimes \rho_E(0) H_{\text{int}}(t) + \int_0^\infty ds \rho(t) \otimes \rho_E(0) H_{\text{int}}(t-s) H_{\text{int}}(t) \Bigg]. \end{aligned} \tag{2.28}$$

[3] It is not always the case under certain conditions for the Redfield equation [26].

[4] In the next section, we will provide the precise definition of a superoperator. For now, we can describe it as an operation that takes operators as inputs and returns operators as outputs.

Applying the decomposition in terms of $S_i(\omega)$ for $H_{\text{int}}(t)$ and $S_i^\dagger(\omega)$ for $H_{\text{int}}(t-s)$, we find for the first term

$$\text{Tr}_E[H_{\text{int}}(t)H_{\text{int}}(t-s)\rho(t)\otimes\rho_E(0)] = \sum_{\substack{k,l\\ \omega,\omega'}} e^{-i\omega t}S_k(\omega)e^{-i\omega'(t-s)}S_l^\dagger(\omega')\rho(t)\text{Tr}_E[E_k(t)E_l^\dagger(t-s)\rho_E]. \tag{2.29}$$

We now define the spectral correlation function Γ_{kl} that contains the information about the effect of the environment.

$$\Gamma_{kl}(\omega) \equiv \int_0^\infty ds e^{i\omega s}\text{Tr}_E[E_k^\dagger(t)E_l(t-s)\rho_E]. \tag{2.30}$$

Doing the same expansion for each terms of 2.28, we find

$$\dot{\rho}_S(t) = \sum_{\substack{k,l\\ \omega,\omega'}} \left(e^{i(\omega-\omega')t}\Gamma_{kl}(\omega)\left[S_l(\omega)\rho(t), S_k^\dagger(\omega')\right] + e^{i(\omega-\omega')t}\Gamma_{lk}^*(\omega')\left[S_l(\omega)\rho(t), S_k^\dagger(\omega')\right]\right). \tag{2.31}$$

In equation (2.31), we can do a *Rotating wave approximation* (RWA). The terms with $|\omega-\omega'| \gg 1$ oscillate much faster around 0 than the typical timescale of the system evolution. Thus, they do not contribute to the time evolution of the system. Considering the weak coupling, we must only consider the terms where $\omega = \omega'$ as the other terms vanish.[5] Our equation now reads

$$\dot{\rho}_S(t) = \sum_{\substack{k,l\\ \omega}} \left(\Gamma_{kl}(\omega)\left[S_l(\omega)\rho(t), S_k^\dagger(\omega)\right] + \Gamma_{lk}^*(\omega)\left[S_l(\omega)\rho(t), S_k^\dagger(\omega)\right]\right). \tag{2.32}$$

To end this section, we still have to put our equation in the standard form by showing explicitly the jump operators. To do so, we decompose our Γ_{kl} coefficients as a sum their Hermitian and anti-Hermitian part, $\Gamma_{kl}(\omega) = \frac{1}{2}\gamma_{kl}(\omega) + i\pi_{kl}$, with

$$\begin{aligned}\pi_{kl} &\equiv \frac{-i}{2}(\Gamma_{kl}(\omega) - \Gamma_{kl}^*(\omega)),\\ \gamma_{kl} &\equiv \Gamma_{kl}(\omega) + \Gamma_{kl}^*(\omega) = \int_{-\infty}^\infty ds e^{i\omega s}\text{Tr}_E\left[E_k^\dagger(s)E_l\rho_E\right].\end{aligned} \tag{2.33}$$

Here we can write $\text{Tr}_E\left[E_k^\dagger(s)E(t-s)_l\rho_E\right] = \text{Tr}_E\left[E_k^\dagger(s)E_l\rho_E\right]$ because ρ_E commute with $exp(iH_Et)$[6]. At this point, it is relevant to note that γ_{kl} is the Fourier Transform of $\text{Tr}_E\left[E_k^\dagger(s)E_l\rho_E\right]$. As explained in [20], it can be shown that the last function is positive, which implies that its Fourier Transform is positive too. Using the decomposition and turning back to Schrödinger picture, we have

$$\dot{\rho}(t) = -i[H_S + H_{LS}, \rho(t)] + \sum_{\substack{k,l\\ \omega}} \gamma_{kl}(\omega)\left(S_l(\omega)\rho(t)S_k^\dagger(\omega) - \frac{1}{2}\left\{S_k^\dagger(\omega)S_l(\omega), \rho(t)\right\}\right), \tag{2.34}$$

with $H_{LS} = \sum_{k,l\omega}\pi_{kl}(\omega)S_k^\dagger(\omega)S_l(\omega)$. We recall that this term will always be neglected in the following. As γ_{kl} is positive $\forall k,l$ the matrix composed of these coefficients is positive and can be diagonalized. Thus, the master equation can be written in a diagonal form, i.e., it exists $L_i(\omega)$ such that

$$\boxed{\dot{\rho}(t) = -i[H_S + H_{LS}, \rho(t)] + \sum_{i,\omega}\left(L_i(\omega)\rho(t)L_i^\dagger(\omega) - \frac{1}{2}\left\{L_i^\dagger(\omega)L_i(\omega), \rho(t)\right\}\right),} \tag{2.35}$$

[5] Essentially, the RWA is equivalent to multiplying by $\delta_{\omega,\omega'}$

[6] Since ρ_E is a thermal state.

which is the expected master equation.

To summarize this section, we started from the Liouville-Von Neumann equation for the density operator of the total system, equation (2.11). We perform a series of approximations, namely the Born-Markov approximation to arrive to a local time evolution equation for the density matrix of the system only that depend to environment only trough the jump operators in a general framework. Example of the derivation for specific cases will be given in the Appendix B.

2.4 Fock-Liouville Hilbert space

In this section, we define the framework of the third quantization. Considering linear combinations of density matrix that conserve their positivity and trace, we construct a linear space of density matrix. Besides, if we define a scalar product over this space, it is a Hilbert space. This space is usually called the Fock-Liouville space and is noted $\rho(\mathcal{H})$.[7] The construction of such space is still valid for an infinite space $\mathcal{H}$.

With this in hand, we can define properly what is a superoperator. A superoperator $\mathcal{S}$ is an operator acting on $\mathcal{B}(\mathcal{H})$, the space of the operators acting on $\mathcal{H}$. For $A \in \mathcal{B}(\mathcal{H})$,

$$A \to A' = \mathcal{S}[A]. \tag{2.36}$$

If we restrict ourselves to superoperator acting on $\rho(\mathcal{H})$, they can define a mapping of $\rho(\mathcal{H})$ over itself, $\mathcal{S} : \rho(\mathcal{H}) \to \rho(\mathcal{H})$. To ensure that the result is a density matrix, the superoperator must fulfill the following properties

- Trace preserving: $\mathrm{Tr}[\mathcal{S}[\rho]] = 1 \forall \rho \in \rho(\mathcal{H})$.
- Completely positive. It must map to a positive density matrix but this sole condition is not enough. If the system of interest is entangled with another system R, the superoperator $(\mathcal{I} \otimes \mathcal{S})$ must also map to a positive density matrix. Here the $\mathcal{I}$ is the identity superoperator.

The class of superoperator satisfying these two conditions are called *completely positive maps* or CPT-maps [9]. These superoperators represent physical processes such as measurement or dynamics. Indeed, we already encountered a superoperator previously, the *Liouvillian*. We can rewrite equation (2.10) as

$$\dot{\rho}_S = \mathcal{L}[\rho_S], \tag{2.37}$$

where $\mathcal{L}$ is the Liouvillian, the superoperator that gives the dynamics of the system. Now that we have introduced the concept of superoperators, there is an alternative notation for the Lindblad equation that we will prefer over the one in (2.10),

$$\boxed{\dot{\rho}_S(t) = \mathcal{L}[\rho_S(t)] = -i[H, \rho_S(t)] + \sum_\mu \gamma_\mu \mathcal{D}_{x_\mu}[\rho_S(t)].} \tag{2.38}$$

where γ_μ are the dissipative rates. For master equation in the Lindblad form, $\gamma_\mu > 0 \ \forall \mu$. The corresponding dissipative superoperators $\mathcal{D}_{x_\mu}[\rho_S(t)]$, are defined as

$$\mathcal{D}_{x_\mu}[\rho_S(t)] = x_\mu \rho_S(t) x_\mu^\dagger - \frac{1}{2}\{x_\mu^\dagger x_\mu, \rho_S\}. \tag{2.39}$$

We can see that the x_μ are nothing else than a rewriting of the jump operators, $L_\mu = \sqrt{\gamma_\mu} x_\mu \forall \mu$.

Note that we have not yet defined a scalar product for our space $\rho(\mathcal{H})$.

To summarize, we have constructed a well-defined Hilbert space of density operators and introduced a class of mappings over this space, known as superoperators, which act like operators at the level of density operators. This structure shares many similarities with the original Hilbert

[7] We have $\rho(\mathcal{H}) \subsetneq \mathcal{B}(\mathcal{H})$

space $\mathcal{H}$ of state vectors $|\psi\rangle$ of the system, where the operators of $\mathcal{B}(\mathcal{H})$ map the ket vectors of $\mathcal{H}$ to themselves. However, there is a key difference in the generator of the dynamics. In $\mathcal{H}$, the Hamiltonian H can be represented as a matrix and diagonalized to solve the Schrödinger equation (see Sec. 1.2). Therefore, the goal of the next section is to find a matrix representation of the generator of the dynamics for $\rho(\mathcal{H})$, which is the Liouvillian $\mathcal{L}$.

2.5 Choi-Jamiołkowski isomorphism

Through the previous section, we constructed a linear space of density matrix. It is straightforward to see that an isomorphism can be easily established between an $N \times N$ matrix and a vector of size $N^2 \times 1$. Formally, we have $|i\rangle\langle j| \to |i\rangle \otimes |j\rangle$. Noting $|\rho\rangle$ the vectorized density operator,

$$\boxed{\rho = \begin{pmatrix} \rho_{11} & \rho_{12} & \cdots & \rho_{1N} \\ \rho_{21} & \rho_{22} & \cdots & \rho_{2N} \\ \vdots & \vdots & \ddots & \vdots \\ \rho_{N1} & \rho_{N2} & \cdots & \rho_{NN} \end{pmatrix} \xrightarrow{\text{Isomorphism}} |\rho\rangle = \begin{pmatrix} \rho_{11} \\ \rho_{12} \\ \vdots \\ \rho_{1N} \\ \vdots \\ \rho_{NN} \end{pmatrix}.} \tag{2.40}$$

This representation for the density operators allow us to define a scalar product. Let ρ, ϕ be elements of $\rho(\mathcal{H})$, their vectorized representation are $|\rho\rangle$ and $|\phi\rangle$. We define the scalar product in the Fock-Liouville space as

$$\langle\rho|\phi\rangle \equiv \mathrm{Tr}[\rho^\dagger \phi]. \tag{2.41}$$

The name of this isomorphism is the *Choi-Jamiołkowski isomorphism*, developed and presented in [27, 28]. This isomorphism also implies the existence of a matrix representation for the Liouvillian $\mathcal{L}$, or any other CPT-map. With a matrix representation of $\mathcal{L}$, we will be able to perform a sort of Bogoliubov transformation in order to find the eigenvalues and eigenvectors of the dynamic. This is the aim of the third quantization.

The Choi-Jamiołkowski isomorphism implies that for any CPT-map $\mathcal{S}$ acting on the density operator space $\rho(\mathcal{H})$ such that $\mathcal{S}[\rho] = A\rho B$ for $\rho \in \rho(\mathcal{H})$, $A, B \in \mathcal{B}(\mathcal{H})$, its matrix representation S is given by[8]

$$\boxed{S = A \otimes B^T,} \tag{2.42}$$

where S is a matrix of size $N^2 \times N^2$ for a Hilbert space $\mathcal{H}$ of dimension N. The demonstration of this isomorphism is done in details in the Appendix A.

Note that in the standard form of the Lindblad equation (2.10), the density operator appears in several terms. Therefore, representing $\mathcal{L}$ in matrix form provides a mathematical object that encapsulates the system's dynamics without explicitly including any density operator. At this point, an example will probably help the comprehension.

2.5.1 Example

We consider the following master equation for a bosonic case:

$$\mathcal{L}[\rho(t)] = \dot{\rho}(t) = -i[H, \rho(t)] + \gamma \mathcal{D}_a[\rho(t)],$$

[8] We shall specify that the tensor product in this equation has a particular name, the *Kronecker product*, defined by the relation

$$A \otimes B = \begin{pmatrix} a_{11}B & \cdots & a_{1n}B \\ \vdots & \ddots & \vdots \\ a_{m1}B & \cdots & a_{mn}B \end{pmatrix},$$

for a matrix A of size $m \times n$ and B of size $p \times q$.

where $H = \omega a^\dagger a$ is the Hamiltonian of the system, ω the frequency of the mode and $a^\dagger, a$ the creation and annihilation operators corresponding to this mode and $\gamma > 0$ the dissipation rate. This equation could model the motion of an atom in an harmonic trap, where the dissipation can correspond to cooling of the atomic motion. In this case, the Fock basis of $\mathcal{H}$ is given by $\{|0\rangle, |1\rangle\}$, the state $|0\rangle$ corresponding to the ground state and the state $|1\rangle$, is the excited one. With this basis, the matrix representation of H, a and ρ are respectively

$$H = \begin{pmatrix} 0 & 0 \\ 0 & \omega \end{pmatrix}, \quad a = \begin{pmatrix} 0 & 1 \\ 0 & 0 \end{pmatrix} \text{and} \quad \rho = \begin{pmatrix} \rho_{11} & \rho_{12} \\ \rho_{21} & \rho_{22} \end{pmatrix}.$$

Following the application of the isomorphism, we have

$$\begin{aligned} [H, \rho] &= H\rho - \rho H \to H \otimes \mathbb{1} - \mathbb{1} \otimes H^T, \\ \mathcal{D}_a[\rho] &= a\rho a^\dagger - \frac{1}{2}\{a^\dagger a, \rho\} \to a \otimes (a^\dagger)^T - \frac{1}{2} a^\dagger a \otimes \mathbb{1} - \frac{1}{2}\mathbb{1} \otimes (a^\dagger a)^T \end{aligned}$$

and

$$L = \begin{pmatrix} 0 & 0 & 0 & \gamma \\ 0 & -\frac{\gamma}{2} + i\omega & 0 & 0 \\ 0 & 0 & -\frac{\gamma}{2} - i\omega & 0 \\ 0 & 0 & 0 & -\gamma \end{pmatrix}.$$

With this representation of the Liouvillian, determining its eigenvalues becomes straightforward, allowing for an analytical solution to the master equation.

In the next section, we will deeply study the spectrum of the Liouvillian to understand how it could affect the dynamics of the system.

2.6 Spectrum of the Liouvillian

In this section, we compare the spectrum of the Hamiltonian with the one of the Liouvillian. We also review the main properties of the eigenvalues and eigenvectors of the Liouvillian.

On the first hand, the Hamiltonian is an operator defined in $\mathcal{B}(\mathcal{H})$, it is therefore hermitian and its eigenvalues are necessarily real. In addition, its left and right eigenvectors are the same, i.e., if $H|\phi_i\rangle = E_i|\phi_i\rangle$, $E_i \in \mathbb{R}$ and $\langle\phi_i| H = \langle\phi_i| E_i$. As the set of eigenvalues is real, we can order them and find the smallest, E_0 such that $E_i > E_0 \; \forall i \neq 0$. The eigenstate associated with the eigenvalue E_0 is called the ground state[9].

On the other hand, the matrix representation of the Liouvillian is not hermitian, which implies different properties for its spectrum. Firstly, Evans theorem [29, 30] assure the existence of at least one zero eigenvalue for finite size systems. The eigenstate associated with this value is the steady state, i.e., we have

$$L[\rho_{\text{NESS}}] = 0. \tag{2.43}$$

The uniqueness of the steady state is not assured, in particular when the Liouvillian admits some specific symmetries, see [31, 32, 33] for more details. To fully determine the dynamics of the system, one has to find the full spectrum of the Liouvillian. One consequence of the non-Hermiticity of L is that its left and right eigenvectors might be different. For a given eigenvalue λ_i, we can find the eigenvectors $|\Lambda_i^R\rangle$ and $\langle\Lambda_i^L|$ such that

$$\boxed{L|\Lambda_i^R\rangle = \lambda_i |\Lambda_i^R\rangle, \quad \langle\Lambda_i^L| L = \langle\Lambda_i^L| \lambda_i.} \tag{2.44}$$

We impose that the norm of the eigenvectors is 1. However, the eigenvectors does not necessarily represent density operators. Having the eigenvalues and eigenvectors of the Liouvillian, we can

[9] Remember equation (1.20) and take $i = 0$.

write the state of the system in any time t,

$$\boxed{|\rho(t)\rangle = \sum_i e^{\lambda_i t} \langle \Lambda_i^L | \rho(0) \rangle |\Lambda_i^R\rangle .} \tag{2.45}$$

Given the previous equation, one can understand that in order to describe a physical system, we must have $\mathrm{Re}[\lambda_i] \leq 0 \forall i$ [26]. Indeed, for $t \to \infty$, $\rho(t) \to \rho_{\mathrm{NESS}}$, the real part of the eigenvalues is responsible for the relaxation to the steady state. Similarly to the Hamiltonian case, we can sort the eigenvalues via their real part: $0 = \mathrm{Re}[\lambda_0] < \mathrm{Re}[\lambda_1] < ... < \mathrm{Re}[\lambda_n]$. We also identify a relevant quantity, the *Liouvillian gap*, $\lambda = \mathrm{Re}[\lambda_1]$ which gives the slowest relaxation rate[10]. It is shown in [32] that if the Liouvillian gap tends toward 0, a dissipative phase transition can occur because the steady state is now degenerated. Many recent articles show the links between dissipative phase transitions, symmetries breaking and study of the spectrum of the Liouvillian. See for example [34, 35, 36].

The Liouvillian admits the following properties

- $e^{Lt} |\Lambda_i^R\rangle = e^{\lambda_i t} |\Lambda_i^R\rangle$.
- As the Liouvillian conserve the trace, we have $\mathrm{Tr}[\Lambda_i^R] = 0$ if $\mathrm{Re}[\lambda_i] \neq 0$. Indeed, for $t \to \infty$, $e^{Lt} |\Lambda_i^R\rangle = e^{\lambda_i t} |\Lambda_i^R\rangle \to 0$. We can understand why the eigenvectors of the Liouvillian are not necessarily density operators.
- The eigenvalues of the Liouvillian are either real or complex conjugated two by two. Indeed, if $L |\Lambda_i^R\rangle = \lambda_i |\Lambda_i^R\rangle$ then $L |\Lambda_i^R\rangle^\dagger = \lambda_i^* |\Lambda_i^R\rangle^\dagger$. Thus, if $|\Lambda_i^R\rangle$ is Hermitian, λ_i has to be real. We can also show that if an eigenvalue is real, the associated eigenvector must be Hermitian.
- If the eigenvalue 0 has a algebraic multiplicity n, then there exists$n$ independent eigenvectors of the Liouvillian. Therefore, there exists n different steady states towards which the system can evolve, depending on the initial condition [32].

In Fig. 2.2, we summarized and compared the properties of the spectrum of the Liouvillian and the Hamiltonian.

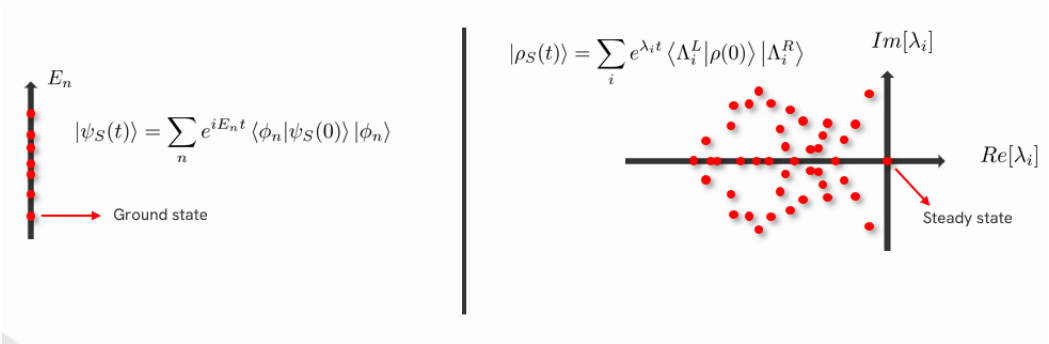

Figure 2.2: Comparison between the spectrum of a typical Hamiltonian and a typical Liouvillian. We see that for H, the spectrum is real while for L, it is complex. We also remark that the eigenvalues of the Liouvillian are two by two complex conjugate. We recall equation (2.45) that gives the time evolution of an arbitrary state $|\rho(t)\rangle \forall t$.

[10]The careful reader will surely have made the connection with the relaxation time defined in Sec. 2.3. Indeed, we have $\tau_{\mathrm{rel}} = 1/\lambda$.

2.7 Summary of the chapter

Throughout the chapter, we developed the mathematical tools required to build a solid theory to study the dynamics of the state of an open quantum system. We described the density operator, which contains the physical information about the system. Then, we presented and derived the Lindblad master equation, a differential equation that generate the dynamics of open quantum systems. Afterwards, we introduced the Fock-Liouville space, an equivalent of the Hilbert space $\mathcal{H}$ where the vectors are now density operators. We also showed that these matrices could be vectorized. With vectorized density operators, the Choi-Jamiołkowski isomorphism allowed us to find a matrix representation for superoperators. Especially for the Liouvillian, the generator of the dynamics of the system. In the previous section, we studied its spectrum and showed that if we have the eigenvalues and eigenvectors of the Liouvillian, we are able to calculate the state of the system for any time t.

However, diagonalizing the Liouvillian is often a very complex problem due to the matrix size, which contains N^4 elements. Performing this manually is tedious, and numerical methods are typically preferred. But for large N, the computation time grows exponentially. Another common numerical approach is integrating the Lindblad equation. Similar issues with computation time arise for large N and depending on the algorithm used, computational errors may occur. An overview of the common numerical methods is done in [37].

This master's thesis is on a new analytical method for diagonalizing the Liouvillian, known as *third quantization*. Initially developed by Prosen for fermions in [3], he later extended the method to bosons in [4]. Subsequently, the Redfield equation was addressed for both fermions [5] and bosons [6]. In the next chapter, we introduce this formalism for the bosonic case.

Chapter 3

Third quantization

The principle of the *third quantization* is to apply a "second quantization" to the Fock-Liouville space. The objective is to find a diagonal representation of the Liouvillian matrix, thereby obtaining its eigenvalues and associated eigenstates, similar to the Bogoliubov transformation for Hamiltonians. The interest of building such methods is ultimately to develop a theory for open many-body systems involving fermions, bosons, their interactions and coupling with the environment. For such systems, a straightforward numerical resolution seems quite impossible. This is where an analytical method like third quantization becomes more than useful.

The third quantization method presented and utilized in this master's thesis is restricted to the bosonic case. We only consider quadratic Hamiltonian and linear coupling with the bath to ensure the existence of a solution. For non-linear coupling, this method must be used in addition with perturbatives or non-perturbatives methods of many-body physics. In this chapter, we present the philosophy of the method for a two-mode bosonic system, as this type of system will be the focus of the second part of this thesis. An extension for the general case of n bosonic modes can be found in [4].

3.1 Preliminaries and notations

We consider a Hilbert space $\mathcal{H}$ of 2 bosonic modes. We recall that with the second quantization, any state of $\mathcal{H}$ can be written in terms of the vacuum state $|0\rangle$, the creation operators, $a_1^\dagger, a_2^\dagger$ and annihilation operators a_1, a_2. We shall now differentiate the elements of $\mathcal{B}(\mathcal{H})$, the set of operators acting on $\mathcal{H}$ and $\rho(\mathcal{H})$, the set of density operators that represent physical states of $\mathcal{H}$. As in the previous chapter, the elements of $\rho(\mathcal{H})$ are noted $|\rho\rangle$. Furthermore, the elements $\mathcal{B}(\mathcal{H})$ will now be noted $(A|$, a bra operator different of $\langle\rho|$[1]. This notation for the operators allow us to give the expectation value A for a state ρ as

$$(A|\rho\rangle = \langle A\rangle = \mathrm{Tr}[A\rho], \tag{3.1}$$

where the last equation comes from equation (2.4).

As the multiplication of matrices is usually not commutative, we are not assured that the outcomes of $b\rho$ and ρb are the same, where b is one of the creation or annihilation operators. The same question can be asked for bA and Ab. Thus, we define the left and right multiplication of b over $\rho(\mathcal{H})$

$$b^L\,|\rho\rangle = |b\rho\rangle\,, \quad b^R\,|\rho\rangle = |\rho b\rangle\,. \tag{3.2}$$

Similarly, for $\mathcal{B}(\mathcal{H})$, one finds

$$(A|b^L = (Ab|, \quad (A|b^R = (bA|. \tag{3.3}$$

[1] We use a different notation to make clear that the kets and bras come from different spaces.

The left and right multiplications output a vector belonging to the initial space, thus defining a mapping. Note that for $\mathcal{B}(\mathcal{H})$, the right multiplication of b is noted with b^L. Indeed,

$$(Ab|\rho\rangle = (A|b^L|\rho\rangle = \mathrm{Tr}[Ab\rho].$$

It also noteworthy that we have $[b^L, b^R] = 0$.

We will use this notation to rewrite the Liouvillian. However, we first need to identify the different terms that can appear in the Hamiltonian and in the jump operators. For a quadratic system, the Hamiltonian can contains four types of terms, one linear, in a or $a^\dagger$, and three quadratic, in aa, in $a^\dagger a^\dagger$ or in $a^\dagger a$. Due to the CCR (1.10), the terms in $aa^\dagger$ can be converted in $a^\dagger a$. It is possible to show that the linear terms can be absorbed via a canonical transformation, resulting in a shift for the right vacuum state, which has no importance for the following. We will therefore not consider these terms. The Hamiltonian can be written as

$$H = \begin{pmatrix} a_1^\dagger \\ a_2^\dagger \end{pmatrix}^T \mathbf{H} \begin{pmatrix} a_1 \\ a_2 \end{pmatrix} + \begin{pmatrix} a_1 \\ a_2 \end{pmatrix}^T \mathbf{K} \begin{pmatrix} a_1 \\ a_2 \end{pmatrix} + \begin{pmatrix} a_1^\dagger \\ a_2^\dagger \end{pmatrix}^T \mathbf{K}^* \begin{pmatrix} a_1^\dagger \\ a_2^\dagger \end{pmatrix}, \tag{3.4}$$

where $\mathbf{H}, \mathbf{K}$ are complex matrices of size 2. Moreover, due to the Hermiticity of H, $\mathbf{H} = \mathbf{H}^\dagger$ and $\mathbf{K} = \mathbf{K}^T$. For the jump operators, we only consider linear coupling, thus it can be rewritten as

$$L_\mu = l_{\mu 1} a_1 + l_{\mu 2} a_2 + k_{\mu 1} a_1^\dagger + k_{\mu 2} a_2^\dagger. \tag{3.5}$$

We can now rewrite the Liouvillian in terms of left and right operators. Given equation (2.38), we have

$$\mathcal{L} = -iH^L + iH^R + \sum_\mu \left(L_\mu^L L_\mu^{\dagger R} - \frac{1}{2} L_\mu^{\dagger L} L_\mu^L - \frac{1}{2} L_\mu^{\dagger R} L_\mu^R \right). \tag{3.6}$$

The link between the use of this notation for left and right multiplication and the Choi -Jamiołkowski isomorphism is straightforward. Using the same master equation as in example 2.5.1, we find

$$\begin{aligned} \mathcal{L} &= i\omega \left((a^\dagger a)^R - (a^\dagger a)^L \right) + \gamma \left(a^L a^{\dagger R} - \frac{1}{2} a^{\dagger L} a^L - \frac{1}{2} a^{\dagger R} a^R \right) \\ &= i\omega \left(a^R a^{\dagger R} - a^{\dagger L} a^L \right) + \gamma \left(a^L a^{\dagger R} - \frac{1}{2} a^{\dagger L} a^L - \frac{1}{2} a^{\dagger R} a^R \right). \end{aligned}$$

We can understand why $(a^\dagger a)^R = a^R a^{\dagger R}$ by calculating the effect of $(a^\dagger a)^R$ on $|\rho\rangle$[2].

Before diving into the heart of the matter, we have to define a new set of maps that will be useful later. We want this set of maps to acts like the creation and annihilation operators $a, a^\dagger$, but at the density vector level. For two bosonic modes, we define the set of 8 maps $a_{0,j}, a_{1,j}, a'_{0,j}, a'_{1,j}$ for $i = 1, 2$,

$$\begin{aligned} a_{0,j} &= a_j^L, \quad & a'_{0,j} &= a_j^{\dagger L} - a_j^{\dagger R}, \\ a_{1,j} &= a_j^{\dagger R}, \quad & a'_{1,j} &= a_j^R - a_j^L. \end{aligned} \tag{3.7}$$

To obtain a mapping similar to the creation and annihilation operators at the density vector level, these maps have to follow the same properties:

- Almost-CCR:
$$[a_{\nu,j}, a'_{\mu,k}] = \delta_{\mu,\nu}\delta_{j,k}, \quad [a_{\nu,j}, a_{\mu,k}] = [a'_{\nu,j}, a'_{\mu,k}] = 0 \tag{3.8}$$
for $\mu, \nu = 0, 1$. We can observe that this property is similar to the corresponding one at the Hilbert space level, as shown in equation (1.10). This similarity is demonstrated by utilizing this relation for the left and right creation and annihilation operators.

[2] We have $(a^\dagger a)^R |\rho\rangle = |\rho a^\dagger a\rangle = a^R |\rho a^\dagger\rangle = a^R a^{\dagger R} |\rho\rangle$

- $a'_{\nu,j}$ left annihilate the identity operator

$$(1|a'_{\nu,j} = 0, \tag{3.9}$$

as the creation operator return 0 when applied to the vacuum bra $\langle 0|$.

- $a_{\nu,j}$ right annihilate the vacuum pure state $|\rho_0\rangle = |0\rangle\langle 0|$,

$$a_{\nu,j}\,|\rho_0\rangle = 0, \tag{3.10}$$

as the annihilation operator return 0 when applied to the vacuum state.

Similarly to the Hilbert Fock space defined in chapter 1, we can define a convenient dual-Fock basis of $\rho(\mathcal{H})$ and $\mathcal{B}(\mathcal{H})$ as

$$|\underline{m}\rangle = \prod_{\nu=0,1} \frac{(a'_{\nu,1})^{m_{\nu,1}}(a'_{\nu,2})^{m_{\nu,2}}}{\sqrt{m_{\nu,1}!}\sqrt{m_{\nu,2}!}}\,|\rho_0\rangle\,, \quad (\underline{m}| = (1|\prod_{\nu=0,1} \frac{(a_{\nu,1})^{m_{\nu,1}}(a_{\nu,2})^{m_{\nu,2}}}{\sqrt{m_{\nu,1}!}\sqrt{m_{\nu,2}!}}, \tag{3.11}$$

where

$$\underline{m} = \begin{pmatrix} m_{0,1} \\ m_{0,2} \\ m_{1,1} \\ m_{1,2} \end{pmatrix}.$$

We have the bi-orthonormality $(\underline{m'}|\underline{m}\rangle = \delta_{\underline{m},\underline{m'}}$ guaranteed by equation (3.8).

3.2 Block triangular form of the Liouvillian

In this section, we inject our new maps to the general expression of the Liouvillian, 3.6. The aim is to show that using the CCR, we can find a block triangular form for L. Therefore, diagonalizing each diagonal block will yield the eigenvalues of the Liouvillian. As the derivation is done for a general case, it will be easy to adapt it for our specific systems.

Let us expand the equation (3.6) in terms of the new maps. For the Hamiltonian terms, we find

$$\begin{aligned} H^L - H^R = &\begin{pmatrix} a_1^{\dagger L} \\ a_2^{\dagger L} \end{pmatrix}^T \mathbf{H} \begin{pmatrix} a_1^L \\ a_2^L \end{pmatrix} + \begin{pmatrix} a_1^L \\ a_2^L \end{pmatrix}^T \mathbf{K} \begin{pmatrix} a_1^L \\ a_2^L \end{pmatrix} + \begin{pmatrix} a_1^{\dagger L} \\ a_2^{\dagger L} \end{pmatrix}^T \mathbf{K}^* \begin{pmatrix} a_1^{\dagger L} \\ a_2^{\dagger L} \end{pmatrix} \\ &- \begin{pmatrix} a_1^{\dagger R} \\ a_2^{\dagger R} \end{pmatrix}^T \mathbf{H} \begin{pmatrix} a_1^R \\ a_2^R \end{pmatrix} - \begin{pmatrix} a_1^R \\ a_2^R \end{pmatrix}^T \mathbf{K} \begin{pmatrix} a_1^R \\ a_2^R \end{pmatrix} - \begin{pmatrix} a_1^{\dagger R} \\ a_2^{\dagger R} \end{pmatrix}^T \mathbf{K}^* \begin{pmatrix} a_1^{\dagger R} \\ a_2^{\dagger R} \end{pmatrix}. \end{aligned} \tag{3.12}$$

We shall decompose our computation in two steps for more clarity. First, the terms in $\mathbf{H}$

$$\begin{aligned} \begin{pmatrix} a_1^{\dagger L} \\ a_2^{\dagger L} \end{pmatrix}^T \mathbf{H} \begin{pmatrix} a_1^L \\ a_2^L \end{pmatrix} - \begin{pmatrix} a_1^{\dagger R} \\ a_2^{\dagger R} \end{pmatrix}^T \mathbf{H} \begin{pmatrix} a_1^L \\ a_2^L \end{pmatrix} &= \begin{pmatrix} a_1^{\dagger L} - a_1^{\dagger R} \\ a_2^{\dagger L} - a_2^{\dagger R} \end{pmatrix}^T \mathbf{H} \begin{pmatrix} a_1^L \\ a_2^L \end{pmatrix} + \begin{pmatrix} a_1^{\dagger R} \\ a_2^{\dagger R} \end{pmatrix}^T \mathbf{H} \begin{pmatrix} a_1^L \\ a_2^L \end{pmatrix} - \begin{pmatrix} a_1^{\dagger R} \\ a_2^{\dagger R} \end{pmatrix}^T \mathbf{H} \begin{pmatrix} a_1^R \\ a_2^R \end{pmatrix} \\ &= \begin{pmatrix} a'_{0,1} \\ a'_{0,2} \end{pmatrix}^T \mathbf{H} \begin{pmatrix} a_{0,1} \\ a_{0,2} \end{pmatrix} - \begin{pmatrix} A_{11} \\ A_{12} \end{pmatrix}^T \mathbf{H} \begin{pmatrix} a'_{1,1} \\ a'_{1,2} \end{pmatrix} \\ &= \begin{pmatrix} a'_{0,1} \\ a'_{0,2} \end{pmatrix}^T \mathbf{H} \begin{pmatrix} a_{0,1} \\ a_{0,2} \end{pmatrix} - \begin{pmatrix} a'_{1,1} \\ a'_{1,2} \end{pmatrix}^T \mathbf{H}^* \begin{pmatrix} A_{11} \\ A_{12} \end{pmatrix}. \end{aligned} \tag{3.13}$$

In the last equation, we switched the a and the a' by using the Hermiticity of $\mathbf{H}$. Then, for the term in $\mathbf{K}$

$$\begin{aligned}\begin{pmatrix}a_1^L\\a_2^L\end{pmatrix}^T\mathbf{K}\begin{pmatrix}a_1^L\\a_2^L\end{pmatrix}-\begin{pmatrix}a_1^R\\a_2^R\end{pmatrix}^T\mathbf{K}\begin{pmatrix}a_1^R\\a_2^R\end{pmatrix}&=\begin{pmatrix}a_1^L\\a_2^L\end{pmatrix}^T\mathbf{K}\begin{pmatrix}a_1^L+a_1^R\\a_2^L+a_2^R\end{pmatrix}-\begin{pmatrix}a_1^L\\a_2^L\end{pmatrix}^T\mathbf{K}\begin{pmatrix}a_1^R\\a_2^R\end{pmatrix}\\&\quad-\begin{pmatrix}a_1^R\\a_2^R\end{pmatrix}^T\mathbf{K}\begin{pmatrix}a_1^L+a_1^R\\a_2^L+a_2^R\end{pmatrix}+\begin{pmatrix}a_1^R\\a_2^R\end{pmatrix}^T\mathbf{K}\begin{pmatrix}a_1^L\\a_2^L\end{pmatrix}\\&=-\begin{pmatrix}a'_{1,1}\\a'_{1,2}\end{pmatrix}^T\mathbf{K}\begin{pmatrix}2a_{0,1}+A'_{11}\\2a_{0,2}+A'_{12}\end{pmatrix}+\begin{pmatrix}a_1^R\\a_2^R\end{pmatrix}^T\mathbf{K}\begin{pmatrix}a_1^L\\a_2^L\end{pmatrix}-\begin{pmatrix}a_1^L\\a_2^L\end{pmatrix}^T\mathbf{K}\begin{pmatrix}a_1^R\\a_2^R\end{pmatrix}\\&=-\begin{pmatrix}a'_{1,1}\\a'_{1,2}\end{pmatrix}^T\mathbf{K}\begin{pmatrix}2a_{0,1}+A'_{11}\\2a_{0,2}+A'_{12},\end{pmatrix},\end{aligned}\tag{3.14}$$

since[3]

$$\begin{pmatrix}a_1^R\\a_2^R\end{pmatrix}^T\mathbf{K}\begin{pmatrix}a_1^L\\a_2^L\end{pmatrix}=\begin{pmatrix}a_1^L\\a_2^L\end{pmatrix}^T\cdot\mathbf{K}\begin{pmatrix}a_1^R\\a_2^R\end{pmatrix}.$$

Similarly, for the term in $\mathbf{K}^*$, we find

$$\begin{pmatrix}a_1^{\dagger L}\\a_2^{\dagger L}\end{pmatrix}^T\mathbf{K}^*\begin{pmatrix}a_1^{\dagger L}\\a_2^{\dagger L}\end{pmatrix}-\begin{pmatrix}a_1^{\dagger R}\\a_2^{\dagger R}\end{pmatrix}^T\mathbf{K}^*\begin{pmatrix}a_1^{\dagger R}\\a_2^{\dagger R}\end{pmatrix}=\begin{pmatrix}a'_{0,1}\\a'_{0,2}\end{pmatrix}^T\mathbf{K}^*\begin{pmatrix}2A_{11}+a'_{0,1}\\2A_{12}+a'_{0,2}\end{pmatrix}.\tag{3.16}$$

We now have to expand the jump operators with the new maps. The derivation follows the same steps as for the Hamiltonian, introducing the new mappings and utilizing the commutation properties. We will not show the derivation here but at some point, we have to define the following 2×2 matrices

$$\mathbf{M}=\sum_\mu\begin{pmatrix}|l_{\mu,1}|^2&l_{\mu,1}l^*_{\mu,2}\\l_{\mu,2}l^*_{\mu,1}&|l_{\mu,2}|^2\end{pmatrix},\quad\mathbf{N}=\begin{pmatrix}|k_{\mu,1}|^2&k_{\mu,1}k^*_{\mu,2}\\k_{\mu,2}k^*_{\mu,1}&|k_{\mu,2}|^2\end{pmatrix},\quad\mathbf{L}=\begin{pmatrix}l_{\mu,1}k^*_{\mu,1}&l_{\mu,1}k^*_{\mu,2}\\l_{\mu,2}k^*_{\mu,1}&l_{\mu,2}k^*_{\mu,2}\end{pmatrix}.\tag{3.17}$$

Notice that the matrices $\mathbf{M}$ and $\mathbf{N}$ are Hermitian. We eventually obtain an expression for the Liouvillian in terms of the new maps

$$\begin{aligned}\mathcal{L}=&-i\begin{pmatrix}a'_{0,1}\\a'_{0,2}\end{pmatrix}^T\mathbf{H}\begin{pmatrix}a_{0,1}\\a_{0,2}\end{pmatrix}+i\begin{pmatrix}a'_{1,1}\\a'_{1,2}\end{pmatrix}^T\mathbf{H}^*\begin{pmatrix}A_{11}\\A_{12}\end{pmatrix}\\&+i\begin{pmatrix}a'_{1,1}\\a'_{1,2}\end{pmatrix}^T\mathbf{K}\begin{pmatrix}2a_{0,1}+A'_{11}\\2a_{0,2}+A'_{12},\end{pmatrix}-i\begin{pmatrix}a'_{0,1}\\a'_{0,2}\end{pmatrix}^T\mathbf{K}^*\begin{pmatrix}2A_{11}+a'_{0,1}\\2A_{12}+a'_{0,2}\end{pmatrix}\\&+\begin{pmatrix}a'_{0,1}\\a'_{0,2}\end{pmatrix}^T(\mathbf{N}-\mathbf{M}^*)\begin{pmatrix}a_{0,1}\\a_{0,2}\end{pmatrix}+\begin{pmatrix}a'_{1,1}\\a'_{1,2}\end{pmatrix}^T(\mathbf{N}^*-\mathbf{M})\begin{pmatrix}A_{11}\\A_{12}\end{pmatrix}\\&+\begin{pmatrix}a'_{0,1}\\a'_{0,2}\end{pmatrix}^T\left(\mathbf{L}^\dagger-\mathbf{L}^*\right)\begin{pmatrix}A_{11}\\A_{12}\end{pmatrix}+\begin{pmatrix}a'_{1,1}\\a'_{1,2}\end{pmatrix}^T\left(\mathbf{L}^T-\mathbf{L}\right)\begin{pmatrix}a_{0,1}\\a_{0,2}\end{pmatrix}\\&-\begin{pmatrix}a'_{0,1}\\a'_{0,2}\end{pmatrix}^T\mathbf{L}^*\begin{pmatrix}a'_{0,1}\\a'_{0,2}\end{pmatrix}-\begin{pmatrix}a'_{1,1}\\a'_{1,2}\end{pmatrix}^T\mathbf{L}\begin{pmatrix}a'_{1,1}\\a'_{1,2}\end{pmatrix}+2\begin{pmatrix}a'_{0,1}\\a'_{0,2}\end{pmatrix}^T\mathbf{N}\begin{pmatrix}a'_{1,1}\\a'_{1,2}\end{pmatrix}.\end{aligned}\tag{3.18}$$

It is worth noting that the primed maps appear always at the left side of the matrices, which implies $(1|\mathcal{L}=0$.

We are now very close to the diagonal form of the the Liouvillian. Setting

$$\underline{b}=\begin{pmatrix}a_{0,1}&a_{0,2}&A_{11}&A_{12}&a'_{0,1}&a'_{0,2}&a'_{1,1}&a'_{1,2}\end{pmatrix}^T,\tag{3.19}$$

[3]If we calculate the matrix product, we find the same expression in both sides by remembering that $[b^L,b^R]=0$

we can rewrite (3.18) as

$$\mathcal{L} = L = \underline{b} \cdot \mathbf{S}\underline{b} - S_0 \mathbb{1}_8, \tag{3.20}$$

where $\mathbf{S}$ is a 2×2 block matrix, where each block is of size 4.

$$\mathbf{S} = \begin{pmatrix} S_1 & S_2 \\ S_3 & S_4 \end{pmatrix}. \tag{3.21}$$

Let us expand $\underline{b} \cdot \mathbf{S}\underline{b}$ to identify which block of $\mathbf{S}$ is associated with each term in (3.18).

$$\underline{b} \cdot \mathbf{S}\underline{b} = \begin{pmatrix} a_{0,1} \\ a_{0,2} \\ A_{11} \\ A_{12} \end{pmatrix}^T S_1 \begin{pmatrix} a_{0,1} \\ a_{0,2} \\ A_{11} \\ A_{12} \end{pmatrix} + \begin{pmatrix} a_{0,1} \\ a_{0,2} \\ A_{11} \\ A_{12} \end{pmatrix}^T S_2 \begin{pmatrix} a'_{0,1} \\ a'_{0,2} \\ a'_{1,1} \\ a'_{1,2} \end{pmatrix} + \begin{pmatrix} a'_{0,1} \\ a'_{0,2} \\ a'_{1,1} \\ a'_{1,2} \end{pmatrix}^T S_3 \begin{pmatrix} a_{0,1} \\ a_{0,2} \\ A_{11} \\ A_{12} \end{pmatrix} + \begin{pmatrix} a'_{0,1} \\ a'_{0,2} \\ a'_{1,1} \\ a'_{1,2} \end{pmatrix}^T S_4 \begin{pmatrix} a'_{0,1} \\ a'_{0,2} \\ a'_{1,1} \\ a'_{1,2} \end{pmatrix}.$$

In equation (3.18), there is no terms in $a(\cdot)a$, thus S_1 is necessarily equal to 0. Due to the almost-CCR condition, we must have $aS_2a' = (a'S_3a)^T$, which implies $S_2 = S_3^T$. To remain consistent with Prosen's notation, we substitute S_2 by $-\mathbf{X}$ and S_4 by $\mathbf{Y}$. Eventually, $\mathbf{S}$ must be in the form

$$\boxed{\mathbf{S} = \begin{pmatrix} \mathbf{0} & -\mathbf{X} \\ -\mathbf{X}^T & \mathbf{Y} \end{pmatrix}.} \tag{3.22}$$

We still have to identify $\mathbf{X}$ and $\mathbf{Y}$ in (3.18) using (3.8). We have

$$\begin{aligned}
\mathcal{L} = &- \frac{i}{2} \begin{pmatrix} a'_{0,1} \\ a'_{0,2} \end{pmatrix}^T \mathbf{H} \begin{pmatrix} a_{0,1} \\ a_{0,2} \end{pmatrix} - \frac{i}{2} \begin{pmatrix} a_{0,1} \\ a_{0,2} \end{pmatrix}^T \mathbf{H}^* \begin{pmatrix} a'_{0,1} \\ a'_{0,2} \end{pmatrix} + \frac{i}{2}\mathbf{H}^* \\
&+ \frac{i}{2} \begin{pmatrix} a'_{1,1} \\ a'_{1,2} \end{pmatrix}^T \mathbf{H}^* \begin{pmatrix} A_{11} \\ A_{12} \end{pmatrix} - \frac{i}{2} \begin{pmatrix} A_{11} \\ A_{12} \end{pmatrix}^T \mathbf{H} \begin{pmatrix} a'_{1,1} \\ a'_{1,2} \end{pmatrix} - \frac{i}{2}\mathbf{H} \\
&+ \frac{i}{2} \begin{pmatrix} a'_{1,1} \\ a'_{1,2} \end{pmatrix}^T 2\mathbf{K} \begin{pmatrix} a_{0,1} \\ a_{0,2} \end{pmatrix} + \frac{i}{2} \begin{pmatrix} a_{0,1} \\ a_{0,2} \end{pmatrix}^T 2\mathbf{K}^* \begin{pmatrix} a'_{1,1} \\ a'_{1,2} \end{pmatrix} + \frac{i}{2} \begin{pmatrix} a'_{1,1} \\ a'_{1,2} \end{pmatrix}^T 2\mathbf{K} \begin{pmatrix} a'_{1,1} \\ a'_{1,2} \end{pmatrix} \\
&- \frac{i}{2} \begin{pmatrix} a'_{0,1} \\ a'_{0,2} \end{pmatrix}^T 2\mathbf{K}^* \begin{pmatrix} A_{11} \\ A_{12} \end{pmatrix} - \frac{i}{2} \begin{pmatrix} A_{11} \\ A_{12} \end{pmatrix}^T 2\mathbf{K} \begin{pmatrix} a'_{0,1} \\ a'_{0,2} \end{pmatrix} - \frac{i}{2} \begin{pmatrix} a'_{0,1} \\ a'_{0,2} \end{pmatrix}^T 2\mathbf{K}^* \begin{pmatrix} a_{0,1} \\ a_{0,2} \end{pmatrix} \\
&+ \frac{1}{2} \begin{pmatrix} a'_{0,1} \\ a'_{0,2} \end{pmatrix}^T (\mathbf{N} - \mathbf{M}^*) \begin{pmatrix} a_{0,1} \\ a_{0,2} \end{pmatrix} + \frac{1}{2} \begin{pmatrix} a_{0,1} \\ a_{0,2} \end{pmatrix}^T (\mathbf{N}^* - \mathbf{M}) \begin{pmatrix} a'_{0,1} \\ a'_{0,2} \end{pmatrix} - \frac{1}{2}(\mathbf{N}^* - \mathbf{M}) \\
&+ \frac{1}{2} \begin{pmatrix} a'_{1,1} \\ a'_{1,2} \end{pmatrix}^T (\mathbf{N}^* - \mathbf{M}) \begin{pmatrix} A_{11} \\ A_{12} \end{pmatrix} + \frac{1}{2} \begin{pmatrix} A_{11} \\ A_{12} \end{pmatrix}^T (\mathbf{N} - \mathbf{M}^*) \begin{pmatrix} a'_{1,1} \\ a'_{1,2} \end{pmatrix} - \frac{1}{2}(\mathbf{N} - \mathbf{M}^*) \\
&+ \frac{1}{2} \begin{pmatrix} a'_{0,1} \\ a'_{0,2} \end{pmatrix}^T (\mathbf{L}^\dagger - \mathbf{L}^*) \begin{pmatrix} A_{11} \\ A_{12} \end{pmatrix} + \frac{1}{2} \begin{pmatrix} A_{11} \\ A_{12} \end{pmatrix} (\mathbf{L}^* - \mathbf{L}^\dagger) \begin{pmatrix} a'_{0,1} \\ a'_{0,2} \end{pmatrix} \\
&+ \frac{1}{2} \begin{pmatrix} a'_{1,1} \\ a'_{1,2} \end{pmatrix}^T (\mathbf{L}^T - \mathbf{L}) \begin{pmatrix} a_{0,1} \\ a_{0,2} \end{pmatrix} + \frac{1}{2} \begin{pmatrix} a_{0,1} \\ a_{0,2} \end{pmatrix}^T (\mathbf{L} - \mathbf{L}^T) \begin{pmatrix} a'_{1,1} \\ a'_{1,2} \end{pmatrix} - \frac{1}{2} \begin{pmatrix} a'_{0,1} \\ a'_{0,2} \end{pmatrix}^T (\mathbf{L}^* + \mathbf{L}^\dagger) \begin{pmatrix} a'_{0,1} \\ a'_{0,2} \end{pmatrix} \\
&- \frac{1}{2} \begin{pmatrix} a'_{1,1} \\ a'_{1,2} \end{pmatrix}^T (\mathbf{L} + \mathbf{L}^T) \begin{pmatrix} a'_{1,1} \\ a'_{1,2} \end{pmatrix} + \frac{1}{2} \begin{pmatrix} a'_{0,1} \\ a'_{0,2} \end{pmatrix}^T 2\mathbf{N} \begin{pmatrix} a'_{1,1} \\ a'_{1,2} \end{pmatrix} + \frac{1}{2} \begin{pmatrix} a'_{1,1} \\ a'_{1,2} \end{pmatrix}^T 2\mathbf{N}^T \begin{pmatrix} a'_{0,1} \\ a'_{0,2} \end{pmatrix}
\end{aligned}$$

and we can finally write the Liouvillian in a block triangular form

$$L = \underline{b}^T \begin{pmatrix} 0 & -\mathbf{X} \\ -\mathbf{X}^T & \mathbf{Y} \end{pmatrix} \underline{b} - \frac{1}{2}[\mathbf{M} + \mathbf{M}^* - (\mathbf{N}^* + \mathbf{N})], \tag{3.23}$$

where

$$\boxed{\mathbf{X} = \frac{1}{2} \begin{pmatrix} i\mathbf{H}^* - \mathbf{N}^* + \mathbf{M} & -2i\mathbf{K} - \mathbf{L} + \mathbf{L}^T \\ 2i\mathbf{K} - \mathbf{L}^* + \mathbf{L}^\dagger & -i\mathbf{H} - \mathbf{N} + \mathbf{M}^* \end{pmatrix},} \tag{3.24}$$

$$\boxed{\mathbf{Y} = \frac{1}{2}\begin{pmatrix} -2i\mathbf{K}^* - \mathbf{L}^* - \mathbf{L}^\dagger & 2\mathbf{N} \\ 2\mathbf{N}^T & 2i\mathbf{K} - \mathbf{L} - \mathbf{L}^T \end{pmatrix} = \mathbf{Y}^T,} \tag{3.25}$$

$$S_0 \mathbb{1}_{4n} = \frac{1}{2}[\mathbf{M} + \mathbf{M}^* - (\mathbf{N}^* + \mathbf{N})] = (\text{Tr } \mathbf{M} - \text{Tr } \mathbf{N})\mathbb{1}_{4n}. \tag{3.26}$$

The latest correspondsto the reordering of maps.

In his paper, Prosen showed that the eigenvalues of the Liouvillian are proportional to the *rapidities*, the eigenvalues of $\mathbf{X}$. Thus, if $\mathbf{X}$ is diagonalizable, we could have the eigenvalues and associated eigenstates, leading to a fully analytical solution of the master equation.

3.3 Eigensystem of the Liouvillian

In this section, we will show how the eigenvalues of $\mathbf{X}$ are related to these of $\mathcal{L}$. We will also show that a Bogoliubov-like transformation can be performed to obtain the normal master mods, equivalent of the normal modes in the section 1.2.

We will assume that $\mathbf{X}$ is diagonalizable[4]. Thus, it exists $\mathbf{\Delta} = \text{diag}(\beta_1, .., \beta_4)$, $\beta_j \in \mathbb{C}, \forall j \in \{1, ..., 4\}$ and $\mathbf{P}$ such that

$$\mathbf{X} = \mathbf{P}\mathbf{\Delta}\mathbf{P}^{-1}. \tag{3.27}$$

As said in the previous section, the eigenvalues of $\mathbf{X}$ are called the *rapidities*. Furthermore, the rapidities should come in complex conjugate pairs[5], β_j, β_j^*. It is due to the fact that $\mathbf{X}$ (and $\mathbf{Y}$) is unitarily similar to a real matrix.

The expression of the eigenstates of $\mathcal{L}$ requires a matrix $\mathbf{Z}$ which is the solution of the following equation

$$\mathbf{X}^T\mathbf{Z} + \mathbf{Z}\mathbf{X} = \mathbf{Y}. \tag{3.28}$$

This equation is known as the *continuous Lyapunov equation*, originally studied by Lyapunov in [38] to investigate the stability of motion. It is known that a solution exists and is unique if no pairs of rapidities exists such that $\beta_j + \beta'_j = 0$. Thus, a solution is guaranteed to exists if all the rapidities have a non-zero real part[6]. With the matrix $\mathbf{Z}$, we can define the 8 *normal master modes* (NMM) (ξ, ξ') as

$$\boxed{\begin{pmatrix} \xi_1 \\ \xi_2 \\ \xi_3 \\ \xi_4 \end{pmatrix} = \mathbf{P}^T \left(\begin{pmatrix} a_{0,1} \\ a_{0,2} \\ A_{11} \\ A_{12} \end{pmatrix} - \mathbf{Z} \begin{pmatrix} a'_{0,1} \\ a'_{0,2} \\ a'_{1,1} \\ a'_{1,2} \end{pmatrix} \right), \quad \begin{pmatrix} \xi'_1 \\ \xi'_2 \\ \xi'_3 \\ \xi'_4 \end{pmatrix} = \mathbf{P}^{-1} \begin{pmatrix} a'_{0,1} \\ a'_{0,2} \\ a'_{1,1} \\ a'_{1,2} \end{pmatrix}.} \tag{3.29}$$

It can be shown that these NMM satisfy the almost-CCR

$$[\xi_r, \xi'_s] = \delta_{r,s}, \quad [\xi_r, \xi_s] = [\xi'_r, \xi'_s] = 0. \tag{3.30}$$

And finally, we have

$$\boxed{L = -2\sum_{r=1}^{4} \beta_r \xi'_r \xi_r.} \tag{3.31}$$

We just showed that the Liouvillian can be expressed in a diagonal form. In the basis of the NMM, the eigenvalues of the Liouvillian are $-2\beta_r$ for $r = 1, ..., 4$. To compare with the Hamiltonian case, $H = \hbar\omega a^\dagger a$ has a single eigenvalue $\hbar\omega$ in the basis $a, a^\dagger$. However, we know that the full

[4] The general case for a non-diagonalizable $\mathbf{X}$ has yet to be explored.

[5] Just as the complex eigenvalues of the Liouvillian.

[6] Unlike the Liouvillian, which has necessarily at least a 0 eigenvalue.

spectrum of the Hamiltonian of a harmonic oscillator is given by $\hbar\omega n$ for $n \in \mathbb{N}$. We still have to find the equivalent for the Liouvillian. Before that, we must note that the existence of a stable solution of the Lindblad master equation is not guaranteed. Indeed, if at least one rapidity is at the left of the imaginary axis, i.e., $\exists j : \mathrm{Re}[\beta_j] < 0$, we would have at least one eigenvalue of $\mathcal{L}$ with a positive real part, which does not corresponds to a physical system, as the system would continuously absorbs excitations from the environment. This case will be explained and discussed in detail in the chapter 4.

We now express the properties of the NMM

1. As expected, a unique *non-equilibrium steady state*[7] (NESS) exists. Indeed, we have $|\rho_{NESS}\rangle \in \rho(\mathcal{H})$, the "right vacuum state" of the Liouvillian, defined by

$$\mathcal{L}\,|\rho_{NESS}\rangle = 0. \tag{3.32}$$

We thus can determine the steady state via the NMM annihilation relations, $\forall r = 1, ..., 4$,

$$\boxed{\xi_r\,|\rho_{NESS}\rangle = 0.} \tag{3.33}$$

We also have that the primed NMM annihilate the identity operator, $(1|\xi'_r = 0$.

2. The spectrum of the Liouvillian is completely determined analytically in term of a 4 component multi-index of super-quantum numbers $\underline{m} = (m_1, m_2, m_3, m_4)$, $m_r \in \mathbb{N}$,

$$\boxed{\lambda_{\underline{m}} = -2\sum_{r=1}^{4} m_r\beta_r.} \tag{3.34}$$

The associated left and right eigenvectors associated are given by

$$\boxed{\mathcal{L}\,|\Lambda_{\underline{m}}\rangle = \lambda_{\underline{m}}\,|\Lambda_{\underline{m}}\rangle\,, \quad (\Lambda_{\underline{m}}|\mathcal{L} = \lambda_{\underline{m}}(\Lambda_{\underline{m}}|,} \tag{3.35}$$

where

$$\boxed{|\Lambda_{\underline{m}}\rangle = \prod_{r=1}^{4} \frac{(\xi'_r)^{m_r}}{\sqrt{m_r!}}\,|\rho_{NESS}\rangle\,, \quad (\Lambda_{\underline{m}}| = (1|\prod_{r=1}^{4} \frac{(\xi_r)^{m_r}}{\sqrt{m_r!}}.} \tag{3.36}$$

The main idea of this point is that the eigenvalues of the Liouvillian are given by $-2\mathbb{CL}$ where $\mathbb{CL}$ are all the possible linear combination of the rapidities, $\mathbb{CL} = \{x : x = m_1\beta_1 + m_2\beta_2 + m_3\beta_3 + m_4\beta_4, \forall m_r \in \mathbb{N}\}$.

3. The 2-point correlator of $|\rho_{NESS}\rangle$ is given by the solution of the Lyapunov equation (3.28). Considering b_r, b_s among the 4 creation or annihilation operators $(a_1, a_1^\dagger, a_2, a_2^\dagger)$, we have

$$\mathrm{Tr}[:b_r b_s:\rho_{\mathrm{NESS}}] = \langle :b_r b_s:\rangle_{\mathrm{NESS}} = Z_{rs}, \tag{3.37}$$

where $:b_r b_s:$ designate the normal order of $b_r b_s$. It is a convention in quantum field theory, the creation operators are to the left of all annihilation operators [39]. This property will be of great interest in the next chapters as it will allows us to obtain the time evolution of the occupation numbers of each mode.

We should also add that the NESS is a Gaussian state[8] and we can express any higher-order correlation thanks to the Wick's theorem [41].

[7] The words "non equilibrium" are there to emphasise that the steady state does not corresponds to an equilibrium situation

[8] A Gaussian state is essentially a state that can be written as

$$\rho_G = \frac{e^{-\beta H}}{\mathrm{Tr}[e^{-\beta H}]}, \tag{3.38}$$

for $\beta > 0$ and a positive definite Hamiltonian [40].

3.4 Summary of the chapter

In this chapter, we introduced a new formalism that acts like a second quantization at the density operator space level. This formalism gives exact analytical solution for master equations of the Lindblad form for quadratic Hamiltonians and linear couplings to the bath. This method shows how to calculate the eigenvalues of the Liouvillian. Instead of diagonalizing a matrix of n^4 elements, where n is the number of bosonic modes, this method diagonalizes a n size matrix and solve the Lyapunov equation for another n size matrix. Once we have obtained these two expressions, the method gives a formula for the normal master mode, an equivalent of the normal modes for the Hamiltonian, that allows us to calculate the steady-state. In addition, the solution of the Lyapunov equation is the 2-point correlation matrix.

In the next part, we will apply this method to a quite general problem of open quantum transport. To ensure clarity, we will address a simple case in Chapter 4 and show most of the calculation steps to illustrate how third quantization operates.

Part II

Application in quantum transport

The second part of this master's thesis is dedicated to the study of quantum transport. We study here simple cases: only one ore two bosonic modes although the extension of the formalism for n bosonic modes could be done. We present the application of the third quantization method together with the results that we were able to draw from it. In the following chapters, we will study the transport of bosons between two baths, passing through a junction. In chapter 4, the junction will be constituted of one single site or mode, namely the *single-site junction* and in chapter 5 it will be constituted of two sites, the *two-sites junction*. The study of quantum transport for this kind of system is the first step towards the study of quantum thermal engines, which is a field of quantum thermodynamics.

Chapter 4

Single-site junction

In this chapter, we will study a simple but non trivial system consisting of a bosonic harmonic oscillator of frequency ω coupled with two bosonic baths of different temperatures. A thermal bosonic bath is modeled here by a collection of different bosonic harmonics oscillators. The interest of this first system is to show how the third quantization should be used to find an analytical solution for the time evolution of the system only. Thus, we consider simplified interactions between the baths and studied system. We assume the baths interact only in a unique manner: the system absorbs particles from the left bath and emitsto the right bath. The absorption and emission rates are chosen constant. A representation of the situation is given in figure 4.1.

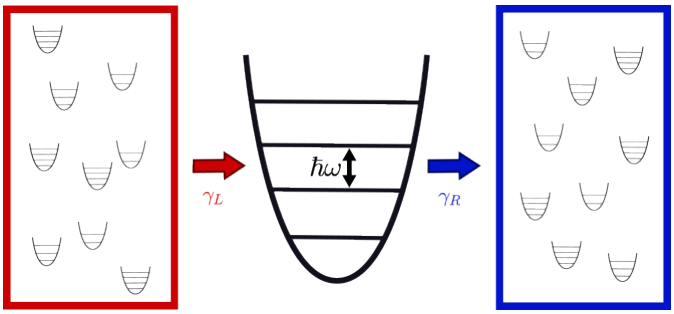

Figure 4.1: Sketch of the bosonic harmonic oscillator coupled with two bosonic baths of different temperatures. The red and blue arrow represent the influence of the left and right baths respectively. For this system, we consider that the left bath only emits particles in the system with rate γ_L while the right bath absorbs from the system with rate γ_R.

The Hamiltonian of the system of study is

$$H_S = \omega a^\dagger a, \tag{4.1}$$

where $a^\dagger$ and a are respectively the creation and annihilation operators of a bosonic mode of frequency ω. The Hamiltonian of each bath is

$$H_\alpha = \sum_k \omega_{k,\alpha} b^\dagger_{k,\alpha} b_{k,\alpha}, \tag{4.2}$$

where $b^\dagger_{k,\alpha}$ and $b_{k,\alpha}$ are respectively the creation and annihilation operators of a bosonic mode of frequency $\omega_{k,\alpha}$, for $\alpha = L, R$. Subscript L denote the left bath and subscript R the right one[1]. It remains the interaction Hamiltonian, given by

$$H_{\text{int}} = \sum_k v_{k,L} a^\dagger b_{k,L} + v_{k,R} a^\dagger b_{k,R} + h.c., \tag{4.3}$$

[1]We shall point out that this notation is non related to the left and right multiplication defined in the previous chapter.

where $h.c.$ stand for Hermitian conjugate and $v_{k,L}, v_{k,R} \in \mathbb{C}$.

The time evolution of the state of the system is described by the following master equation of Lindblad form

$$\dot{\rho}(t) = \mathcal{L}[\rho(t)] = -i[H_S, \rho(t)] + \gamma_L \mathcal{D}_{a^\dagger}[\rho(t)] + \gamma_R \mathcal{D}_a[\rho(t)], \tag{4.4}$$

where $\rho(t)$ is the density matrix of the system, $\gamma_L, \gamma_R > 0$ are the absorption and emission rates and $\mathcal{D}_x[\rho(t)]$ is the dissipation superoperator defined by

$$\mathcal{D}_x[\rho(t)] = x\rho(t)x^\dagger - \frac{1}{2}\{x^\dagger x, \rho(t)\}.$$

The complete derivation of the master equation from the Liouville-Von Neumann equation is done in details in Appendix B.1.

Study of the differential equation

As a first approach, one could be interested in displaying the coupled differential equation system. This would allow to see explicitly which elements of the density matrix are coupled together. In order to do so, we have to project equation (4.4) on the Fock state $\langle n| \cdot |m\rangle$. Defining $\rho_{nm} = \langle n| \rho |m\rangle$ and $\dot{\rho}_{nm} = \langle n| \dot{\rho} |m\rangle$, with $n, m \in \mathbb{N}$, we have

$$\begin{aligned}\dot{\rho}_{nm} = &-i\omega n\rho_{nm} + i\omega m\rho_{nm} \\ &+ \gamma_L[\sqrt{nm}\rho_{n-1m-1} - \frac{1}{2}(n+1)\rho_{nm} - \frac{1}{2}(m+1)\rho_{nm}] \\ &+ \gamma_R[\sqrt{(n+1)(m+1)}\rho_{n+1m+1} - \frac{1}{2}n\rho_{nm} - \frac{1}{2}m\rho_{nm}].\end{aligned} \tag{4.5}$$

Taking $n = m$, we obtain the differential equation that describes any diagonal element ρ_{nn} (for $n \geq 1$) of the density matrix. Thus, we see that the time evolution of a diagonal element only depends on other diagonal elements and does not depend on any non-diagonal element. We can then decompose the Hilbert space of density operators $\rho(\mathcal{H})$ into two distinct subspaces: one containing the diagonal elements and the other containing the non diagonal ones.

This remarkable structure of the density matrix puts us on the path to a $\mathbb{U}(1)$ symmetry, that will be explored later in Sec. 4.2.

The study of this system is going to be done from several points of view. We first use the third quantization method to obtain the eigenvalues and eigenstates associated of the Liouvillian as well as the steady state.The latter allows us to find an analytical solution to the master equation. Then, we will study the spectrum of the Liouvillian and compare the third quantization method with a numerical method. Finally, we will study the quantum transport between the two baths via the particle current.

4.1 Application of the third quantization

Using the methods of the third quantization, we define successively

$$\begin{gathered}\mathbf{H} = \omega, \quad \mathbf{K} = 0, \\ l_1 = k_2 = 0, \quad l_2 = \sqrt{\frac{\gamma_R}{2}}, \quad k_1 = \sqrt{\frac{\gamma_L}{2}}, \\ \mathbf{M} = \frac{\gamma_R}{2}, \quad \mathbf{N} = \frac{\gamma_L}{2}, \quad \mathbf{L} = 0.\end{gathered}$$

Following (3.24) and (3.25), we find

$$\mathbf{X} = \frac{1}{2}\begin{pmatrix} i\omega + \frac{\gamma_R-\gamma_L}{2} & 0 \\ 0 & -i\omega + \frac{\gamma_R-\gamma_L}{2} \end{pmatrix}, \tag{4.6}$$

$$\mathbf{Y} = \begin{pmatrix} 0 & \gamma_L/2 \\ \gamma_L/2 & 0 \end{pmatrix}. \tag{4.7}$$

The diagonal form of $\mathbf{X}$ gives immediately the rapidities of our system:

$$\boxed{\beta_1, \beta_2 = \frac{\gamma_R - \gamma_L}{4} \pm \frac{i\omega}{2}.} \tag{4.8}$$

Thus, we just have to solve the Lyapunov equation (3.28) to find the NMM. Its solution is

$$\mathbf{Z} = \begin{pmatrix} 0 & \frac{\gamma_L}{\gamma_R-\gamma_L} \\ \frac{\gamma_L}{\gamma_R-\gamma_L} & 0 \end{pmatrix}. \tag{4.9}$$

Then, using equations (3.29), we can express the NMM

$$\begin{pmatrix} \xi_1 \\ \\ \xi_2 \end{pmatrix} = \begin{pmatrix} a_L \frac{\gamma_R}{\gamma_R-\gamma_L} - a_R \frac{\gamma_L}{\gamma_R-\gamma_L} \\ \\ a_R^\dagger \frac{\gamma_R}{\gamma_R-\gamma_L} - a_L^\dagger \frac{\gamma_L}{\gamma_R-\gamma_L} \end{pmatrix}, \tag{4.10}$$

$$\begin{pmatrix} \xi_1' \\ \xi_2' \end{pmatrix} = \begin{pmatrix} a_L^\dagger - a_R^\dagger \\ a_R - a_L \end{pmatrix}. \tag{4.11}$$

Once we calculated the NMM, the steady state can be found in a few steps via the property (3.33).

4.1.1 Derivation of the steady state

Before calculating the steady state, we need to do an ansatz that makes the calculation realisable. We will see in Sec. 4.2 that the existence of a symmetry completely justifies this ansatz.

As said in Sec. 3.3, the steady state of the system is guaranteed to be a Gaussian thermal state. Furthermore, there is no term in $a \cdot a$ nor in $a^\dagger \cdot a^\dagger$ in the Liouvillian. We can then make the ansatz that the steady state is diagonal in the Fock basis. In other words, we suppose

$$\rho_{NESS} = R \sum_n C_n \left|n\right\rangle \left\langle n\right|, \tag{4.12}$$

or, for the vectorized density operator,

$$\left|\rho_{NESS}\right\rangle = R \sum_n C_n \left|n\right\rangle \left|n\right\rangle, \tag{4.13}$$

where R is a constant that ensure the trace to be one.

Using equation (3.33) for ξ_1, we can now calculate the steady state. We have

$$\xi_1 \left|\rho_{NESS}\right\rangle = 0. \tag{4.14}$$

For now on, we use the matrix representation of the density operator as it is more intuitive, even if they are both equivalent in a mathematical sense.

$$\begin{aligned} &\Leftrightarrow \sum_{n=0}^{\infty} \frac{\gamma_R C_n}{\gamma_R - \gamma_L} a_L \left|n\right\rangle \left\langle n\right| - \frac{\gamma_L C_n}{\gamma_R - \gamma_L} a_R \left|n\right\rangle \left\langle n\right| = 0 \\ &\Leftrightarrow \sum_{n=0}^{\infty} \frac{C_n}{\gamma_R - \gamma_L} (\gamma_R a \left|n\right\rangle \left\langle n\right| - \gamma_L \left|n\right\rangle \left\langle n\right| a) = 0. \end{aligned}$$

Separating the sum and re-indexing the first one while keeping in mind that $a|0\rangle = 0$, we have

$$\sum_{n=0}^{\infty} C_{n+1}\gamma_R\sqrt{n+1}\,|n\rangle\langle n+1| - C_n\gamma_L\sqrt{n+1}\,|n\rangle\langle n+1| = 0.$$

The aim is to find a recurrence relation over the coefficients C_n. Thus, we have to impose that the factor in front of $|n\rangle\langle n-1|$ is equal to 0. One finds

$$\begin{aligned}&\gamma_R C_{n+1}\sqrt{n+1} - \gamma_L C_n\sqrt{n+1} = 0\\ &\Leftrightarrow C_{n+1} = \frac{\gamma_L}{\gamma_R}C_n.\end{aligned}$$

This recurrence relation implies that

$$C_0 = C, \tag{4.15}$$

$$C_n = C\left(\frac{\gamma_L}{\gamma_R}\right)^n, \tag{4.16}$$

for $n \in \mathbb{N}\backslash\{0\}$ and C a constant that still needs to be determined. To do so, we use the definition of the density operator, it must have a trace of one. We have

$$\mathrm{Tr}[\rho_{NESS}] = 1 \tag{4.17}$$

$$\Leftrightarrow \sum_n \langle n|\, R \sum_{n'} C\left(\frac{\gamma_L}{\gamma_R}\right)^{n'} |n'\rangle\langle n'|n\rangle = 1 \tag{4.18}$$

$$\Leftrightarrow RC\sum_n \langle n| \sum_{n'}\left(\frac{\gamma_L}{\gamma_R}\right)^{n'} |n'\rangle\langle n'|n\rangle = 1 \tag{4.19}$$

$$\Leftrightarrow \sum_n \left(\frac{\gamma_L}{\gamma_R}\right)^n \langle n|n\rangle = \frac{1}{RC} \tag{4.20}$$

$$\Leftrightarrow \sum_n \left(\frac{\gamma_L}{\gamma_R}\right)^n = \frac{1}{RC}. \tag{4.21}$$

The left hand side of the last equation is a geometric series where the ratio between two successive terms is $\frac{\gamma_L}{\gamma_R}$. The series is diverging if $\gamma_L \geq \gamma_R$ and converging if $\gamma_L < \gamma_R$, the limit being $\frac{\gamma_R}{\gamma_R - \gamma_L}$. Thus, we find an expression for the steady state,

$$\boxed{|\rho_{NESS}\rangle = \begin{cases}\mathbb{1} & \text{if } \gamma_L \geq \gamma_R,\\ \frac{\gamma_R-\gamma_L}{\gamma_R}\sum_n \left(\frac{\gamma_L}{\gamma_R}\right)^n |n\rangle\,|n\rangle & \text{if } \gamma_L < \gamma_R.\end{cases}} \tag{4.22}$$

When $\gamma_L \geq \gamma_R$, the system cannot be normalizable. The result is a non physical state. Physically, we add more excitation into the system than we remove, which leads to an accumulation of energy in the system. As we consider a bosonic harmonic oscillator, it can absorb excitation indefinitely. Thus, the "steady state", should correspond to the eigenvalue 0 of the Liouvillian is a superposition of all the possible states in the Fock basis.

Having an analytical expression for the steady state will allow us to find an expression for the state of the system at any time, i.e., a solution of the Lindblad master equation (4.4).

4.1.2 Solution of the master equation

We are now interested to find an expression of the state of the system at any time. We will first express it in the basis of the NMM that we just found in equation (4.10) and then in the Fock basis[2].

[2]The reader not interested by the mathematical development should only look at the boxed equation and skip the rest of this subsection.

For the state in the NMM basis, we follow equation (2.45). The state of the system $|\rho(t)\rangle$ for a time t is given by

$$\boxed{|\rho(t)\rangle = \sum_{m_1,m_2} e^{-(m_1+m_2)\frac{\gamma_R-\gamma_L}{2}t} e^{-i\omega(m_1-m_2)t} c_{m_1,m_2} \frac{(\xi_1')^{m_1}(\xi_2')^{m_2}}{\sqrt{m_1!}\sqrt{m_2!}} |\rho_{NESS}\rangle} \tag{4.23}$$

with

$$c_{m_1,m_2} = (1|\frac{\xi_1^{m_1}\xi_2^{m_2}}{\sqrt{m_1!}\sqrt{m_2!}}|\rho(0)\rangle\,.$$

We now want to switch to the Fock basis. In this basis, any state $|\rho(t)\rangle$ is written as $|\rho(t)\rangle = \sum_{n,n'} c_{n,n'} |n\rangle\langle n'|$. As the steady state is diagonal in the Fock basis, we first have to compute the power of ξ', then apply ξ_2' to $|n\rangle\langle n|$ and ξ_1' to the result.

Computing explicitly the powers of ξ_i' in terms of a_L, a_R, we find

$$(\xi_1')^{m_1} = \left(a_L^\dagger - a_R^\dagger\right)^{m_1} = \sum_{k=0}^{m_1} \binom{m_1}{k} a_L^{\dagger m_1-k}(-a_R^{\dagger k}), \tag{4.24}$$

$$(\xi_2')^{m_2} = (a_R - a_L)^{m_2} = \sum_{k=0}^{m_2} \binom{m_2}{k} a_R^k(-a_L)^{m_2-k}. \tag{4.25}$$

For ξ_2', we have

$$(\xi_2')^{m_2}|n\rangle\langle n| = \sum_{\substack{k=0\\k>m_2-n}}^{m_2} \binom{m_2}{k}(-1)^{m_2-k}\sqrt{\frac{(n+k)!}{(n-m_2+k)!}}\,|n-m_2+k\rangle\langle n+k|\,, \tag{4.26}$$

where the condition $k > m_2 - k$ comes from the $|n-m_2+k\rangle$, as $a|0\rangle = 0$. For ξ_1', that must be applied to $|n\rangle\langle n'|$, we find

$$(\xi_1')_1^m|n\rangle\langle n'| = \sum_{\substack{k=0\\k<n'}}^{m_1} \binom{m_1}{k}(-1)^k\sqrt{\frac{(n+m_1-k)!}{n!}\frac{(n')!}{(n'-k)!}}\,|n+m_1-k\rangle\langle n'-k|\,, \tag{4.27}$$

where we have the condition $k < n'$ for the same reason. Combining the two previous equations,

$$\begin{aligned}(\xi_1')^{m_1}(\xi_2')^{m_2}|n\rangle\langle n| = \sum_{\substack{k=0\\k>m_2-n}}^{m_2}\sum_{\substack{k'=0\\\times k'<n+k}}^{m_1} \binom{m_1}{k'}\binom{m_2}{k}(-1)^{m_2-k+k'}\frac{(k+n)!}{(k-m_2+n)!}\\ \sqrt{\frac{(k-k'+m_1-m_2+n)!}{(n+k-k')!}}|n-m_2+m_1-k'+k\rangle\langle n+k-k'|\,.\end{aligned} \tag{4.28}$$

Gathering all our equations, we can display the solution of the master equation as a function of the time in the Fock basis:

$$\begin{aligned}\boxed{|\rho(t)\rangle = \sum_{m_1,m_2}\sum_{n}\sum_{k,k'} e^{-(m_1+m_2)\frac{\gamma_R-\gamma_L}{2}t}e^{-i\omega(m_1-m_2)t}c_{m_1,m_2}\binom{m_1}{k'}\binom{m_2}{k}}\\ \times\frac{(k+n)!}{(k-m_2+n)!}\sqrt{\frac{(k-k'+m_1-m_2+n)!}{m_1!m_2!(k-k'+n)!}}\\ \times(-1)^{m_2-k+k'}\left|n-m_2+m_1-k'+k\right\rangle\left|n+k-k'\right\rangle.\end{aligned} \tag{4.29}$$

In the limit for $t(\gamma_R-\gamma_L) \gg 1$, the first exponential decreases to 0 except for $m_1 = m_2 = 0$. We have

$$\lim_{t\to+\infty} e^{-(m_1+m_2)\frac{\gamma_R-\gamma_L}{2}t} \sim \delta_{m_1,0}\delta_{m_2,0}. \tag{4.30}$$

Therefore in this limit, we obtain the steady state, as expected. It is associated with a zero eigenvalue, as $m_1 = 0 = m_2$.

4.2 Symmetries of the system

The studied system displays a $\mathbb{U}(1)$ weak discrete symmetry. A weak symmetry is found when a given unitary transformation leaves the full Lindbladian invariant (i.e. the transformation commutes with the Lindbladian) without necessarily keeping the jump operators invariant. Furthermore, the symmetry ensures that the matrix form of the Liouvillian has a block-diagonal structure in the appropriate basis, the basis of the eigenvectors of the generator [42]. The size of the blocks is given by the algebraic multiplicity of the eigenvalues of the generator of the transformation [31]. In this section we will first show the symmetry by studying the commutator of the Liouvillian and an arbitrary unitary superoperator. Secondly, we will demonstrate that given this symmetry, the steady state is diagonal in the Fock basis.

The generator of the symmetry is unitary, we can write it as $\mathcal{U} = U \cdot U^\dagger$, with $U = e^{-ia^\dagger a}$. Showing that the system admits a $\mathbb{U}(1)$ weak symmetry is equivalent to show that $[\mathcal{L},\mathcal{U}] = 0$. We recall that $\mathcal{U}$, as $\mathcal{L}$, is a superoperator acting on $\rho(\mathcal{H})$. Let us compare the two following expressions

$$\mathcal{L}\mathcal{U}[\rho] = \mathcal{L}[\rho'] \tag{4.31}$$

with $\rho' = e^{-i\phi a^\dagger a}\rho e^{i\phi a^\dagger a}$ and

$$\mathcal{U}\mathcal{L}[\rho] = -iU[H,\rho]U^\dagger + \gamma_L U\mathcal{D}_{a^\dagger}[\rho]U^\dagger + \gamma_R U\mathcal{D}_{[}\rho]U^\dagger. \tag{4.32}$$

At some point of the derivation, we will have to commute a and $a^\dagger$ with U and $U^\dagger$. Let us show once and for all how they commute. Expanding the exponential, we have

$$aU = a\sum_k \frac{(-i\phi)^k}{k!}(a^\dagger a)^k. \tag{4.33}$$

We rearrange $a(a^\dagger a)^k$ in $(aa^\dagger)^k a$ and using the CCR, we find

$$aU = e^{-i\phi}Ua. \tag{4.34}$$

Similarly, we have the following expressions

$$Ua^\dagger = e^{-i\phi}a^\dagger U, \tag{4.35}$$

$$aa^\dagger U = Uaa^\dagger \tag{4.36}$$

and trivially,

$$a^\dagger aU = Ua^\dagger a. \tag{4.37}$$

We now compare term by term the expressions (4.31) and (4.32). For the first one, we have

$$a^\dagger aU\rho U^\dagger - U\rho U^\dagger a^\dagger a = a^\dagger e^{-i\phi(a^\dagger a+1)}a\rho U^\dagger - U\rho a^\dagger e^{i\phi(a^\dagger a+1)}a \tag{4.38}$$

and

$$Ua^\dagger a\rho U^\dagger - U\rho a^\dagger aU^\dagger = a^\dagger e^{-i\phi(a^\dagger a+1)}a\rho U^\dagger - U\rho a^\dagger e^{i\phi(a^\dagger a+1)}a. \tag{4.39}$$

The second term of (4.31),

$$a^\dagger U\rho U^\dagger a - \frac{1}{2}aa^\dagger U\rho U^\dagger - \frac{1}{2}U\rho U^\dagger aa^\dagger = Ua^\dagger\rho aU^\dagger - \frac{1}{2}Uaa^\dagger\rho U^\dagger\frac{1}{2}U\rho U^\dagger aa^\dagger, \tag{4.40}$$

is equal to the second term of (4.32). For the thirds ones, we also have identical terms. Thus, the $\mathbb{U}(1)$ symmetry is displayed.

We notice here that the eigenvectors of the generator is the Fock basis and algebraic multiplicities of the associated eigenvalues are 1. This implies that the matrix form of the Liouvillian

is diagonal, which explains the particular structure of the density matrix showed in the beginning of this chapter.

Now, we want to use this symmetry to justify the ansatz in equation (4.12), i.e., demonstrate that if the steady state is unique, it must be diagonal in the Fock basis. Here the uniqueness of the steady state is an assumption, as all our systems will admit a unique steady state. We recall that by definition, from equation (2.43), the steady state is the eigenvector of $\mathcal{L}$ associated with the eigenvalue 0: $\mathcal{L}[\rho_{\text{NESS}}] = 0$. Moreover, we have

$$\mathcal{U}\mathcal{L}[\rho_{\text{NESS}}] = \mathcal{U}[0] = 0. \tag{4.41}$$

As $\mathcal{U}$ and $\mathcal{L}$ commute, we also have

$$\mathcal{L}\mathcal{U}[\rho_{\text{NESS}}] = 0. \tag{4.42}$$

So, $\mathcal{U}[\rho_{\text{NESS}}]$ is also the eigenvector associated with the eigenvalue 0, which is the definition of the steady state. Nevertheless, the steady state is unique, so we must have

$$\mathcal{U}[\rho_{\text{NESS}}] = e^{-i\phi a^\dagger a}\rho_{\text{NESS}}e^{i\phi a^\dagger a} = \rho_{\text{NESS}}. \tag{4.43}$$

Projecting this equation on $\langle n| \cdot |m\rangle$, with $n, m \in \mathbb{N}$, we obtain

$$\begin{aligned} &\langle n|\, e^{-i\phi a^\dagger a}\rho_{\text{NESS}}e^{i\phi a^\dagger a}\,|m\rangle = \langle n|\,\rho_{\text{NESS}}\,|m\rangle \\ \Leftrightarrow\, &\langle n|\, e^{-i\phi n}\rho_{\text{NESS}}e^{i\phi m}\,|m\rangle = \langle n|\,\rho_{\text{NESS}}\,|m\rangle\,. \end{aligned}$$

The last equation being true if and only if $e^{-i\phi n}e^{i\phi m} = 1$ which implies $n = m$.

We just demonstrated that when a $\mathbb{U}(1)$symmetry occurs and if the steady state is unique, it must be diagonal in the Fock Basis.

4.3 Spectrum of the Liouvillian

We will now study the spectrum of the Liouvillian. We mentioned earlier the existence of numerical methods. Thus, as the system is quite simple, it is relevant to compare one of these methods with our analytical results obtained via the third quantization. Below, we detail the two approaches and compare the results.

4.3.1 Analytical method

The computation of the analytical eigenvalues is done using formula (3.34). Essentially, the eigenvalues are given by all the possible linear combinations of β_1, β_2 where the coefficients are integers. As there is an infinite number of eigenvalues, we have to fix a limit for the coefficients of the linear combinations. We introduce the integer M such that $m_1, m_2 \leq M$. For the comparison between the two methods, we choose $M = 10$.

4.3.2 Numerical method

The numerical method is based on the direct diagonalization of the matrix representation of the Liouvillian. This method is here quite simple as we demonstrated earlier than L is already diagonal due to the $\mathbb{U}(1)$ symmetry.

We chose here to start from the definition (4.4) of the Liouvillian for the system of study and use the following matrix representation for the creation and annihilation operators, a and $a^\dagger$. In the Fock basis,

$$a_{ij} = \sqrt{i}\delta_{i,j-1} \tag{4.44}$$

and $a^\dagger_{i,j} = a_{j,i}$. We obtain the matrix representation of $\mathcal{L}$ using the Choi-Jamiołkowski isomorphism, as described in Sec. 2.5. We shall note that a cutoff must be defined in order to deal with non-infinite size matrices. Formally, we have to choose N_{cutoff} such that $n, m \leq N_{\text{cutoff}}$. This cutoff value should influence the accuracy of the results.

4.3.3 Results

In figure 4.2, we compare the eigenvalues obtained via the third quantization, and the eigenvalues of L for different values of N_{cutoff}. The numerical computation is done for four different cutoff values, one for each plot: 10 for panel (a), 30 for panel (b), 50 for panel (c) and 70 for panel (d). In each plot, ϵ, γ and ω are respectively equal to 1.3, 1 and 1. Analytical eigenvalues are represented in red while numerical are represented in blue. The real part of the eigenvalues are represented in the horizontal axis while the imaginary part is represented in the vertical axis.

We can see that for each panel, there is a blue and a red dot in $(0, 0)$. This corresponds to the eigenvalue 0 associated with the steady state. Increasing the cutoff, we see the blue dot are lining up to the red ones. This lign-up starts on the right, for eigenvalues of greater real part. As expected, increasing N_{cutoff} will give numerical eigenvalues closer to the (exact) analytical eigenvalues.

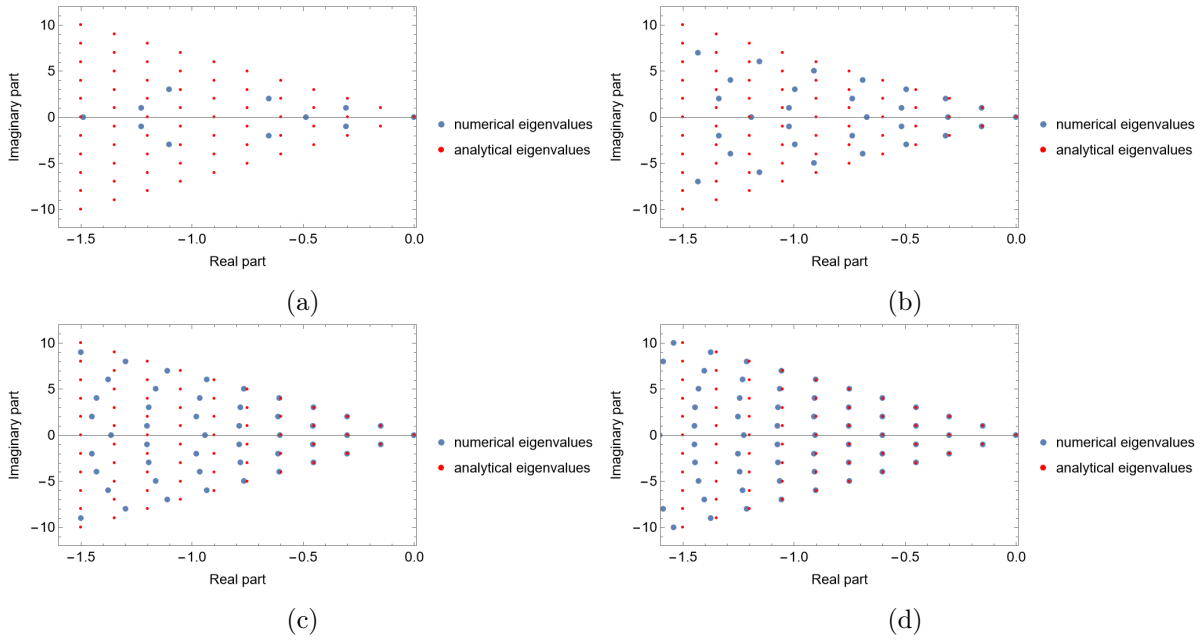

Figure 4.2: Eigenvalues of the Liouvillian using two different methods. The first one is numerical, via the matrix representation of the Liouvillian, L, which is already diagonal due to the $\mathbb{U}(1)$ symmetry. The numerical eigenvalues are represented by the blue dots in the figures. For the second method, we use (3.34) for $m_1, m_2 \leq 10$. The eigenvalues obtained via third quantization are represented in red. Moreover, we plotted the eigenvalues for 4 different values of Ncutoff: 10 for panel (a), 30 for panel (b), 50 for panel (c) and 70 for panel (d). In each plot, ϵ, γ and ω are respectively equal to 1.3, 1 and 1. The real part of the eigenvalues are represented in the horizontal axis while the imaginary part is represented in the vertical axis.

4.4 Particle current

In this section, we study the particle current which characterizes the heat and energy diffusion trough the baths and sites. Its definition is given by

$$J \equiv \frac{d(a^\dagger a)}{dt}. \tag{4.45}$$

Formally, it is the variation of particles passing throughout the site. We can also define its mean value,

$$\langle J \rangle \equiv \frac{d\langle a^\dagger a \rangle}{dt}. \tag{4.46}$$

For the steady state, the theory of the third quantization gives directly the quantity $\langle a_i a_j \rangle$ for $i, j = 1, 2$ via the $\mathbf{Z}$ matrix. We have

$$\langle a_i a_j \rangle = (1|a_i a_j \, |\rho_{NESS}\rangle = Z_{ij}. \tag{4.47}$$

In this particular system, we find

$$\langle a^\dagger a \rangle = \frac{\gamma_L}{\gamma_R - \gamma_L}. \tag{4.48}$$

As the steady state corresponds to long time dynamics of our system, we can infer that this limit for $t(\gamma_R - \gamma_L) \gg 1$ should appear during the derivation.

We derive the expression of $J(t)$ using the master equation in Heisenberg picture. For any operator A, its time evolution is given by

$$\dot{A} = i[H_S, A] + \sum_i \gamma_i \left(L_i^\dagger A L_i - \frac{1}{2} \left\{ L_i^\dagger L_i, A \right\} \right). \tag{4.49}$$

For its mean counterpart, we use the Heisenberg picture to "project" $a^\dagger a$ into the master equation: $\frac{d\langle a^\dagger a \rangle}{dt} = \mathrm{Tr}[\dot{\rho}(t) a^\dagger a]$.

Deriving equation (4.49) for $A = a^\dagger a$, one finds

$$J(t) = \frac{d\left(a^\dagger a\right)}{dt} = i[H_S, a^\dagger a] + \gamma_L [a a^\dagger a a^\dagger - \frac{1}{2}\{a a^\dagger, a^\dagger a\}] + \gamma_R [a^\dagger a^\dagger a a - \frac{1}{2}\{a^\dagger a, a^\dagger a\}] \tag{4.50}$$

$$= \gamma_L a a^\dagger - \gamma_R a^\dagger a \tag{4.51}$$

$$= -(\gamma_R - \gamma_L) a^\dagger a + \gamma_L. \tag{4.52}$$

Solving the differential equation,

$$(a^\dagger a)(t) = C e^{-(\gamma_R - \gamma_L)t} + \frac{\gamma_L}{\gamma_R - \gamma_L} \tag{4.53}$$

with $C \in \mathbb{C}$. It is relevant to rewrite this expression in terms of the initial conditions to get rid of the C constant,

$$(a^\dagger a)(t) = e^{-(\gamma_R - \gamma_L)t} \left((a^\dagger a)(0) - \frac{\gamma_L}{\gamma_R - \gamma_L} \right) + \frac{\gamma_L}{\gamma_R - \gamma_L}. \tag{4.54}$$

As predicted, the limit for $t(\gamma_R - \gamma_L) \gg 1$ is the one expected even for the operator quantity. In addition, we can highlight the divergence when $\gamma_L \geq \gamma_R$. And finally,

$$\boxed{J(t) = e^{-(\gamma_R - \gamma_L)t} [\gamma_L - a^\dagger a(0)(\gamma_R - \gamma_L)]}. \tag{4.55}$$

We can see that this operator is a scalar, which means that its mean value should be the same expression. Indeed, we find

$$\begin{aligned} \mathrm{Tr}[\dot{\rho} a^\dagger a] = &- i\mathrm{Tr}[H_S \rho a^\dagger a - \rho H_S a^\dagger a] \\ &+ \gamma_L (\mathrm{Tr}[a^\dagger \rho a a^\dagger a] - \frac{1}{2}\mathrm{Tr}[a a^\dagger \rho a^\dagger a] - \frac{1}{2}\mathrm{Tr}[\rho a a^\dagger a^\dagger a]) \\ &+ \gamma_R (\mathrm{Tr}[a \rho a^\dagger a^\dagger a] - \frac{1}{2}\mathrm{Tr}[a^\dagger a \rho a^\dagger a] - \frac{1}{2}\mathrm{Tr}[\rho a^\dagger a a^\dagger a]), \end{aligned} \tag{4.56}$$

which leads to the same differential equation.

For the purpose of plotting, we define two new variables, $\gamma = \gamma_L$ and $\epsilon = \gamma_R / \gamma_L$ such that $\gamma_R = \gamma\epsilon$. The particle current reads now

$$J(t) = e^{-(\epsilon - 1)\gamma t} [1 - a^\dagger a(0)(\epsilon - 1)]\gamma. \tag{4.57}$$

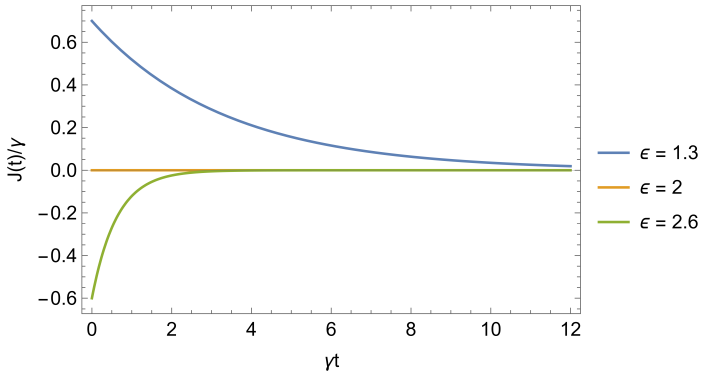

Figure 4.3: Normalized particle current J/γ as a function of γt for $\gamma = 1$, $(a^\dagger a)(0) = 1$ for three different values of $\epsilon = \gamma_R/\gamma_L$ as obtained in equation (4.57). The blue curve shows the behavior for $\epsilon = 1.3$, the yellow one for $\epsilon = 2$ and the green one for $\epsilon = 2.6$.

The particle current $J(t)$ is plotted in Fig. 4.3 for $\gamma = 1$ and $a^\dagger a(0) = 1$ for different values of ϵ. We can see that three different behavior can be outlined, depending on the value of ϵ. For $1 < \epsilon < 2$, the blue curve, the particle current is a positive decreasing function. For $\epsilon = 2$, in other words when the rate of incoming particles is exactly 2 times smaller than the rate of outgoing particles, the yellow curve, the function is null for any time. And if $\epsilon > 2$, the green curve, it is a negative increasing function. We can see that for the three cases, the limit for $t\gamma \gg 1$ is 0. As the system tends towards its stationary state for sufficiently long periods of time, the number of particles within it remains constant, as dictated by the definition of the steady state.

It is relevant to say that for $\gamma_L = \gamma_R$, the particle current is γ_L, a constant. This is coherent with the diverging steady state in this case as excitation are brought constantly into the system. The case $\gamma_L > \gamma_R$ gives a exponential growth: the system gain more and more particles and this gain is exponential.

4.5 Numerical comparison

It is interesting to compare the particle current obtained from the third quantization method and the one we can find using a "brute force" numerical method. Here we will solve numerically the system of equations (4.5). As in Subsec 4.3.2, we have to define a cutoff in order to deal with non-infinite size matrices. We will see that the choice of the cutoff will be relevant regarding the dynamics of the system.

As said at the beginning of this chapter, the dynamics of the populations only depends on the populations. It is straightforward to show that the particle current, $\mathrm{Tr}[\rho a^\dagger a]$, only depends on the populations too. This reduce efficiently the computation time.

The results of the numerical computations are shown in Figure 4.4. We plot the normalized particle current for four values of the cutoff value $(5, 10, 20$ and $50)$ and for four different values of ϵ: 1.3 in Fig (a), 2 in Fig(b), 2.6 in Fig (c) and 0.85 in Fig (d). The choice of ϵ allows to displays the four different possible behaviors for the particle current. In each plot, we choose $n_0 = 1$ and $\gamma = 1$, where n_0 is the initial number of particles in the system.

In panel (a), we see that the blue and yellow curves do not fit well, although the behavior is the right one, a decreasing exponential to zero. For the case $N_{\text{cutoff}} = 20$, we see that the gap between the green curve and the theoretical expectation is near to zero. For the last curve, the fit is perfect. In panel (b), we see that for the blue curve, the particle current is negative around $\gamma t = 0.6$, which is not consistent with the expected behavior. The same remark applies to the orange curve around $\gamma t = 1$. While the two last fit perfectly. In panel (c), every curve converge rapidly, even the blue one. This is due to the large value of ϵ which appears in exponential.

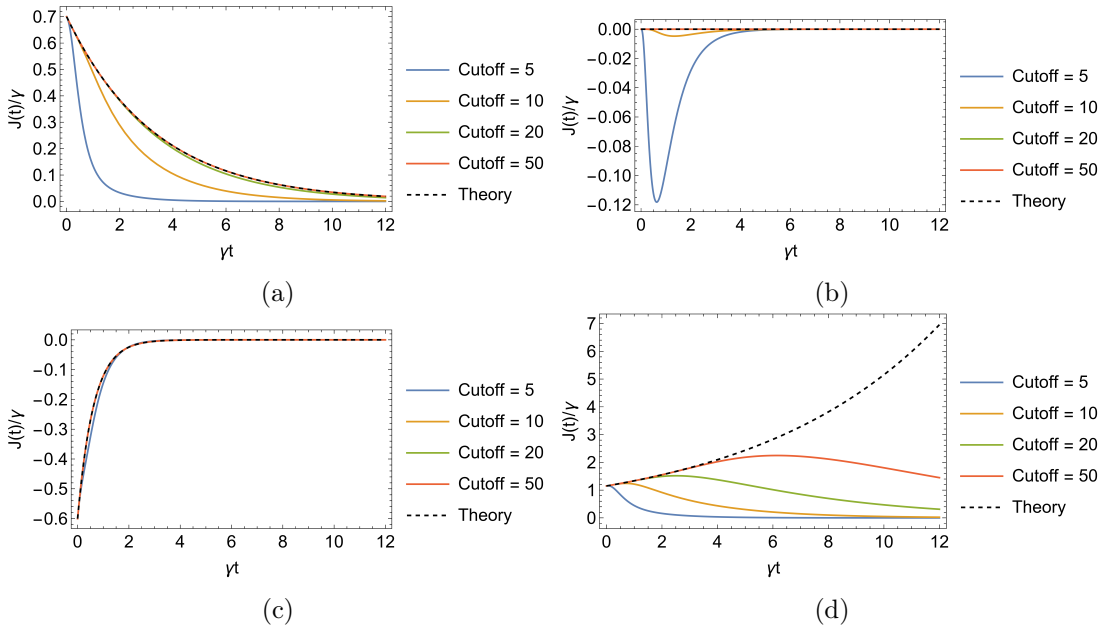

Figure 4.4: Comparison between analytical and numerical computation of the normalized particle current J/γ as a function of the normalized time for four different values of ϵ. The numerical method comes from the resolution of equation (4.5) while the analytical method is given in equation (4.57). The computations for four different cutoffs values (5 in blue, 10 in yellow, 20 in green, 50 in orange) are compared with the analytical curve (in black) obtained with the third quantization method. In panel (a), the particle current is plotted for $\epsilon = 1.3$, in panel (b) it is for $\epsilon = 2$, in panel (c) it is for $\epsilon = 2.6$ and in panel (d) it is for $\epsilon = 0.85$. In each plot, we chose $n_0 = 1$ and $\gamma = 1$.

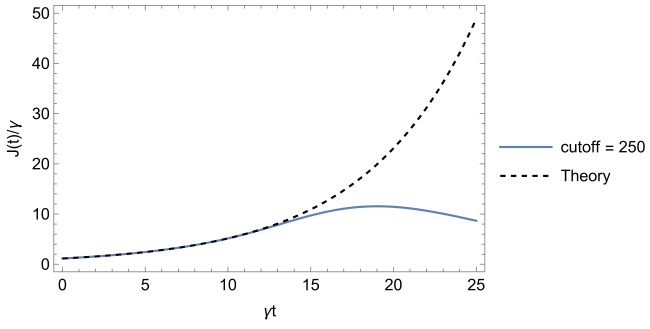

Figure 4.5: Comparison between analytical and numerical computation of the normalized particle current J/γ as a function of the normalized time for $\epsilon = 0.85$ and $N_{\text{cutoff}} = 250$ (in blue) compared to the analytical curve (in black) found with the third quantization method. The numerical method comes from the resolution of equation (4.5) while the analytical method is given in equation (4.57). We chose $n_0 = 1$ and $\gamma = 1$.

In panel (d), the limits of the numerical computation are found. For all cutoff values, we observe a decrease towards zero, whereas an exponential increase was expected. Even if we increase the cutoff to 250, see figure 4.5, we see that the numerical curve does not fit the theoretical one for long time and eventually decreases towards 0.

Overall, we find that for values of ϵ great enough, numerical curves converge for reasonable values of N_{cutoff}. For $\epsilon < 1$, the numerical curve always tends to zero which is not the behavior expected by the analytic curve and the physic behind the system.

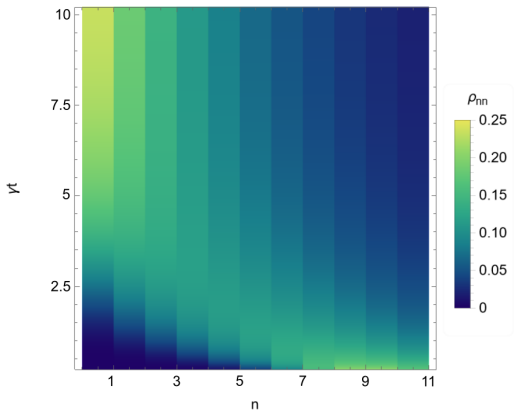

Figure 4.6: Time evolution of the numerical population ρ_{nn} in the Fock basis as a function of the index n. Parameters ϵ, γ and ω are respectively $1.3, 1$ and 1. The initial number of particles is $n_0 = 8$ and $N_{\text{cutoff}} = 11$.

In figure 4.6, we see the time evolution of the populations ρ_{nn} in the Fock basis, computed with the numerical method. Parameters ϵ, γ and ω are respectively $1.3, 1$ and 1 and $N_{\text{cutoff}} = 11$. Note that the origin of the time axis is not taken at 0 but 0.04 to remove the peak for short times.

Initially, the system is in a state with 8 particles, i.e., ρ_{nn} is equal to 0 for all n excepted for $n = 8$ where we have $\rho_{88} = 1$. Then, the system evolves with $\mathcal{L}$ and the state tends towards the steady state defined in 4.22. This corresponds to the content of the figure for $\gamma t > 7.5$: the populations with smaller index n weight more than the others. The populations with index n close to N_{cutoff} are not negligible if the cutoff value is not taken large enough. This leads to a wrong behavior for the curves of panel (b) of Fig. 4.4 for a cutoff value of 5. A balance must therefore be struck between a threshold value large enough to avoid miscalculation and one that is too large, which could lead to too much unnecessary calculation time.

4.6 Summary of the chapter

In this chapter we studied in details the single-site junction with the use of the third quantization method. We first showed how it was utilized to solve the Lindblad master equation with an analytical method. We found that the steady state was unique and had a physical meaning only if the emission rate γ_R was greater than the absorption rate γ_L. Then, we compared the eigenvalues of the Liouvillian obtained via the third quantization with a numerical method. We saw that if a great precision was required for the numerical method, a large cutoff value, i.e., the size of the matrices, was needed. Afterwards, we studied the particle current which is the time derivative of the number of particles in the site. We identified three regimes of parameters, depending on the ratio between the absorption and emission rates. We finally compared our results with a numerical method.

Chapter 5

Two-site junction

In this chapter, we will demonstrate how the third quantization method can be applied to a more complex case than in the previous chapter: a two-site junction. We will study this system using three different approaches, each corresponding to a distinct master equation that models the system's time evolution under various assumptions. Our objectives in this chapter are multifaceted. First, we will apply third quantization to solve the master equation for the first two approaches. Next, we will compare the spectrum of their respective Liouvillian, just as the particle currant, within a parameter range where both approaches are valid. We want to illustrate that one approach may be more suitable than the other depending on the chosen parameters. Finally, we will apply the third quantization to the third approach, demonstrating that although it is more complex to solve, this method provides superior results across all parameter regimes.

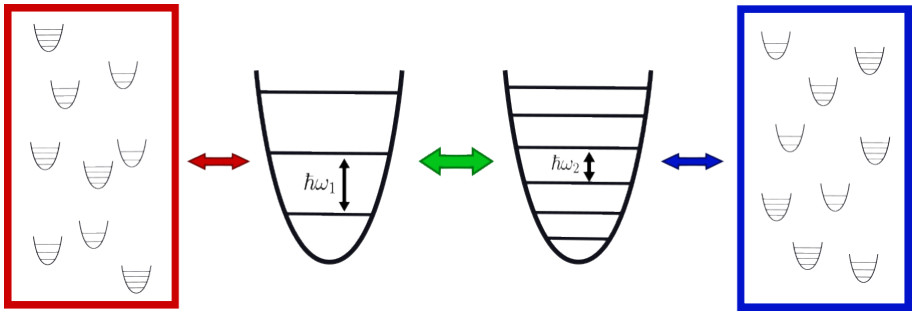

Figure 5.1: Sketch of the two-site junction. The system consists of two bosonic harmonic oscillators with different frequencies coupled with two bosonic baths of different temperature. The arrows represent the interactions governing the evolution of the system. In green, we see the coupling between the two sites. In red, we see the interactions between the left bath and the first site. Similarly, the blue double arrow represents the interactions between the second site and the right bath. To model a more realistic system, we consider that the interaction between the sites and the baths are in both ways: the system can absorb and emit particles in both sides.

The second system to be considered is sketched in figure 5.1. It consists of two harmonic oscillators, with frequencies ω_1 and ω_2, each coupled to a separate bath. The first harmonic oscillator, referred to as the *site*, couples to the left bath, while the second oscillator couples to the right bath[1]. Unlike the previous system, we consider a more general coupling with the baths where absorption and emission coexist for each side. Furthermore, we consider a coupling between the two sites. The source of this coupling is not the subject of interest here but an example of coupling mediated by an external field is proposed in [43].

The Hamiltonian of the system of study is

$$H_S = \omega_1 a_1^\dagger a_1 + \omega_2 a_2^\dagger a_2 + g(a_1^\dagger a_2 + a_2^\dagger a_1), \tag{5.1}$$

[1]Note that the left bath does not interacts with the second site, and the right bath does not interacts with the first site.

where the third term corresponds to the coupling between the two sites, with $g > 0$. The Hamiltonian of the baths is same as in equation (4.2). For the interaction Hamiltonian, we have

$$H_{\text{int}} = \sum_k v_{k,L} a_1^\dagger b_{k,L} + v_{k,R} a_2^\dagger b_{k,R} + h.c. \tag{5.2}$$

with $v_{k,L}, v_{k,R} \in \mathbb{C}$.

Local vs global & Redfield

There is two main approaches to derive a Lindblad master equation for our system. The first one, the *local approach*, consists in considering a free Hamiltonian when computing the effects of the environment on the system [44]. In our case, the coupling between the two sites is neglected when calculating the jumps operators. Thus, each jump operator only affects one site at a time. The effect of the coupling only appears in the commutator, i.e., the first term of the master equation. This approach is more phenomenological and is expected to be valid for sufficiently small coupling as it relies on a different approximation than the secular one.

The second approach is the *global approach*. This approach consists in coupling the environment with the eigenvalues of the system. Thus, we have to consider the full Hamiltonian when deriving the jump operators which can then act on both sites simultaneously rather than just one site at a time. It is convenient to diagonalize the initial Hamiltonian to identify the normal modes. As in Sec. 1.2, we have to find linear combinations of the initial modes $a_1^\dagger, a_1, a_2^\dagger, a_2$ such that there is no interaction terms in the Hamiltonian of the system. In this picture, the two sites are uncoupled and each bath is interacting with each mode. This method is supposed to be valid for sufficient coupling between the two sites. Moreover, this approach requires the secular approximation to derive a standard form of the Lindblad equation.

Finally, the *Redfield approach* is the same approach as the global one but without the secular approximation. As it is based on less assumptions that the other methods, this approach is expected to give better results than the two others.

We shall add that for the first system, the three approaches lead to the same master equation.

We will use the numerical results from [43] as a reference point for comparing our different approaches. In this paper, they describe the two-site junction where a time-dependant external field mediates the coupling between the two sites. Although their system is slightly different, it aligns with ours when we set the site frequencies to be equal, $\omega_1 = \omega_2$.

5.1 Local approach

The first approach that we study is the local one. A sketch of the situation can be found in Fig. 5.2. As we consider here a "phenomenological approach", the master equation will contain several terms. First, the unitary evolution of the system, then the jump operators. There are two jump operators per site, one for the absorption and the other for the emission. Each dissipative term acts only on one site. Thus, the time evolution of the system state is given by the following Lindblad master equation

$$\dot{\rho} = \mathcal{L}[\rho(t)] = -i[H_S, \rho(t)] + \gamma_L(\omega_1)\mathcal{D}_{a_1^\dagger}[\rho(t)] + \bar{\gamma}_L(\omega_1)\mathcal{D}_{a_1}[\rho(t)] + \gamma_R(\omega_2)\mathcal{D}_{a_2^\dagger}[\rho(t)] + \bar{\gamma}_R(\omega_2)\mathcal{D}_{a_2}[\rho(t)], \tag{5.3}$$

with the same definition for dissipation superoperators. Unlike the previous system, the absorption and emission rates are not constant in this case. They are defined by

$$\begin{aligned} \gamma_\alpha(\omega) &= \kappa(\omega) n_\alpha(\omega), \\ \bar{\gamma}_\alpha(\omega) &= \kappa(\omega)[n_\alpha(\omega) + 1] \end{aligned} \tag{5.4}$$

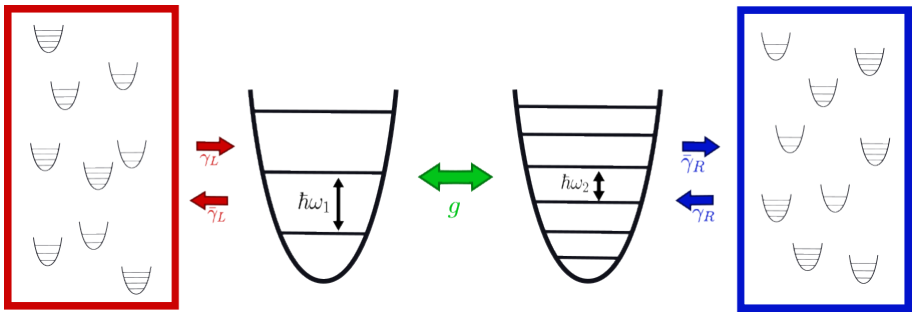

Figure 5.2: Sketch of the two-site junction. The system consists of two bosonic harmonic oscillators with different frequencies coupled with two bosonic baths of different temperature. The arrows represent the interactions governing the evolution of the system. In green, we see the coupling between the two sites, whose intensity is given by g. In red, we see the interactions between the left bath and the first site, with absorption rate γ_L and emission rate $\bar{\gamma}_L$. Similarly, the blue arrows represents the dissipation between the second site and the right bath, with absorption rate γ_R and emission rate $\bar{\gamma}_R$.

with $\kappa(\omega)$ the spectral density and $n_\alpha(\omega)$ for $\alpha = L, R$ being the Bose-Einstein distribution. We choose an ohmic spectral density, $\kappa(\omega) \propto \omega$. Taking units where $k_B = 1$, the Bose-Einstein distribution is given by

$$n_\alpha(\omega) = \frac{1}{e^{\omega/T_\alpha} - 1} \tag{5.5}$$

where T_α is the temperature of the bath α. Note that with this definition, the absorption rate is always smaller than the emission rate for a positive frequency. While we could consider negative frequencies for the left bath to encourage absorption instead of dissipation, we stick to positive frequencies in order to compare of results with [43].

A partial derivation of the local master equation can be found in Subsec. B.2.1. This approach is said to be valid for a small coupling between the two sites, i.e., $g \ll \omega$.

5.1.1 Application of the third quantization

In contrary of the single-site junction, we have two modes here, which doubles the dimension of $\mathbf{X}, \mathbf{Y}$ and $\mathbf{Z}$. However, the calculation remains quite similar. Hence, we leave the details for the Appendix, see Sec. C.1.

For $\mathbf{X}$, we obtain a 2×2 block diagonal matrix, whose diagonalization gives the rapidities

$$\boxed{\begin{aligned}
\beta_1 &= \frac{\bar{\gamma}(\omega_1,\omega_2) - \gamma(\omega_1,\omega_2)}{4} - i\frac{\omega_1+\omega_2}{4} - \frac{\sqrt{\lambda_+(\omega_1,\omega_2)}}{8}, \\
\beta_2 &= \frac{\bar{\gamma}(\omega_1,\omega_2) - \gamma(\omega_1,\omega_2)}{4} - i\frac{\omega_1+\omega_2}{4} + \frac{\sqrt{\lambda_+(\omega_1,\omega_2)}}{8}, \\
\beta_3 &= \frac{\bar{\gamma}(\omega_1,\omega_2) - \gamma(\omega_1,\omega_2)}{4} - i\frac{\omega_1+\omega_2}{4} - \frac{\sqrt{\lambda_-(\omega_1,\omega_2)}}{8}, \\
\beta_4 &= \frac{\bar{\gamma}(\omega_1,\omega_2) - \gamma(\omega_1,\omega_2)}{4} - i\frac{\omega_1+\omega_2}{4} + \frac{\sqrt{\lambda_-(\omega_1,\omega_2)}}{8},
\end{aligned}} \tag{5.6}$$

where we defined

$$\begin{aligned}
2\bar{\gamma}(\omega_1,\omega_2) &= \bar{\gamma}_L(\omega_1) + \bar{\gamma}_R(\omega_2), \\
2\gamma(\omega_1,\omega_2) &= \gamma_L(\omega_1) + \gamma_R(\omega_2), \\
\lambda_\pm(\omega_1,\omega_2) &= \left(\gamma_L(\omega_1) - \bar{\gamma}_L(\omega_1) - \gamma_R(\omega_2) + \bar{\gamma}_R(\omega_2) \pm 2i(\omega_1-\omega_2)\right)^2 - 16g^2.
\end{aligned}$$

Here, $2\bar{\gamma}$ is the total absorption, 2γ, the total emission and $\lambda_\pm$ the correction term due to the coupling. We can see that the rapidities for the two-site junction are similar to the ones found for the single-site junction (4.8). The solution of the Lyapunov equation (3.28) is given by the block matrix

$$\mathbf{Z} = \left(\begin{array}{c|c} 0 & A \\ \hline A^T & 0 \end{array}\right), \tag{5.7}$$

where the matrix A is expressed as

$$A_{11} = n_{L,1} + \frac{4g^2(\kappa_1+\kappa_2)\kappa_2(n_{R,2}-n_{L,1})}{(\kappa_1+\kappa_2)^2(4g^2+\kappa_1\kappa_2)+4\kappa_1\kappa_2(\omega_1-\omega_2)^2},$$

$$A_{12} = \frac{2g(n_{L,1}-n_{R,2})\kappa_1\kappa_2[2(\omega_1-\omega_2)+i(\kappa_1+\kappa-2)]}{(\kappa_1+\kappa_2)^2(4g^2+\kappa_1\kappa_2)+4\kappa_1\kappa_2(\omega_1-\omega_2)^2},$$

$$A_{21} = \frac{2g(n_{L,1}-n_{R,2})\kappa_1\kappa_2[2(\omega_1-\omega_2)-i(\kappa_1+\kappa-2)]}{(\kappa_1+\kappa_2)^2(4g^2+\kappa_1\kappa_2)+4\kappa_1\kappa_2(\omega_1-\omega_2)^2} = A_{12}^*,$$

$$A_{22} = n_{R,2} + \frac{4g^2(\kappa_1+\kappa_2)\kappa_1(n_{L,1}-n_{R,2})}{(\kappa_1+\kappa_2)^2(4g^2+\kappa_1\kappa_2)+4\kappa_1\kappa_2(\omega_1-\omega_2)^2},$$

where

$$\kappa_i = \kappa(\omega_i), \quad n_{\alpha,i} = n_\alpha(\omega_i).$$

The reader must bear in mind equation (3.37): the matrix elements of $\mathbf{Z}$ give the mean values of the creation and annihilation operators for the steady state. Explicitly,

$$\begin{aligned} A_{11} &= \langle a_1^\dagger a_1\rangle_{\text{NESS}}, \quad A_{12} = \langle a_1^\dagger a_2\rangle_{\text{NESS}}, \\ A_{21} &= \langle a_2^\dagger a_1\rangle_{\text{NESS}}, \quad A_{22} = \langle a_2^\dagger a_2\rangle_{\text{NESS}}. \end{aligned} \tag{5.8}$$

From the $\mathbf{Z}$ matrix, we also deduce that $\langle a_i a_j\rangle = \langle a_i^\dagger a_j^\dagger\rangle = 0$ for $i,j = 1,2$, the steady-state is diagonal in the Fock basis.

The derivation of the steady state relies on the same property (3.32) and the ansatz (justified here) that it is diagonal in the Fock basis. At one point of the derivation, we have to study the convergence of a series that guarantees that the trace of the steady state is one. We have the following condition

$$\begin{aligned} |A_{11}+A_{12}| &< |1+A_{11}+A_{12}|, \\ |A_{22}+A_{12}^*| &< |1+A_{22}+A_{12}^*|. \end{aligned} \tag{5.9}$$

If one of these two conditions are not fulfilled, the existence of a unique steady state is not guaranteed. these conditions correspond to the case where all rapidities β_i defined in (5.6) have their reel part positive. The expression of the steady state of the two-site junction is

$$\boxed{|\rho_{NESS}\rangle = \sum_{n,n'} \frac{\left(\frac{A_{11}+A_{12}}{1+A_{11}+A_{12}}\right)^n \left(\frac{A_{12}^*+A_{22}}{1+A_{12}^*+A_{22}}\right)^{n'} |n,n'\rangle\,|n,n'\rangle}{(1+A_{11}+A_{12})\,(1+A_{22}+A_{12}^*)}.} \tag{5.10}$$

It is interesting to note that the steady state depends directly of the number of particles in each site, i.e., A_{11} and A_{22} and the cross term, A_{12}. Intuitively, we can understand that if the first site accumulates particles without sending them to the right site, for example if the coupling is too weak, the system will never reach a steady state.

5.1.2 Symmetries of the system

In this subsection, we will study in detail the symmetries of the system. Firstly, we will display that this system admits a $\mathbb{U}(1)$ as the previous system, with an adapted unitary generator. Afterwards, we will show how the symmetry deeply affects the matrix representation of the Liouvillian.

As is the previous section, we define the superoperator $\mathcal{U} = U \cdot U^\dagger$ for $U = e^{-i\phi\left(a_1^\dagger a_1 + a_2^\dagger a_2\right)}$ for $\phi \in \mathbb{R}$. We seek for conditions for ϕ under which $[\mathcal{L}, \mathcal{U}] = 0$.
The operator U can be rewritten as

$$U = e^{-i\phi a_1^\dagger a_1} e^{-i\phi a_2^\dagger a_2} = U_1 U_2 = U_2 U_1. \tag{5.11}$$

This allows us to reuse the relations (4.34) - (4.37) found in the previous chapter. We have now

$$a_i U = e^{-i\phi} U a_i, \tag{5.12}$$
$$U a_i^\dagger = e^{-i\phi} a_i^\dagger U, \tag{5.13}$$
$$a_i^\dagger a_i U = U a_i^\dagger a_i, \tag{5.14}$$
$$a_i a_j^\dagger U = U a_i a_j^\dagger. \tag{5.15}$$

The last relation can be demonstrated in a few lines,

$$\begin{aligned} a_i a_j^\dagger U &= a_i a_j^\dagger U_i U_j \\ &= a_i U_i a_j^\dagger U_j. \end{aligned}$$

Using (5.12) and (5.13), we find successively

$$\begin{aligned} a_i a_j^\dagger U &= e^{-i\phi} U_i a_i a_j^\dagger U_j \\ &= U_i a_i U_j a_j^\dagger \\ &= U a_i a_j^\dagger. \end{aligned}$$

All that remains is to compute $\mathcal{LU}[\rho]$ and $\mathcal{UL}[\rho]$, keeping in mind that we partially did the computations for the previous system.
Firstly, we derive $\mathcal{LU}[\rho]$. Denoting $\rho' = U_1 U_2 \rho U_1^\dagger U_2^\dagger$ and $\rho_1 = U_1 \rho U_1^\dagger$, $\rho_2 = U_2 \rho U_2^\dagger$, we have

$$\begin{aligned} \mathcal{LU}[\rho] = &- i\left[H_S, \rho'\right] + \gamma_L \left(a_1^\dagger \rho' a_1 - \frac{1}{2}\left\{a_1 a_1^\dagger \rho'\right\}\right) + \bar{\gamma}_L \left(a_1 \rho' a_1^\dagger - \frac{1}{2}\left\{a_1^\dagger a_1 \rho'\right\}\right) \\ &+ \gamma_R \left(a_2^\dagger \rho' a_2 - \frac{1}{2}\left\{a_2 a_2^\dagger \rho'\right\}\right) + \bar{\gamma}_R \left(a_2 \rho' a_2^\dagger - \frac{1}{2}\left\{a_2^\dagger a_2 \rho'\right\}\right). \end{aligned} \tag{5.16}$$

Expanding the commutator, we have for the first term

$$\begin{aligned} -i\left[H_S, \rho'\right] &= - i\omega_1 \left[a_1^\dagger a_1, \rho'\right] - i\omega_2 \left[a_2^\dagger a_2, \rho'\right] - i\left[g\left(a_1^\dagger a_2 + a_1 a_2^\dagger\right), \rho'\right] \\ &= - i\omega_1 U_2 \left[a_1^\dagger a_1, \rho_1\right] U_2^\dagger - i\omega_2 U_1 \left[a_2^\dagger a_2, \rho_2\right] U_1^\dagger - i\left[g\left(a_1^\dagger a_2 + a_1 a_2^\dagger\right), \rho'\right], \end{aligned} \tag{5.17}$$

where we used property (5.14) to split U_1 and U_2 and made appear ρ_1 and ρ_2. For the single-site junction, we showed the equality of (4.38) and (4.39). We can reuse this here for the two first terms of (5.17), which implies that we only have to compare the coupling terms. Similarly, by applying what has already been proven for the single-site junction, we can demonstrate that all other terms in (5.16) match the corresponding terms in $\mathcal{UL}\rho$. Thus, we have

$$\mathcal{LU}\rho = \mathcal{UL}\rho \tag{5.18}$$

if and only if

$$\left[g\left(a_1^\dagger a_2 + a_1 a_2^\dagger\right), \rho'\right] = U\left[g\left(a_1^\dagger a_2 + a_1 a_2^\dagger\right), \rho\right] U^\dagger. \tag{5.19}$$

Expanding the left side of the equation, we have

$$\begin{aligned}\left[g\left(a_1^\dagger a_2 + a_1 a_2^\dagger\right), \rho'\right] =& g\left(a_1^\dagger a_2 U_1 U_2 \rho U_1^\dagger U_2^\dagger + a_1 a_2^\dagger U_1 U_2 \rho U_1^\dagger U_2^\dagger\right) \\ & - g\left(U_1 U_2 \rho U_1^\dagger U_2^\dagger a_1^\dagger a_2 + U_1 U_2 \rho U_1^\dagger U_2^\dagger a_1 a_2^\dagger\right).\end{aligned} \tag{5.20}$$

Using relation (5.15) in each term, the left side of equation (5.19) reads

$$\begin{aligned}\left[g\left(a_1^\dagger a_2 + a_1 a_2^\dagger\right), \rho'\right] &= g\left(U a_1^\dagger a_2 \rho U^\dagger + U a_1 a_2^\dagger \rho U^\dagger\right) - g\left(U \rho a_1^\dagger a_2 U^\dagger + U \rho a_1 a_2^\dagger U^\dagger\right) \\ &= U g\left(a_1^\dagger a_2 + a_1 a_2^\dagger\right) \rho U^\dagger - U g \rho \left(a_1^\dagger a_2 + a_1 a_2^\dagger\right) U^\dagger \\ &= U\left[g\left(a_1^\dagger a_2 + a_1 a_2^\dagger\right), \rho\right] U^\dagger,\end{aligned} \tag{5.21}$$

which is the right side of equation (5.19).

As any condition over ϕ has been encountered during the development, we have established that the two-site junction admits a $\mathbb{U}(1)$ symmetry.

Implications of the symmetry

We want to show here how a $\mathbb{U}(1)$ weak symmetry on the superoperator level could affect the dynamics of the system. We state that this kind of symmetry on the superoperator implies another symmetry, on the operator level. Indeed, we have

$$[U, H_S] = 0. \tag{5.22}$$

We prove this equality in a few lines

$$\begin{aligned}U H_S &= U_1 U_2 \left(\omega_1 a_1^\dagger a_1 + \omega_2 a_2^\dagger a_2 + g(a_1^\dagger a_2 + a_2^\dagger a_1)\right) \\ &= (\omega_1 a_1^\dagger a_1 + \omega_2 a_2^\dagger a_2) U_1 U_2 + U_1 U_2 g(a_1^\dagger a_2 + a_2^\dagger a_1),\end{aligned}$$

using property (5.14) and

$$\begin{aligned}U H_S &= (\omega_1 a_1^\dagger a_1 + \omega_2 a_2^\dagger a_2) U_1 U_2 + g(a_1^\dagger a_2 + a_2^\dagger a_1) U_1 U_2 \\ &= H_S U,\end{aligned}$$

using property (5.15). Thus, the matrix representation of H_S is block diagonal in the basis of the eigenvectors of U. To better understand the strength of the symmetries, an example is required.

We represent the creation and annihilation operator of each site as

$$\begin{aligned}a_1 &= a \otimes \mathbb{1}, \\ a_2 &= \mathbb{1} \otimes a,\end{aligned} \tag{5.23}$$

where we use the definition (4.44) of the annihilation operator a. The creation operators are defined by the transpose of the annihilation operators. Taking $N_{\text{cutoff}} = 3$, the matrix representation of H_S in the Fock basis is

$$H_S = \begin{pmatrix} 0 & 0 & 0 & 0 & 0 & 0 & 0 & 0 & 0 \\ 0 & \omega_2 & 0 & g & 0 & 0 & 0 & 0 & 0 \\ 0 & 0 & 2\omega_2 & 0 & \sqrt{2}g & 0 & 0 & 0 & 0 \\ 0 & g & 0 & \omega_1 & 0 & 0 & 0 & 0 & 0 \\ 0 & 0 & \sqrt{2}g & 0 & \omega_1 + \omega_2 & 0 & \sqrt{2}g & 0 & 0 \\ 0 & 0 & 0 & 0 & 0 & \omega_1 + 2\omega_2 & 0 & 2g & 0 \\ 0 & 0 & 0 & 0 & \sqrt{2}g & 0 & 2\omega_1 & 0 & 0 \\ 0 & 0 & 0 & 0 & 0 & 2g & 0 & 2\omega_1 + \omega_2 & 0 \\ 0 & 0 & 0 & 0 & 0 & 0 & 0 & 0 & 2\omega_1 + 2\omega_2 \end{pmatrix}. \tag{5.24}$$

In the same basis, the matrix representation of the generator U is

$$U = \mathrm{diag}(1, e^{-i\phi}, e^{-2i\phi}, e^{-i\phi}, e^{-2i\phi}, e^{-3i\phi}, e^{-2i\phi}, e^{-3i\phi}, e^{-4i\phi}). \tag{5.25}$$

The generator U is already diagonal but its eigenvalues are not sorted. We define P as the unitary matrix that sorts the eigenvalues of U, i.e.

$$PUP^T = \mathrm{diag}(e^{-4i\phi}, e^{-3i\phi}, e^{-3i\phi}, e^{-2i\phi}, e^{-2i\phi}, e^{-2i\phi}, e^{-i\phi}, 1). \tag{5.26}$$

The matrix P contains the change of basis required to display H_S in a block diagonal form,

$$\tilde{H}_S = PH_SP^T = \begin{pmatrix} 2\omega_1+2\omega_2 & 0 & 0 & 0 & 0 & 0 & 0 & 0 & 0 \\ 0 & 2\omega_1+\omega_2 & 2g & 0 & 0 & 0 & 0 & 0 & 0 \\ 0 & 2g & \omega_1+2\omega_2 & 0 & 0 & 0 & 0 & 0 & 0 \\ 0 & 0 & 0 & 2\omega_1 & \sqrt{2}g & 0 & 0 & 0 & 0 \\ 0 & 0 & 0 & \sqrt{2}g & \omega_1+\omega_2 & \sqrt{2}g & 0 & 0 & 0 \\ 0 & 0 & 0 & 0 & \sqrt{2}g & 2\omega_2 & 0 & 0 & 0 \\ 0 & 0 & 0 & 0 & 0 & 0 & \omega_1 & g & 0 \\ 0 & 0 & 0 & 0 & 0 & 0 & g & \omega_2 & 0 \\ 0 & 0 & 0 & 0 & 0 & 0 & 0 & 0 & 0 \end{pmatrix}.$$

Note that the size of the matrices is N_{cutoff}^2 as we have two sites here. In the superoperator level, the size of the matrices are $N_{\mathrm{cutoff}}^{n^2}$ where n is the number of sites. The growth is exponential for a large number of modes, which explains why analytic exact methods are important.

By setting $N_{\mathrm{cutoff}} = 2$, we can observe the changes when transitioning from the Hamiltonian to the Liouvillian. We reduce the cutoff value by one because, if we kept the previous value, the matrix representation of the Liouvillian would be of size 81, which is too large to represent here. When sorted, the eigenvalues of U are $e^{-2i\phi}, e^{-i\phi}, 1$ with algebraic multiplicity respectively $1, 2, 1$. Thus, in this basis, the Hamiltonian is

$$\tilde{H}_S = \begin{pmatrix} \omega_1+\omega_2 & 0 & 0 & 0 \\ 0 & \omega_1 & g & 0 \\ 0 & g & \omega_2 & 0 \\ 0 & 0 & 0 & 0 \end{pmatrix}. \tag{5.27}$$

Then, the generator at the superoperator level, $\mathcal{U}$, has the following eigenvalues

$$\begin{aligned} &\lambda_1 = e^{-2i\phi} \text{ of multiplicity 1,} \\ &\lambda_2 = e^{-i\phi} \text{ of multiplicity 4,} \\ &\lambda_3 = 1 \text{ of multiplicity 6,} \\ &\lambda_4 = e^{i\phi} \text{ of multiplicity 4,} \\ &\lambda_5 = e^{2i\phi} \text{ of multiplicity 1} \end{aligned}$$

and the Liouvillian in the appropriate basis is

$$L = \begin{pmatrix} L_1 & 0 & 0 & 0 & 0 \\ 0 & L_2 & 0 & 0 & 0 \\ 0 & 0 & L_3 & 0 & 0 \\ 0 & 0 & 0 & L_4 & 0 \\ 0 & 0 & 0 & 0 & L_5 \end{pmatrix}, \tag{5.28}$$

where

$$L_1 = \frac{-\gamma - \bar{\gamma} - 2i(\omega_1 + \omega_2)}{2} = L_5^*,$$

$$L_2 = \frac{1}{2}\begin{pmatrix} -\gamma_R - \bar{\gamma}_R - 2(\bar{\gamma}_L + i\omega_2) & 2ig & 0 & 2\gamma_L \\ 2ig & -\gamma_L - \bar{\gamma}_L - 2(\bar{\gamma}_R + i\omega_1) & 2\gamma_R & 0 \\ 0 & 2\bar{\gamma}_R & -\gamma_L - \bar{\gamma}_L - 2(\gamma_R + i\omega_1) & -2ig \\ 2\bar{\gamma}_L & 0 & -2ig & -\gamma_R - \bar{\gamma}_R - 2(\gamma_L + i\omega_2) \end{pmatrix}$$

$$= L_4^*,$$

$$L_3 = \begin{pmatrix} -\bar{\gamma}_L - \bar{\gamma}_R & \gamma_R & 0 & 0 & \gamma_L & 0 \\ \bar{\gamma}_R & -\bar{\gamma}_L - \gamma_R & ig & -ig & 0 & \gamma_L \\ 0 & ig & \frac{1}{2}(-\gamma - \bar{\gamma} - 2(i\omega_1 - i\omega_2) & 0 & -ig & 0 \\ 0 & -ig & 0 & \frac{1}{2}(-\gamma - \bar{\gamma} + 2i(\omega_1 - \omega_2)) & ig & 0 \\ \bar{\gamma}_L & 0 & -ig & ig & -\gamma_L - \bar{\gamma}_R & \gamma_R \\ 0 & \bar{\gamma}_L & 0 & 0 & \bar{\gamma}_R & -\gamma_L - \gamma_R \end{pmatrix}.$$

We can see that the size of each block is related to the multiplicity of the associated eigenvalue of $\mathcal{U}$.

The connection between $\tilde{H}_S$ and L can be understood by examining the diagonal elements of each matrix, particularly by counting the occurrences of a site frequency, ω_1 or ω_2. This analysis provides an in-depth understanding of what occurs when transitioning from a closed to an open system. For the Hamiltonian, the diagonal elements respectively show 2, 1, and 0 frequencies. We count two frequencies for the first element due to their addition; for a subtraction, we would count zero. These numbers correspond to the coefficients in front of ϕ in the exponential terms for the eigenvalues of U. Applying the same logic to L, we get -2 and 2 for the first and last elements, -1 and 1 for the second and fourth blocks, and 0 for the third block. For the third block, we could also represent the third and fourth elements as $-1+1$ and $1-1$. Again, these values are related to the eigenvalues of $\mathcal{U}$ and match those found for $\tilde{H}$, establishing the link between the two matrices. Figure 5.3 illustrates this reasoning, with colors added to help visualize how each block from $\tilde{H}$ transforms into L.

At first glance, the reader might think that the study of symmetries is not directly related to third quantization methods. However, several recent studies have combined both approaches to find analytical solutions to Lindblad master equations [45, 46, 47, 48].

5.1.3 Particle current

It this subsection, we want to derive an expression for the particle current. We shall recall that the particle current corresponds to the amount of particles passing from the left to the right bath per unit of time. Tracing the path of a particle, it begins at the left bath, moves through the left junction, continues through the right junction, and finally reaches the right bath. The definition of the particle current should reflect this trajectory. Thus, we define the total particle current by

$$\langle J_T \rangle = \mathrm{Tr}[\dot{\rho}(t)(a_1^\dagger a_1 + a_2^\dagger a_2)] = \frac{d}{dt}\langle a_1^\dagger a_1 + a_2^\dagger a_2 \rangle. \tag{5.29}$$

Defining the left and right current as

$$\langle J_L \rangle = \frac{d}{dt}\langle a_1^\dagger a_1 \rangle, \tag{5.30}$$

$$\langle J_R \rangle = \frac{d}{dt}\langle a_2^\dagger a_2 \rangle, \tag{5.31}$$

$$\tag{5.32}$$

we have

$$\langle J_T \rangle = \langle J_L \rangle + \langle J_R \rangle. \tag{5.33}$$

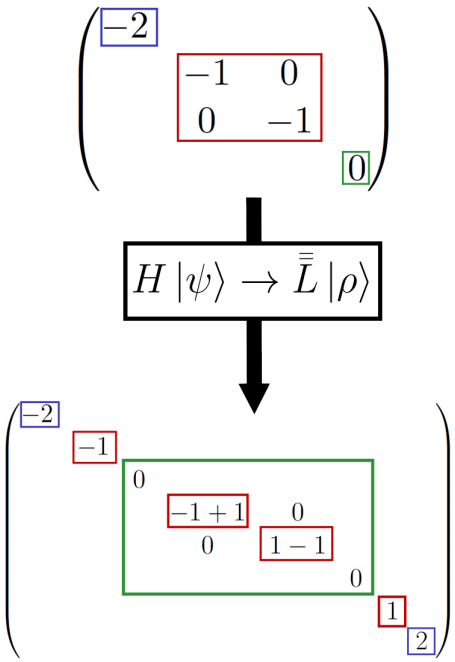

Figure 5.3: Sketch of the link that can be found between $\tilde{H}$ and L when counting the occurrences of the site frequencies of each diagonal element or block. Blocks framed in the same color share their count of frequencies and are related.

After some algebra, we find

$$\langle J_L \rangle = ig\langle a_2^\dagger a_1 - a_1^\dagger a_2 \rangle + \langle a_1^\dagger a_1 \rangle (\gamma_L(\omega_1) - \bar{\gamma}_L(\omega_1)) + \gamma_L(\omega_1), \tag{5.34}$$

$$\langle J_R \rangle = ig\langle a_1^\dagger a_2 - a_2^\dagger a_1 \rangle + \langle a_2^\dagger a_2 \rangle (\gamma_R(\omega_2) - \bar{\gamma}_R(\omega_2)) + \gamma_R(\omega_2). \tag{5.35}$$

We now exploit the covariance matrix $\mathbf{Z}$ using (5.8). Replacing the corresponding terms, we obtain an analytical solution for the particle current at the steady state

$$\begin{aligned} \langle J_L \rangle &= \frac{8g^2(n_{L,1} - n_{R,2})(\kappa_1 + \kappa_2)\kappa_1\kappa_2}{4g^2(\kappa_1 + \kappa_2)^2 + \kappa_1\kappa_2\left((\kappa_1 + \kappa_2)^2 + 4(\omega_1 - \omega_2)^2\right)}, \\ \langle J_R \rangle &= -\frac{8g^2(n_{L,1} - n_{R,2})(\kappa_1 + \kappa_2)\kappa_1\kappa_2}{4g^2(\kappa_1 + \kappa_2)^2 + \kappa_1\kappa_2\left((\kappa_1 + \kappa_2)^2 + 4(\omega_1 - \omega_2)^2\right)} = -\langle J_L \rangle. \end{aligned} \tag{5.36}$$

We can already know that at the steady state, the total particle current is null for every regime of parameter. There are as much particles entering the system than particles going out.

Ultimately, we derived an analytical solution for the left and right particle current which depends on the frequency of each site, the coupling strength g and the temperatures of each bath through the Bose-Einstein distribution.

5.2 Global approach

We now study our system with the second approach, the global one. As explained at the beginning of this chapter, we must apply a Bogoliubov transformation to the system Hamiltonian. This will allow us to find the eigenstates and eigenvalues associated such that the Hamiltonian is in a diagonal form, without an interaction term. Thus, we will effectively have a coupling between the baths and the eigenvalues of the system, which means that the frequencies of the normal modes must appear in the expression of the jump operators. A sketch of this situation is shown in figure 5.4. We must define new absorption and emission rates, for a total of eight:

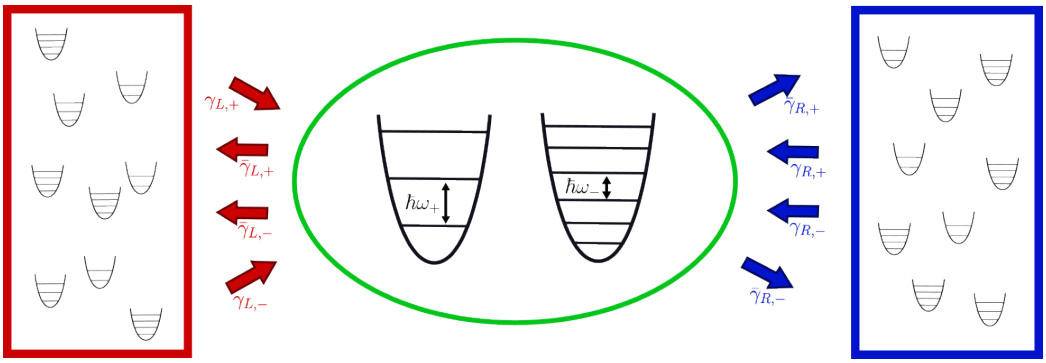

Figure 5.4: Sketch of the two-site junction in the global approach. Instead of the previous two sites, we diagonalized the Hamiltonian to find the normal modes, namely the "+" and "-" modes of frequency ω_+ and ω_-. Using the normal modes, the two sites are now uncoupled. Thus, a boson going from the left to the right bath cross the junction via one mode only. In addition, each mode absorbs and emits particles to each bath, which leads to eight rates, one for each combination of absorption/emission to the left/right bath for the "+"/"-" mode.

$\gamma_{\alpha,\sigma}$ is the absorption rate for the mode σ and bath α, $\bar{\gamma}_{\alpha,\sigma}$ is the emission rate for the mode σ and bath α.

This approach is less intuitive than the local one but according to [44, 43, 49], it tends to give better results, especially for a large coupling between the two sites.

After the Bogoliubov transformation, the Hamiltonian of the system reads now

$$H_S = \omega_+ a_+^\dagger a_+ + \omega_- a_-^\dagger a_-, \tag{5.37}$$

where

$$\omega_\pm = \frac{\omega_1 + \omega_2 \pm \sqrt{4g^2 + (\omega_1 - \omega_2)^2}}{2} \tag{5.38}$$

and the new creation and annihilation operators are given by

$$\begin{aligned} a_+ &= a_1 \cos\theta + a_2 \sin\theta, \\ a_- &= a_1 \sin\theta - a_2 \cos\theta. \end{aligned} \tag{5.39}$$

The angle θ, assuring that the new mapping admits the CCR, is defined as

$$\tan\theta = \frac{2g}{(\omega_1 - \omega_2) - \sqrt{4g^2 + (\omega_1 - \omega_2)^2}}. \tag{5.40}$$

We shall take $\omega_1 = \omega_2$ for more simplicity. Otherwise we would obtain a master equation containing terms in $\cos\theta$ and $\sin\theta$. Taking $\omega_1 = \omega_2$, the new mapping reads now

$$a_+ = \frac{1}{\sqrt{2}}(a_1 + a_2), \tag{5.41}$$

$$a_- = \frac{1}{\sqrt{2}}(a_1 - a_2). \tag{5.42}$$

$$\tag{5.43}$$

The global form of the Lindblad master equation is

$$\begin{aligned} \dot{\rho}(t) = -i\,[H_S, \rho(t)] &+ (\bar{\gamma}_{L,+} + \bar{\gamma}_{R,+})\,\mathcal{D}_{a_+}[\rho(t)] + (\bar{\gamma}_{L,-} + \bar{\gamma}_{R,-})\,\mathcal{D}_{a_-}[\rho(t)] \\ &+ (\gamma_{L,+} + \gamma_{R,+})\,\mathcal{D}_{a_+^\dagger}[\rho(t)] + (\gamma_{L,-} + \gamma_{R,-})\,\mathcal{D}_{a_-^\dagger}[\rho(t)]. \end{aligned} \tag{5.44}$$

We can see here that the modes are effectively uncoupled, the coupling factor g only appearsin the definition of the new frequencies. Furthermore, if we neglected the absorption for left bath and emission for right bath, we would obtain an equation similar to Eq. (4.4) for two independent modes.

The dissipation rates are defined as follows

$$\begin{aligned}\gamma_{\alpha,\sigma} &= \kappa(\omega_\sigma) n_\alpha(\omega_\sigma),\\ \bar{\gamma}_{\alpha,\sigma} &= \kappa(\omega_\sigma)[n_\alpha(\omega_\sigma)+1],\end{aligned} \tag{5.45}$$

for $\alpha = L, R$, $\sigma = +, -$.

The complete derivation of the global master equation can be found in Subsec. B.2.2. This approach is said to be valid for a large coupling, $g \gg \kappa(\omega)$.

5.2.1 Application of the third quantization

The calculation details are not showed here as the resolution is quite similiar to the two previous cases. We only show here the obtained results.

As the the two modes absorbed the interaction term, the $\mathbf{X}$ matrix is diagonal. We find immediately the rapidities,

$$\begin{aligned}\beta_1 &= \frac{\bar{\gamma}_{L,-}(\omega_-) + \bar{\gamma}_{R,-}(\omega_-) - \gamma_{L,-}(\omega_-) - \gamma_{R,-}(\omega_-)}{4} - \frac{i\omega_-}{2},\\ \beta_2 &= \frac{\bar{\gamma}_{L,-}(\omega_-) + \bar{\gamma}_{R,-}(\omega_-) - \gamma_{L,-}(\omega_-) - \gamma_{R,-}(\omega_-)}{4} + \frac{i\omega_-}{2},\\ \beta_3 &= \frac{\bar{\gamma}_{L,+}(\omega_+) + \bar{\gamma}_{R,+}(\omega_+) - \gamma_{L,+}(\omega_+) - \gamma_{R,+}(\omega_+)}{4} - \frac{i\omega_+}{2},\\ \beta_4 &= \frac{\bar{\gamma}_{L,+}(\omega_+) + \bar{\gamma}_{R,+}(\omega_+) - \gamma_{L,+}(\omega_+) - \gamma_{R,+}(\omega_+)}{4} + \frac{i\omega_+}{2}.\end{aligned}$$

Using definition (5.45), the rapidities reduce to

$$\boxed{\begin{aligned}\beta_1 &= \frac{\kappa(\omega_-)}{2} - \frac{i\omega_-}{2},\\ \beta_2 &= \frac{\kappa(\omega_-)}{2} + \frac{i\omega_-}{2},\\ \beta_3 &= \frac{\kappa(\omega_+)}{2} - \frac{i\omega_+}{2},\\ \beta_4 &= \frac{\kappa(\omega_+)}{2} + \frac{i\omega_+}{2}.\end{aligned}} \tag{5.46}$$

With these expressions, we can already infer that $\mathrm{Re}[\beta_1]$ and $\mathrm{Re}[\beta_2]$ are negatives when $\kappa(\omega_-)$ is negative. As $\kappa(\omega) \propto \omega$, we find a negative real part when $g > \sqrt{\omega_2/\omega_1}$.

Similarly to the local approach, the solution of the Lyapunov equation is given by a 2×2 block equation. However, here we are only interested by two matrix elements. The elements in $\langle aa \rangle$ or $\langle a^\dagger a^\dagger \rangle$ are equal to zero, just like in the local case, and additionally, the modes are no longer interacting. The latter lead to matrix elements corresponding to different modes, in $\langle a_\sigma^\dagger a_\tau \rangle$, also equal to 0. Thus, we have

$$\mathbf{Z}_{13} = \mathbf{Z}_{31} = \langle a_+^\dagger a_+ \rangle_{NESS} = \frac{n_{L,+} + n_{R,+}}{2}, \tag{5.47}$$

$$\mathbf{Z}_{24} = \mathbf{Z}_{42} = \langle a_-^\dagger a_- \rangle_{NESS} = \frac{n_{L,-} + n_{R,-}}{2}, \tag{5.48}$$

where

$$n_{\alpha,\sigma} = n_\alpha(\omega_\sigma),$$

for $\alpha = L, R$, $\sigma = +, -$.

The derivation of the steady state brings a condition for the stability of the system. The steady state is well defined if

$$|\langle a_+^\dagger a_+\rangle_{NESS}| < |\langle a_+^\dagger a_+\rangle_{NESS} + 1|, \quad |\langle a_-^\dagger a_-\rangle_{NESS}| < |\langle a_-^\dagger a_-\rangle_{NESS} + 1|. \tag{5.49}$$

The first condition is always true as $\langle a_+^\dagger a_+\rangle_{NESS}$ is positive for all range of parameters. For the second condition, we find an instability if $\langle a_-^\dagger a_-\rangle_{NESS} < 1/2$, i.e., if $g \geq \sqrt{\omega_2/\omega_1}$, the same condition that led to $\mathrm{Re}[\beta_i] < 0$ for $i = 1, 2$. Considering $g < \sqrt{\omega_2/\omega_1}$, we find for the steady state

$$\boxed{|\rho_{\mathrm{NESS}}\rangle = \sum_{n,n'} \frac{\left(\frac{\langle a_+^\dagger a_+\rangle_{NESS}}{\langle a_+^\dagger a_+\rangle_{NESS}+1}\right)^n \left(\frac{\langle a_-^\dagger a_-\rangle_{NESS}}{\langle a_-^\dagger a_-\rangle_{NESS}+1}\right)^{n'}}{(\langle a_+^\dagger a_+\rangle_{NESS} + 1)(\langle a_-^\dagger a_-\rangle_{NESS} + 1)} |n, n'\rangle\, |n, n'\rangle\,.} \tag{5.50}$$

5.2.2 Symmetries of the system

The previous section already included a thorough analysis of the symmetries of the system. Given the similitude of this system and the previous ones, it seems to us that the study of the symmetries of the system would not add new elements. We simply state that the system admits a $\mathbb{U}(1)$ weak symmetry.

5.2.3 Particle current

In this subsection, we want to find an analytical expression for the particle currents. Given that the master equation is different from the local approach, we must adapt the definitions of the left and right currents. For the local approach, we defined them as

$$\langle J_L\rangle = \mathrm{Tr}\Big[\mathcal{L}_L[\rho(t)](a_+^\dagger a_+ + a_-^\dagger a_-)\Big], \tag{5.51}$$

$$\langle J_R\rangle = \mathrm{Tr}\Big[\mathcal{L}_R[\rho(t)](a_+^\dagger a_+ + a_-^\dagger a_-)\Big], \tag{5.52}$$

where $\mathcal{L}_\alpha$ corresponds to the dissipator related to the bath α,

$$\mathcal{L}_\alpha = \bar{\gamma}_{\alpha,+}\mathcal{D}[a_+] + \bar{\gamma}_{\alpha,-}\mathcal{D}[a_-] + \gamma_{\alpha,+}\mathcal{D}[a_+^\dagger] + \gamma_{\alpha,}\mathcal{D}[a_-^\dagger].$$

The idea behind this definition is to isolate the effect of the coupling for only one bath at a time in the master equation. The reader might think that the contribution of the unitary evolution (the commutator with the Hamiltonian term) has been forgotten. Yet it is trivial to show that $\mathrm{Tr}\Big[-i[H_S, \rho](a_+^\dagger a_+ + a_-^\dagger a_-)\Big] = 0$, due to the properties of the trace. After some algebra, we find

$$\langle J_\alpha\rangle = \langle a_+^\dagger a_+\rangle(\gamma_{\alpha,+} - \bar{\gamma}_{\alpha,+}) + \langle a_-^\dagger a_-\rangle(\gamma_{\alpha,-} - \bar{\gamma}_{\alpha,-}) + \gamma_{\alpha,-} + \gamma_{\alpha,+}, \tag{5.53}$$

for $\alpha = L, R$. We now exploit the covariance matrix $\mathbf{Z}$. Replacing the corresponding terms, we obtain an analytical solution for the particle current at the steady state

$$\begin{aligned}\langle J_L\rangle &= \frac{\kappa_-(n_{L,-} - n_{R,-}) + \kappa_+(n_{L,+} - n_{R,+})}{2},\\ \langle J_R\rangle &= -\frac{\kappa_-(n_{L,-} - n_{R,-}) + \kappa_+(n_{L,+} - n_{R,+})}{2} = -\langle J_L\rangle.\end{aligned} \tag{5.54}$$

Once again, the right current is the exact opposite of the left current.

5.3 Results

In this section, we will compare the spectrum of the Liouvillian and the particle current for each approach. As the master equation for the global approach is only valid for $\omega_1 = \omega_2$, we will not consider different frequencies for the sites. Thus, we will study the influence of the coupling strength g for two regimes: when $T_L = T_R$ and when $T_L \neq T_R$. It might also be interesting to compare the two approaches for g fixed and varying T_L/T_R. For all the computations, we take $\kappa_1 = \kappa_2 = 0.05$ and $\omega_1 = \omega_2 = 1$. Thus $\omega_\pm = 1 \pm g$ and $\kappa_\pm = \kappa/(2\pi)\omega_\pm$. We recall that the validity of the local approach is when $g \ll \omega$ and for the global one, it is valid for $g \gg \kappa$. Thus, there is an overlapping between the regimes of validity for the two approaches, when $\kappa \ll g \ll \omega$.

We shall note that we will not compare our derivations with a numerical method here. Firstly because we can compare our results with the numerical results from [43]. In that paper, they studied a similar problem but instead of having the same frequencies on each site, they considered an external driving. For identical frequencies, both methods are the same. Secondly, the results from our numerical computations were unsatisfactory. Achieving the desired precision would have required a too high N_{cutoff}. Given that the size of the Liouvillian matrix scales as N^4_{cutoff}, this approach was impractical. For this test, instead of straightforwardly solve the coupled differential equations corresponding to the master equation, we wanted to exploit the symmetries of the system. Indeed, as explained in Subsec. 5.1.2, rather than a large matrix of size N^4_{cutoff}, we only had to diagonalize smaller square matrices. However, we still had to diagonalize and find the eigenvectors of the matrix generator of the symmetry, which, despite being unitary, was also of size N^4_{cutoff}. This final step prevented us from performing the necessary computations.

5.3.1 Spectrum of the Liouvillian

In this subsection, we compare the spectrum given by the two approaches. Rather than plotting the spectrum of the Liouvillian using property (3.34), we chose to directly compare the rapidities. We shall note that given the expressions of the rapidities for the local case, equation (5.6) and the global case, equation (5.46), the rapidities are independent of the temperatures in both cases. Thus, it remains to study the influence of the coupling for the real and the imaginary parts of the rapidities.

In the upper panel of Fig. 5.5, we compare the real part of the rapidities for both approaches. We see that all the real parts of the rapidities in the local case are equal and constant with respect to g. For the global case, we see that for $g > 1$, $\text{Re}[\beta_1] = \text{Re}[\beta_2] < 0$. In this case, the Liouvillian has eigenvalues with positive real parts, which would imply that the state does not converge towards the steady state. Instead, the system continuously absorbs excitations from the left bath. In the lower panel, we plotted the imaginary part of the rapidities for the global approach only[2]. We see that for $g = 1$, we have $\beta_1 = \beta_2 = 0$, there is an infinity of eigenvalues 0 instead of one for $g \neq 1$. This implies that for $g = 1$, the steady state is degenerated.

5.3.2 Particle current

In this subsection, we compare the particle current for the two approaches. As the total current is null for the two approaches, we compare the left current, which corresponds to the quantity of particles entering the system per unit of time. The left particle current for the local approach is given in equation (5.36) and in equation (5.54) for the global apprach.

In Fig. 5.6, we compare the left particle current for both approaches as a function of g for $T_L = T_R$. We see that without gradient of temperature, no particle current is found. For $T_L > T_R$, the left particle current is positive, see Fig 5.7. The local approach gives the expected

[2]The imaginary part of the rapidities does not give information about the physical properties of the system if the real parts are constant.

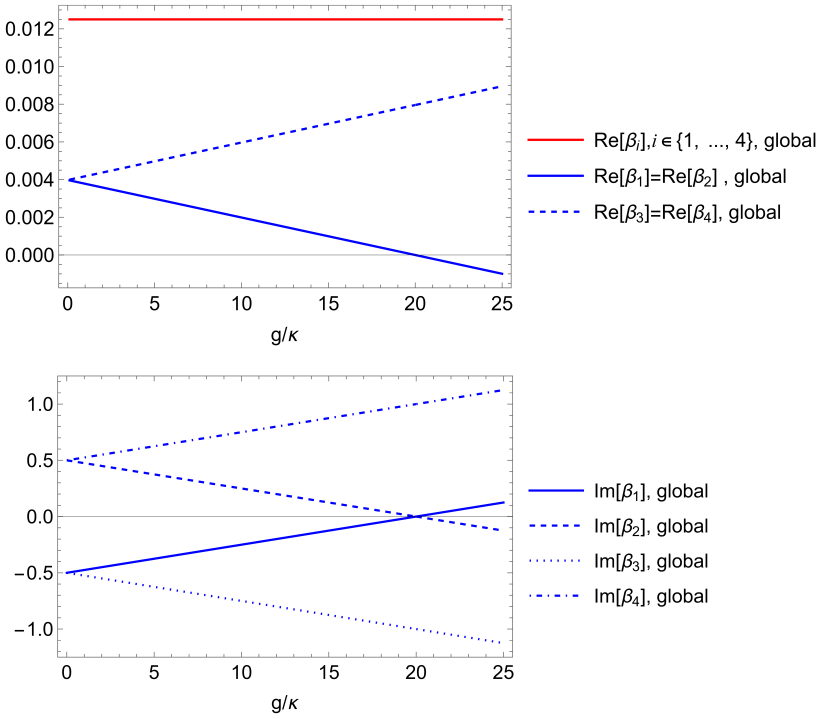

Figure 5.5: Upper panel: Comparison of the real part of the rapidities obtained for the local master equation (5.6) (in red) and the global master equation (5.46) (in blue) as a function of the coupling strength g. The real part of the rapidities are constant in the local approach while $\mathrm{Re}[\beta_1] < 0$ for $g > 1$. Lower panel: Comparison of the imaginary part of the rapidities obtained for the global master equation (5.46). When $g = 1$, $\mathrm{Im}[\beta_1] = \mathrm{Im}[\beta_2] = 0$. Parameters: $\omega_1 = \omega_2 = 1$, $\kappa_1 = \kappa_2 = 0.05, T_L = T_R = 0.5$.

behavior in all range of g, even for $g \approx \omega/2$ where it is expected to break down. The global left current indeed breaks down for small g as it it gives a non-zero current for $g = 0$.

In Figs. 5.8 and 5.9, we compare the left particle current as a function of the temperature of the left bath T_L. We see in the figure 5.8 that the left particle current follows the temperature gradient in both approaches, as it is positive for $T_L > T_R$ and negative for $T_L < T_R$ (see the insets in both panels). In the left panel, as $g = 0.5 = \omega/2$, we expect the local approach to break down, which is not the case and gives similar results than the global approach. In the right panel, both approaches are valid and also give similar results. Note that $|\langle J_{\text{Local}}\rangle| \leq |\langle J_{\text{Global}}\rangle|$ for all T_L. The Fig. 5.9 shows that the global approach break down when $g = 0$ for all T_L.

We see that our results are in accord with the conclusions drawn in [43].

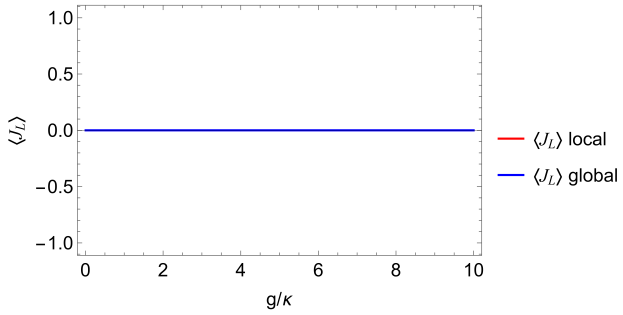

Figure 5.6: Comparison of the left particle current obtained for the local master equation (5.36) (in red) and the global master equation (5.54) (in blue) as a function of the coupling strength g. The left particle current is null everywhere for the two approaches. Parameters: $\omega_1 = \omega_2 = 1$, $\kappa_1 = \kappa_2 = 0.05, T_L = T_R = 0.5$.

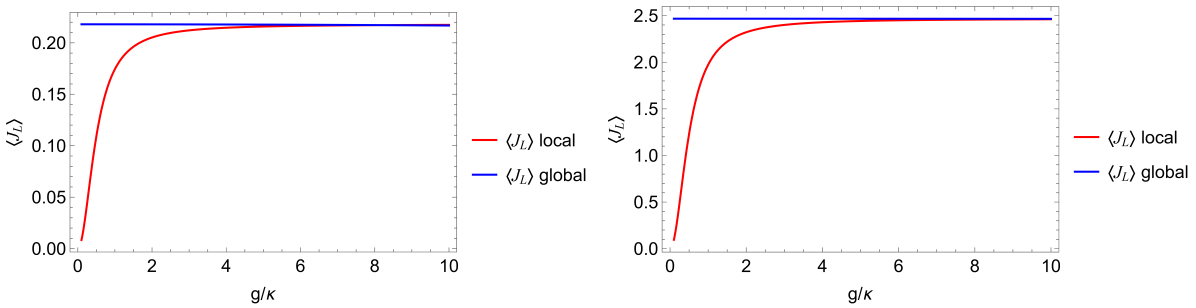

(a) (b)

Figure 5.7: Comparison of the left particle current obtained for the local master equation (5.36) (in red) and the global master equation (5.54) (in blue) as a function of the coupling strength g. The global left current decreases very slowly, remaining nearly constant over this range of parameters. In contrast, the local left current starts at 0 for $g = 0$ then increases significantly for $g < 0.12$, and eventually levels off to reach the value of the global current. Increasing the temperature of the left bath, T_L, by a factor 10 gives a left current multiplied by 10 in both approaches. Panel (a): $T_L = 5$ Panel (b): $T_L = 50$. Parameters: $\omega_1 = \omega_2 = 1$, $\kappa_1 = \kappa_2 = 0.05, T_R = 0.5$.

5.4 Redfield approach

In this section, we study our system with the last approach, the Redfield one. This method follows a derivation similar to the global approach, except that the secular approximation is not performed here.

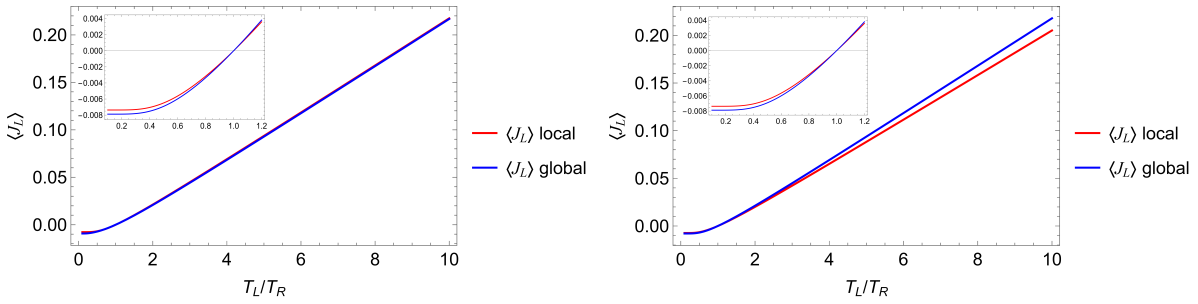

(a) (b)

Figure 5.8: Comparison of the left particle current obtained for the local master equation (5.36) (in red) and the global master equation (5.54) (in blue) as a function of the temperature of the left bath, T_L. The insets show the behavior of the left current for $T_L \leq T_R$. The value of the particle current follows the temperature gradient for both cases. In the left panel, the two approaches give similar results even if the local approach is expected to break down, as $g = \omega/2$.. In the right panel, both approaches are valid and also give similar results. Note that $|\langle J_{\text{Local}}\rangle| \leq |\langle J_{\text{Global}}\rangle|$ for all T_L. Panel (a): $g = 0.5$ Panel (b): $g = 0.1$. Parameters: $\omega_1 = \omega_2 = 1$, $\kappa_1 = \kappa_2 = 0.05, T_R = 0.5$.

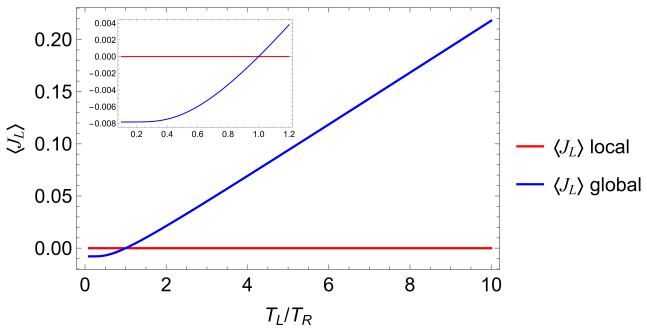

Figure 5.9: Comparison of the left particle current obtained for the local master equation (5.36) (in red) and the global master equation (5.54) (in blue) as a function of the temperature of the left bath, T_L. The inset showsthe behavior of the left current for $T_L \leq T_R$. For $g = 0$, the local approach gives a null left particle current, as expected, while the global approach break down and gives a non-zero one. Parameters: $\omega_1 = \omega_2 = 1$, $\kappa_1 = \kappa_2 = 0.05, g = 0, T_R = 0.5$.

The master equation in the Redfield approach is

$$\begin{aligned}\dot{\rho}(t) = -i\left[H_S, \rho(t)\right] &+ \left(\bar{\gamma}_{L,+} + \bar{\gamma}_{R,+}\right)\mathcal{D}_{a_+}[\rho(t)] + \left(\bar{\gamma}_{L,-} + \bar{\gamma}_{R,-}\right)\mathcal{D}_{a_-}[\rho(t)] \\ &+ \left(\gamma_{L,+} + \gamma_{R,+}\right)\mathcal{D}_{a_+^\dagger}[\rho(t)] + \left(\gamma_{L,-} + \gamma_{R,-}\right)\mathcal{D}_{a_-^\dagger}[\rho(t)] \\ &+ \frac{1}{2}\sum_{\substack{\alpha=L,R \\ \sigma=\pm}} \left(\gamma_\alpha(\omega_\sigma) + \bar{\gamma}_\alpha(\omega_\sigma)\right)\left[a_\sigma \rho(t) a_{\bar{\sigma}}^\dagger - \rho(t) a_\sigma^\dagger a_{\bar{\sigma}} + h.c.\right], \end{aligned} \tag{5.55}$$

where $\bar{\sigma} = \pm$ if $\sigma = \mp$. We see that the only difference between this master equation and the one obtained via the global approach, equation (5.44), is the last term. It contains the "cross terms" that were neglected with the secular approximation. Without this approximation, our equation is expected to be valid for all the ranges of parameters.

5.4.1 Application of the third quantization

The third quantization as shown in chapter 3 is not valid anymore as the master equation is not on the Lindblad form here. Fortunately, the third quantization has been extended to Redfield master equation in [6] with a few modifications. In this subsection, we will discuss how to adapt our equations so that they match the notations presented in the article.

The aim is to obtain a master equation of the form

$$\dot{\rho}(t) = \mathcal{L}[\rho(t] = -[H_S, \rho(t)] + \mathcal{D}[\rho], \tag{5.56}$$

where $\mathcal{D}$ is a new type of dissipator. Its definition is

$$\mathcal{D}[\rho(t)] = \sum_{\mu,\nu} \int_0^\infty d\tau \Gamma_{\mu,\nu}(\tau)[X_m u(\tau)\rho(t), X\nu] + h.c.. \tag{5.57}$$

Here the definition of $\Gamma_{\mu,\nu}$ is different from the one we used in Sec. 2.3. We have

$$\Gamma_{\mu,\nu}(\tau) = \mathrm{Tr}_E[E_1(t)^\dagger E_2(t-\tau)\rho_E].$$

Essentially, we remove the time integral that we hid in our definition (2.30). We need a change of notation to derive the dissipator of form (5.57):

$$\begin{aligned}\tilde{\Gamma}_{1,2}(\tau) &= \sum_k |\gamma_{k,L}|^2 e^{i\omega_{k,L}\tau}[n_L(\omega_{k,L}) + 1] \\ \tilde{\Gamma}_{2,1}(\tau) &= \sum_k |\gamma_{k,L}|^2 e^{i\omega_{k,L}\tau} n_L(\omega_{k,L}) \\ \tilde{\Gamma}_{3,4}(\tau) &= \sum_k |\gamma_{k,R}|^2 e^{i\omega_{k,R}\tau}[n_R(\omega_{k,R}) + 1] \\ \tilde{\Gamma}_{4,3}(\tau) &= \sum_k |\gamma_{k,R}|^2 e^{i\omega_{k,R}\tau} n_L(\omega_{k,R})\end{aligned}$$

and $\Gamma_{i,j} = 0$ for the others combination of i, j. We also set

$$X_1 = \frac{1}{\sqrt{2}}a_+ + a_-, \quad X_2 = X_1^\dagger, \quad X_3 = \frac{1}{\sqrt{2}}a_- - a_+, \quad X_4 = X_3^\dagger.$$

Thus, the nations given in [6] match with ours.

5.5 Comparison with the other approaches

In this section, we compare the three approaches throughout the 2-point correlation matrix $\mathbf{Z}$. We shall precise that for the global and Redfield cases, the correlation matrix is expressed in terms of the mapping a_+, a_- while the local is expressed in terms of a_1, a_2. We chose to express everything in terms of a_1, a_2 in order to capture the Physics of the system as this mapping is more intuitive. We compared the occupation number for both sites, $\langle a_1^\dagger a_1 \rangle_{\text{NESS}}$ and $\langle a_2^\dagger a_2 \rangle_{\text{NESS}}$ and the overlap between the two modes, $\langle a_1^\dagger a_2 \rangle_{\text{NESS}}$ at the steady state. We compared our observables for two regimes: the equilibrium case, without thermal gradient, and the non-equilibrium case, where $T_L > T_R$.

In Fig. 5.10 we compare our observables in the equilibrium case. In both panels, we see that each approach gives the same behavior around $g = 0$. However, for $g > 0$, the local approach breaks down.

In Fig. 5.7 and 5.8, we compare the occupation number in each site for the non-equilibrium case. For g around 0, we expect to have only particles in the first site, which is not the case for the Redfield and global approaches. For $g > 0$, we see that for the local approach, each site tends to have the same number of particles, which is confirmed by Fig 5.8, where we see that the total number of particle is constant for increasing g. For the Redfield and global approach, we have $\langle a_1^\dagger a_1 \rangle_{\text{NESS}} = \langle a_2^\dagger a_2 \rangle_{\text{NESS}}, \forall\ g$.

In Fig. 5.9, we compare the overlap between the two modes for the non-equilibrium case. The local approach breaks down for $g > 0$ and the global and Redfield approaches break down for small g.

Overall, the Redfield and global approaches give in all the studied cases the same results. For the equilibrium case, the Redfield and global approaches give better results than the local approach. For the non-equilibrium case, the Redfield and global approaches do not give the right behavior for g small. while the local approach breaks down for $g > 0$. As the secular approximation was not performed in the Redfield approach, we would have expected this approach to give better results than the global approach for small g. It is not the case here.

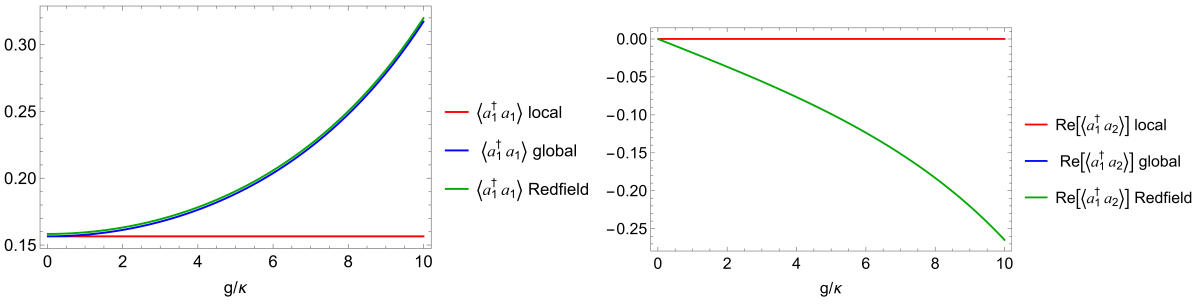

(a) (b)

Figure 5.10: Comparison of elements of the 2-point correlation matrix $\mathbf{Z}$ for the local master equation (5.8) (in red), the global master equation (5.47) (in blue) and for the Redfield master equation (in green) as a function of the coupling strength g in the equilibrium case. Panel (a): Occupation number for the first site $\langle a_1^\dagger a_1 \rangle_{\text{NESS}}$. Panel (b): Overlap between the two modes $\text{Re}[\langle a_1^\dagger a_2 \rangle_{\text{NESS}}]$. The local approach does not give the right behavior for $g > 0$. We also see that the Redfield and global approaches give similar results. In the equilibrium case, $\text{Im}[\langle a_1^\dagger a_2 \rangle_{\text{NESS}}] = 0$. Parameters: $\omega_1 = \omega_2 = 1$, $\kappa_1 = \kappa_2 = 0.05, T_L = T_R = 0.5$.

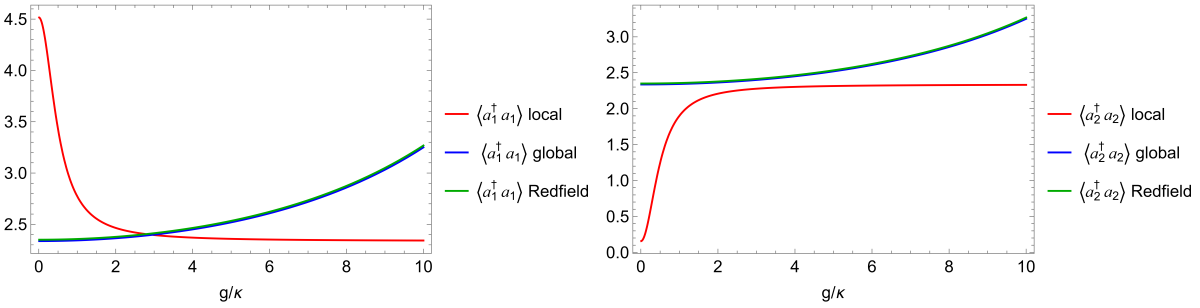

(a) (b)

Figure 5.11: Comparison of the occupation numbers at the steady state computed via the 2-point correlation matrix $\mathbf{Z}$ for the local master equation (5.8) (in red), the global master equation (5.47) (in blue) and for the Redfield master equation (in green) as a function of the coupling strength g with a temperature gradient. Panel (a): Occupation number for the first site $\langle a_1^\dagger a_1 \rangle_{\text{NESS}}$. Panel (b): Occupation number for the second site $\langle a_2^\dagger a_2 \rangle_{\text{NESS}}$. We can observe here the break down of the global approach for small g and we also see that the Redfield approach does not give the right behavior in the same regime. Parameters: $\omega_1 = \omega_2 = 1$, $\kappa_1 = \kappa_2 = 0.05, T_L = 5, T_R = 0.5$.

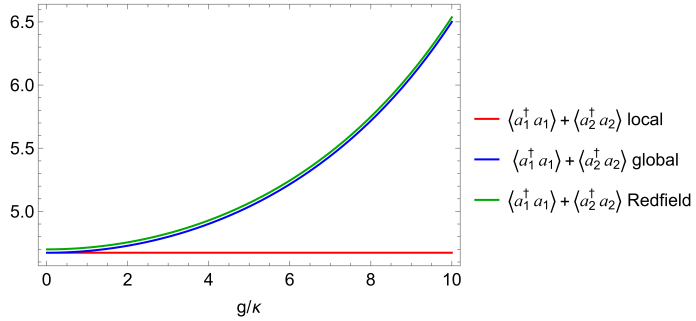

Figure 5.12: Comparison of the total number of particles at the steady state, $\langle a_1^\dagger a_1 \rangle + \langle a_2^\dagger a_2 \rangle_{\text{NESS}}$ computed via the 2-point correlation matrix $\mathbf{Z}$ for the local master equation (5.8) (in red), the global master equation (5.47) (in blue) and for the Redfield master equation (in green) as a function of the coupling strength g with a temperature gradient. In the local case, the total number of particles is constant while it increases for the two other approaches. Parameters: $\omega_1 = \omega_2 = 1$, $\kappa_1 = \kappa_2 = 0.05, T_L = 5, T_R = 0.5$.

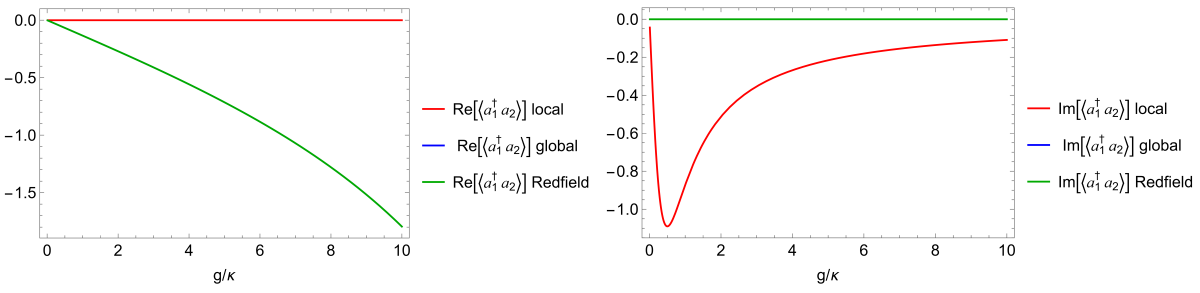

(a) (b)

Figure 5.13: Comparison of the overlap between the two modes computed via the 2-point correlation matrix $\mathbf{Z}$ for the local master equation (5.8) (in red), the global master equation (5.47) (in blue) and for the Redfield master equation (in green) as a function of the coupling strength g. Panel (a): $\text{Re}[\langle a_1^\dagger a_2 \rangle_{\text{NESS}}]$. Panel (b): $\text{Im}[\langle a_1^\dagger a_2 \rangle_{\text{NESS}}]$. Once again, we see in the right panel that the global and Redfield approaches break down for small g. Parameters: $\omega_1 = \omega_2 = 1$, $\kappa_1 = \kappa_2 = 0.05, T_L = 5, T_R = 0.5$.

5.6 Summary of the chapter

In this chapter, we studied the two-site junction in details with the use of the third quantization. We first discussed three different approaches to derive the master equation. The first approach was the local one, presented as more phenomenological and expected to be valid for small coupling between the two sites, i.e., $g \ll \omega$ where g is the coupling strength and ω the frequency of the two sites. In the section dedicated to the local approach, we discussed the implications of a weak symmetry for the matrix representation of the Liouvillian and the Hamiltonian. The second approach was the global one, expected to be valid for strong coupling, i.e., $g \gg \kappa(\omega)$ where $\kappa(\omega)$ is the spectral density and was taken ohmic here ($\kappa(\omega) \propto \omega$). For this method, we had to perform a Bogoliubov transformation in order to find the normal mode to effectively have a coupling between the baths and the eigenvalues of the system. We then compared several quantities such as the particle current at the steady state and the spectrum of the Liouvillian for the two methods in two cases: same temperatures in the two baths or different temperatures. Our conclusions were that, as expected, the global approach broke down for small g while the local approach had the right behavior, even for $g = \omega/2$ where it was expected to break down. We shall note that for the global approach, we found that the steady state was degenerated for $g = 1$. Finally, we showed a third approach, the Redfield one, which had the same features as the global approach, except for the secular approximation which was not performed in this approach. We ended this chapter by comparing the three methods for the occupation numbers of each site and the overlap between the two modes at the steady state, and we drew the same conclusions: the local approach failed to give the right behavior for large coupling while the global and Redfield approaches broke down for small g.

Conclusion

The aim of this master's thesis was to study the dynamics of open quantum systems in the framework of the third quantization, an elegant and exact analytical method of resolution for master equations with quadratic Hamiltonians and linear couplings with baths. We studied its application for a system made of two bosonic thermal baths and a junction of one or two sites, bosonic too. Our final objective was to study different approaches of derivation for the master equation and compare which one was the best in which regime of parameters.

In chapter 1, we introduced the second quantization in closed quantum systems and presented the *Bogoliubov transformation*.
In chapter 2, we introduced the mathematical framework to study the dynamics of open quantum systems. We presented the density operator and its properties. We then derived the *Lindblad master equation* for a general case. After that, we introduced the *Choi-Jamiołkowski isomorphism*, that allowed us to construct a Hilbert space where the vectors are the vectorized density operators. We also presented the *superoperators* and their matrix representation. We ended this chapter with a description of the spectrum of the *Liouvillian*, the generator of the dynamics of open quantum systems.
In chapter 3, we presented the third quantization method in a general case for two bosonic modes. We showed how this method could give an exact analytical solution for Lindblad master equations where the Hamiltonian is quadratic and the couplings to the bath are linear. Furthermore, we presented the features of this method such as obtaining the steady state, the normal master mode, the complete spectrum of the Liouvillian and the two-points correlations matrix.
In chapter 4, we applied this method of resolution for a simple but non-trivial system of quantum transport, the *single-site junction*. We showed the conditions of validity of the steady state: the emission rate must be greater than the absorption rate, otherwise, the system continuously accumulates excitations. We also discussed the symmetries of the system. Finally, we compared the third quantization method with numerical methods throughout the spectrum of the Liouvillian and the time evolution of the particle current between the two baths. We showed that a large cutoff value had to be taken to recover the physical behaviors predicted by the third quantization, highlighting the power this latter approach.
In chapter 5, we studied the *two-site junction* via three methods of derivation for the master equation: the *local approach*, the *global approach* and the *Redfield approach*. We saw that each approach had its regime of validity, depending on the coupling strength. For small coupling, the local approach showed better results while for large coupling, the two others were better. We based our conclusions on the study of the rapidities (for the local and global approaches), the particle current at the steady state for thermal equilibrium and non-equilibrium between the two baths (for the local and global approaches) and the elements of the two-points correlations matrix (for all the approaches). Surprisingly, the Redfield approach should have yielded better results than the global approach for small coupling because the latter required an additional approximation. We found out that both approaches result in the same incorrect behavior for small coupling.

The last chapter of this master thesis contains original results. Although this system has already been studied, it was with the use of numerical methods. The use of the third quantization

for this specific model has not been reported in the literature to our knowledge.

The outlook of this master's thesis would be to study the two-sites junctions with an external drive for the three approaches that we presented here. Indeed, in [43], they do consider the case of an external field, however, they do not take into account the Redfield approach. In contrast, in [49] they take into account the Redfield approach, however, they limit their study to the case where both sites share the same frequency, as we did.The introduction of an external drive will make the system similar to a quantum heat engine and make possible the study of quantum batteries, for example.

Another direction to go further would be to investigate open systems with strong couplings to their environments. In this regime, the Born-Markov approximation no longer holds, necessitating the study of memory effects within the system. Extending third quantization to such cases would enable the exploration of non-Markovian effects in quantum thermodynamics, as studies such as [50, 51, 52, 53] have demonstrated their potential to enhance the efficiency of quantum heat engines.

Appendix A

Choi-Jamiołkowski isomorphism

In this chapter, we recall the result presented in Sec. 2.5 which provides the matrix representation of the Liouvillian. Given the Choi-Jamiołkowski isomorphism, *for any CPT-map* $\mathcal{S}$ *acting on* $\rho(\mathcal{H})$ *such that* $\mathcal{S}[\rho] = A\rho B$ *for* $\rho \in \rho(\mathcal{H})$, $A, B \in \mathcal{B}(\mathcal{H})$, *its matrix representation* S *is given by*

$$S = A \otimes B^T. \tag{A.1}$$

Proof. We have to show that

$$|\mathcal{S}[\rho]\rangle = |A\rho B\rangle = S\,|\rho\rangle\,, \tag{A.2}$$

where $|\rho\rangle$ is the vectorized density operator. Let $\{|i\rangle\}, i \in \{1, ...N\}$ be a basis of $\mathcal{H}$ with N the dimension of $\mathcal{H}$. The spectral theorem gives the decomposition of A and B in this basis,

$$A = \sum_{i,j} a_{ij}\,|i\rangle\langle j|\,, \quad B = \sum_{k,l} b_{kl}\,|k\rangle\langle l|\,. \tag{A.3}$$

The same decomposition can be applied to ρ, $\rho = \sum_{m,n} b_{mn}\,|m\rangle\langle n|$. The element i, j of the matrix $A\rho B$ is given by

$$(A\rho B)_{i,j} = \sum_k a_{ik} \left(\sum_l \rho_{kl} b_{lj} \right) \tag{A.4}$$

and

$$|A\rho B\rangle = \begin{pmatrix} (A\rho B)_{11} \\ \vdots \\ (A\rho B)_{1N} \\ \vdots \\ (A\rho B)_{NN} \end{pmatrix}, \tag{A.5}$$

where $(A\rho B)_{i,j}$ corresponds to the element $(i-1)N + j$ of $|A\rho B\rangle$. On the other side, ρ_{kl} is the element $(k-1)N + l$ of $|\rho\rangle$ and

$$A \otimes B^T\,|\rho\rangle = \begin{pmatrix} a_{11}B^T & \cdots & a_{1N}B^T \\ \vdots & \ddots & \vdots \\ a_{N1}B^T & \cdots & a_{NN}B^T \end{pmatrix} \begin{pmatrix} \rho_{11} \\ \vdots \\ \rho_{1N} \\ \vdots \\ \rho_{NN} \end{pmatrix}. \tag{A.6}$$

Multiplying $A \otimes B^T$ by $|\rho\rangle$, each block$a_{kl}B^T$ multiply the corresponding subpart of $|\rho\rangle$, which gives a sum over the product $a_{ik}\rho_{kl}b_{lj}$. This corresponds to the matrix element i, j of $A\rho B$. □

Appendix B

Lindblad Master equations

B.1 Derivation of the Lindblad master equation for one mode

In this section, we show how to derive a Lindblad master equation of the form of (4.4). We give bellow the expressions of the system, environment and interaction Hamiltonian (respectively H_S, H_E and H_{int}

$$\begin{aligned} H_S &= \Omega a^\dagger a, \\ H_E &= \sum_k \left[\omega_{k,L} b_{k,L}^\dagger b_{k,L} + \omega_{k,R} b_{k,R}^\dagger b_{k,R}\right], \\ H_{\text{int}} &= \sum_k \left[\gamma_{k,L} a^\dagger b_{k,L} + \gamma_{k,R} a^\dagger b_{k,R} + h.c.\right], \end{aligned}$$

where $h.c$ stand for hermitian conjugated.

In the interaction picture, the time evolution of the annihilation and creation operators of the system, $a(t)$ and $a^\dagger(t)$, are given by

$$a(t) = e^{iH_S t} a e^{-iH_S t} = e^{-i\Omega t} a, \quad a^\dagger(t) = e^{i\Omega t} a^\dagger$$

and the interaction Hamiltonian H_{int} becomes

$$\begin{aligned} H_{\text{int}}(t) &= \sum_k \gamma_{k,L} e^{i(H_S+H_E)t} a^\dagger b_{k,L} e^{-i(H_S+H_E)t} + \gamma_{k,R} e^{i(H_S+H_E)t} a^\dagger b_{k,R} e^{-i(H_S+H_E)t} + h.c. \\ &= \sum_k \gamma_{k,L} a^\dagger e^{iH_E t} b_{k,L} e^{-iH_E t} + \gamma_{k,R} a(t)^\dagger e^{iH_E t} b_{k,R} e^{iH_E t} + h.c. \\ &= B^\dagger(t) a(t) + h.c., \end{aligned} \tag{B.1}$$

where we defined the operator $B(t)$ such that

$$B(t) = \sum_{\substack{\alpha=L,R \\ k}} \gamma_{k,\alpha} b_{k,\alpha} e^{-i\omega_{k,\alpha} t}. \tag{B.2}$$

We now have to inject (B.1) in (2.28). For the first term of the right-hand-side, we obtain

$$\text{Tr}_E \left[\int_0^\infty ds \left(B^\dagger(t)a(t) + h.c.\right)\left(B^\dagger(t-s)a(t-s) + h.c.\right)\rho(t) \otimes \rho_E\right], \tag{B.3}$$

with $\rho_E = \rho_L \otimes \rho_R$ where ρ_L and ρ_R are both thermal states. Expanding the product in (B.3), we have a sum of terms of the form $B^\dagger B^\dagger aa + BB^\dagger a^\dagger a + BBa^\dagger a^\dagger$.[1] As the environment is a tensor product of thermal states, we have

$$\text{Tr}_E[B^\dagger(t)B^\dagger(t-s)\rho_E] = 0 = \text{Tr}_E[B(t)B(t-s)\rho_E]. \tag{B.4}$$

[1] We omit on purpose the time dependence here because it is not necessary.

Thus, the integrand of (B.3) is equal to

$$\mathrm{Tr}_E\left[\left(B^\dagger(t)B(t-s)a(t)a^\dagger(t-s)+h.c.\right)\rho_S\otimes\rho_E\right] \\ =\left(a(t)a^\dagger(t-s)+h.c.\right)\rho_S\mathrm{Tr}_E\left[\left(B^\dagger(t)B(t-s)+h.c.\right)\rho_E\right]. \quad \text{(B.5)}$$

By definition, $\mathrm{Tr}_E\left[\left(B^\dagger(t)B(t-s)\right)\rho_E\right] = \langle B^\dagger(t)B(t-s)\rangle_E$ and we can expand B and $B^\dagger$ from (B.2)

$$\langle B^\dagger(t)B(t-s)\rangle_E = \left\langle \sum_{\substack{\alpha,\alpha'\\k,k'}} \gamma^*_{k,\alpha}\gamma_{k',\alpha'}b^\dagger_{k,\alpha}b_{k',\alpha'}e^{i\omega_k t}e^{-i\omega_{k'}(t-s)}\right\rangle_E \\ = \sum_{\substack{\alpha,\alpha'\\k,k'}} \gamma^*_{k,\alpha}\gamma_{k',\alpha'}\left\langle b^\dagger_{k,\alpha}b_{k',\alpha'}\right\rangle_E e^{i\omega_k t}e^{-i\omega_{k'}(t-s)}. \quad \text{(B.6)}$$

Keeping in mind that the baths are thermal, $\left\langle b^\dagger_{k,\alpha}b_{k',\alpha'}\right\rangle = n_{k,\alpha}\delta_{k,k'}\delta_{\alpha,\alpha'}$ where $n_{k,\alpha}$ is the Bose-Einstein distribution,

$$n_{k,\alpha} = \frac{1}{e^{\omega_{k,\alpha}/T}-1}. \quad \text{(B.7)}$$

We can now define the correlation function $C_1(s)$ as

$$C_1(s) = \sum_{k,\alpha}|\gamma_{k,\alpha}|^2 n_{k,\alpha}e^{i\omega_{k,\alpha}s}. \quad \text{(B.8)}$$

Similarly, we find for $\langle B(t)B^\dagger(t-s)\rangle_E$

$$\langle B(t)B^\dagger(t-s)\rangle_E = C_2(s) = \sum_{k,\alpha}|\gamma_{k,\alpha}|^2(1+n_{k,\alpha})e^{-i\omega_{k,\alpha}s}. \quad \text{(B.9)}$$

These two correlations function can be found in each term of (2.28). We then rewrite the time evolution of the density matrix of the system as

$$\dot\rho(t) = \int_0^\infty ds\left(C_1(s)\left[a^\dagger(t-s)\rho(t)a(t)-a(t)a^\dagger(t-s)\rho(t)\right]\right. \\ \left. + C_2(s)\left[a(t-s)\rho a^\dagger(t)-a^\dagger(t)a(t-s)\rho(t)\right]\right)+h.c.. \quad \text{(B.10)}$$

We now elaborate more these correlations functions. Choosing an arbitrary spectral density $J(\omega)$, we change the sum into an integral:

$$C_1(s) = \sum_\alpha\int_0^\infty d\omega_{k,\alpha}J(\omega_{k,\alpha})n_{k,\alpha}(\omega_{k,\alpha})e^{i\omega_{k,\alpha}s}, \\ C_2(s) = \sum_\alpha\int_0^\infty d\omega_{k,\alpha}J(\omega_{k,\alpha})\left(1+n_{k,\alpha}(\omega_{k,\alpha})\right)e^{-i\omega_{k,\alpha}s}. \quad \text{(B.11)}$$

We can show explicitly the effect of this change in the first term of (B.10)

$$\int_0^\infty dsC_1(s)\left(a^\dagger(t-s)\rho(t)a(t)\right) = \sum_\alpha\int_0^\infty ds\int_0^\infty d\omega_{k,\alpha}J(\omega_{k,\alpha})n_{k,\alpha}(\omega_{k,\alpha})e^{i\omega_{k,\alpha}s}e^{-i\Omega s}a^\dagger\rho(t)a \\ = \sum_\alpha\int_0^\infty d\omega_{k,\alpha}J(\omega_{k,\alpha})n_{k,\alpha}(\omega_{k,\alpha})a^\dagger\rho(t)a\left[\int_0^\infty dse^{i(\omega_{k,\alpha}-\Omega)s}\right]. \quad \text{(B.12)}$$

The integral between the brackets is a well-known formula of distribution theory,

$$\int_0^\infty ds e^{i(\omega_{k,\alpha}-\Omega)s} = \pi\delta(w_k-\Omega) + iP.V.\left(\frac{1}{\omega_k-\Omega}\right). \tag{B.13}$$

This is the same decomposition that we made for Γ_{kl} in Sec. 2 of chapter 2. If we account only for the real part, (B.12) is now

$$\int_0^\infty ds C_1(s)\left(a^\dagger(t-s)\rho(t)a(t)\right) = \pi J(\Omega)(n_L(\Omega)+n_R(\Omega))a^\dagger\rho(t)a. \tag{B.14}$$

We removed the subscript k in n_α because this quantity does not depend on k from now on. The other part of the decomposition will appear in the commutator and H_{LS} can be neglected here.

Gathering everything, we can write the master equation in the standard form

$$\begin{aligned}\dot\rho(t) = -i[H_s,\rho(t)] &+ \pi J(\Omega)(n_L(\Omega)+n_R(\Omega))\left(a^\dagger\rho(t)a - \frac{1}{2}\{aa^\dagger,\rho(t)\}\right)\\ &+ \pi J(\Omega)(n_L(\Omega)+n_R(\Omega)+2)\left(a\rho(t)a^\dagger - \frac{1}{2}\{a^\dagger a,\rho(t)\}\right).\end{aligned}$$

We chose the spectral density $J(\omega)$ arbitrary. We now take it such that

$$\pi J(\Omega)(n_L(\Omega)+n_R(\Omega)) = \gamma_L \tag{B.15}$$

and

$$\pi J(\Omega)(n_L(\Omega)+n_R(\Omega)+2) = \gamma_R. \tag{B.16}$$

The master equation studied in Sec. 1 of Chapter 4 is retrieved.

B.2 Derivation of the Lindblad master equation for two modes

This section is dedicated to the computation of a Lindblad master equation for the two mode system in local and global form.

$$\begin{aligned}H_S &= H_L + H_R + g(a_L a_R^\dagger + a_L^\dagger a_R),\\ H_E &= \sum_k \omega_{k,L} b_{k,L}^\dagger b_{k,L} + \omega_{k,R} b_{k,R}^\dagger b_{k,R},\\ H_{\text{int}} &= \sum_{\substack{\alpha=L,R\\k}} \gamma_{k,\alpha} a_\alpha^\dagger b_{k,\alpha} + h.c. = H_{int,L} + H_{int,R},\end{aligned}$$

with $H_\alpha = \Omega_\alpha a_\alpha^\dagger a_\alpha$ the Hamiltonian of the site $\alpha = L,R$. Here, the operators $a_L, a_R, a_L^\dagger, a_R^\dagger$ are operators related to the left and right sites, we do not use the notations $a_1, a_2, a_1^\dagger, a_2^\dagger$ in order to to effectively reduce the size of the sums that we will encounter throughout this section. This notation has nothing to do with the left and right operators defined in Chapter 3.

B.2.1 Local approach

Similarly to the previous case, it is possible to derive a time evolution equation for the reduced density matrix in the form

$$\begin{aligned}\dot\rho(t) = \sum_{\alpha=L,R}\int_0^\infty ds \Big(&C_{1\alpha}(s)\left[a_\alpha^\dagger(t-s)\rho(t)a_\alpha(t) - a_\alpha(t)a_\alpha^\dagger(t-s)\rho(t)\right]\\ &+ C_{2\alpha}(s)\left[a_\alpha(t-s)\rho a_\alpha^\dagger(t) - a_\alpha^\dagger(t)a_\alpha(t-s)\rho(t)\right]\Big) + h.c.,\end{aligned} \tag{B.17}$$

where the bath correlation functions are defined by

$$C_{1,\alpha}(s) = \sum_k |\gamma_{k,\alpha}|^2 n_\alpha(\omega_{k\alpha}) e^{i(\omega_{k,\alpha}-\Omega_\alpha)s}, \tag{B.18}$$

$$C_{2,\alpha}(s) = \sum_k |\gamma_{k,\alpha}|^2 [1 + n_\alpha(\omega_{k\alpha})] e^{i(\omega_{k,\alpha}-\Omega_\alpha)s}, \tag{B.19}$$

$$\tag{B.20}$$

and $n_\alpha(\omega_{k,\alpha})$ is the Bose-Einstein distribution for the bath α,

$$n_\alpha(\omega) = \frac{1}{e^{\omega/(k_B T_\alpha)} - 1}. \tag{B.21}$$

As the correlation functions are peaked around $s = 0$ and decay for large times, we can perform the following approximation:

$$a_\alpha(t - s) \approx a_\alpha(t). \tag{B.22}$$

This approximation directly result in the local master equation given in Sec. 5.1 without need of the secular approximation (that will be required for the global case).

B.2.2 Global approach

To retrieve the global Lindblad master equation, we first have to rewrite the system Hamiltonian in a diagonal form,

$$H_S = H_L + H_R + g(a_L a_R^\dagger + a_L^\dagger a_R) = (a_L^\dagger, a_R^\dagger) \begin{pmatrix} \Omega_L & g \\ g & \Omega_R \end{pmatrix} \begin{pmatrix} a_L \\ a_R \end{pmatrix}. \tag{B.23}$$

Diagonalizing the Hamiltonian is equivalent to find a new pair of creation and annihilation operators. Thus, the system Hamiltonian is a sum of two independent harmonic oscillators, the coupling being included in the definition of the new operators:

$$H_S = \Omega_+ a_+^\dagger a_+ + \Omega_- a_-^\dagger a_-, \tag{B.24}$$

where

$$\Omega_\pm = \frac{\Omega_1 + \Omega_2 \pm \sqrt{4g^2 + (\Omega_1 - \Omega_2)^2}}{2} \tag{B.25}$$

and the new operators are given by

$$\begin{aligned} a_+ &= a_L \cos\theta - a_R \sin\theta, \\ a_- &= a_L \sin\theta + a_R \cos\theta, \end{aligned} \tag{B.26}$$

with the angle θ defined as

$$\tan\theta = \frac{2g}{(\Omega_1 - \Omega_2) - \sqrt{4g^2 + (\Omega_1 - \Omega_2)^2}}. \tag{B.27}$$

It is trivial to verify that these creation and annihilation operators satisfy the bosonic canonical commutation relations $[a_\nu, a_{\nu'}^\dagger] = \delta_{\nu\nu'}$ for $\nu, \nu' = +, -$.

The interest of the diagonalization is that we do not have to deal with the interaction term between the two sites throughout the computation. We can now express these operators in the interaction picture:

$$\begin{aligned} a_+(t) &= e^{iH_S t} a_+ e^{-iH_S t} = e^{-i\Omega_+ t} a_+, \\ a_-(t) &= e^{iH_S t} a_- e^{-iH_S t} = e^{-i\Omega_- t} a_- \end{aligned}$$

and inject it into the expression of H_{int} in the interaction picture

$$H_{\text{int}} = \sum_k \gamma_{kL} \left(a_-^\dagger \sin\theta + a_+^\dagger \cos\theta \right) b_{k,L} + \sum_k \gamma_{kR} \left(a_-^\dagger \cos\theta - a_+^\dagger \sin\theta \right) b_{k,R} + h.c.$$

and

$$\begin{aligned} H_{\text{int}}(t) &= \sum_k \gamma_{kL} \left(a_-^\dagger(t) \sin\theta + a_+^\dagger(t) \cos\theta \right) e^{iH_E t} b_{k,L} e^{-iH_E t} + h.c. \\ &\quad + \sum_k \gamma_{kR} \left(a_-^\dagger(t) \cos\theta - a_+^\dagger(t) \sin\theta \right) e^{iH_E t} b_{k,R} e^{-iH_E t} + h.c. \\ &= B_L(t) \left(a_-^\dagger(t) \sin\theta + a_+^\dagger(t) \cos\theta \right) + B_R(t) \left(a_-^\dagger(t) \cos\theta - a_+^\dagger(t) \sin\theta \right) + h.c.. \end{aligned} \tag{B.28}$$

Similarly to (B.2), we defined $B_\alpha(t)$ for $\alpha = L, R$ as

$$B_\alpha(t) = \sum_k \gamma_{k,\alpha} b_{k\alpha} e^{-i\omega_{k\alpha} t}. \tag{B.29}$$

The interaction between the baths and the system can decomposed in a sum two terms, one corresponding to the interaction with the left bath and the other corresponding to the right bath, $H_{\text{int}} = H_{int,L} + H_{int,R}$. Considering this, we obtain the analogue of (2.22),

$$\begin{aligned} \dot{\rho}(t) &= -\int_0^\infty ds \text{Tr}_{B_L} [H_{int,L}(t), [H_{int,L}(t-s), \rho(t) \otimes \rho_{B_L}]] \\ &\quad - \int_0^\infty ds \text{Tr}_{B_R} [H_{int,R}(t), [H_{int,R}(t-s), \rho(t) \otimes \rho_{B_R}]], \\ &= \mathcal{L}_L[\rho] + \mathcal{L}_R[\rho]. \end{aligned} \tag{B.30}$$

as

$$\text{Tr}_E \left[H_{int,L}(t), [H_{int,R}(t-s), \rho(t)] \right] = 0 = \text{Tr}_E \left[H_{int,R}(t), [H_{int,L}(t-s), \rho(t)] \right].$$

We will first focus on $\mathcal{L}_L$. It is trivial to find a decomposition similar to (2.27) since we already partially did it. By construction, $[H_S, a_\pm] = -\Omega_\pm$ and we can find the expressions for $S_j(\omega)$ and $E_j(t)$

$$\begin{aligned} S_1(\Omega_+) &= a_+ \cos\theta, \quad S_1(\Omega_-) = a_- \sin\theta, \\ S_2(\Omega_+) &= a_+^\dagger \cos\theta, \quad S_2(\Omega_-) = a_-^\dagger \sin\theta, \\ E_1(t) &= B_L^\dagger(t), \quad E_2(t) = B_L(t). \end{aligned} \tag{B.31}$$

With these operators, we can compute the spectral correlation functions (2.30). For the first one, we have

$$\begin{aligned} \Gamma_{11}(\omega) &= \int_0^\infty ds e^{i\omega s} \text{Tr}_L \left[E_1(t) E_1^\dagger(t-s) \rho_L \right] \\ &= \int_0^\infty ds e^{i\omega s} \text{Tr}_L \left[B_L(t) B_L^\dagger(t-s) \rho_L \right] \\ &= \int_0^\infty ds e^{i\omega s} \sum_{k,k'} \gamma_{k,L} \gamma_{k',L}^* e^{-i\omega_{k,L} t} e^{i\omega_{k',L}(t-s)} \left\langle b_{k,L} b_{k',L}^\dagger \right\rangle_L \qquad \text{(B.32)} \\ &= \sum_k |\gamma_{k,L}|^2 [n_L(\omega_{k,L}) + 1] \int_0^\infty ds e^{i(\omega - \omega_{k,L})s}. \qquad \text{(B.33)} \end{aligned}$$

As we did for the single mode, we introduce now the spectral density of the left bath $J_L(\omega) = \sum_j |\gamma_{k,L}|^2 \delta(\omega - \omega_{j,L})$,

$$\Gamma_{11}(\omega) = \int_0^\infty d\nu J_L(\nu) \int_0^\infty ds e^{i(\omega-\nu)s} [n_L(\nu) + 1].$$

Using formula (B.13), we split Γ_{11} into its real and imaginary parts (assuming $\omega > 0$),

$$\Gamma_{11}(\omega) = \gamma_L(\omega)[n_L(\omega) + 1] + i[\Delta_L(\omega) + \Delta'_L(\omega)], \tag{B.34}$$

with

$$\begin{aligned}
\gamma_L(\omega) &= \pi J_L(\omega), \\
\Delta_L(\omega) &= \text{P.V.} \int_0^\infty d\omega \frac{J_L\omega)}{\omega - \omega}, \\
\Delta'_L(\omega) &= \text{P.V.} \int_0^\infty \mathrm{d}\omega \frac{J_L(\omega) n_L(\omega)}{\omega - \omega}.
\end{aligned} \tag{B.35}$$

For the others spectral correlation function, one finds, taking $\omega > 0$,

$$\Gamma_{12}(-\omega) = \Gamma_{21}(\omega) = 0, \Gamma_{22}(-\omega) = \gamma_L(\omega) n_L(\omega) - i\Delta'_L(\omega). \tag{B.36}$$

Having these expressions for Γ_{kl} allows to perform the secular approximation on $\mathcal{L}_1$,

$$\begin{aligned}
\mathcal{L}_1[\rho(t)] = \sum_{\omega,\omega'} & e^{i(\omega'-\omega)t} \Gamma_{11}(\omega) \left[S_1(\omega)\rho(t), S_1^\dagger\left(\omega'\right) \right] + e^{i(\omega-\omega')\mathrm{t}} \Gamma_{11}^*(\omega) \left[S_1\left(\omega'\right), \rho(t) S_1^\dagger(\omega) \right] \\
& + e^{i(\omega'-\omega)\mathrm{t}} \Gamma_{22}(\omega) \left[S_2(\omega)\rho(t), S_2^\dagger\left(\omega'\right) \right] + e^{i(\omega-\omega')t} \Gamma_{22}^*(\omega) \left[S_2\left(w'\right), \rho(t) S_2^\dagger(w) \right].
\end{aligned} \tag{B.37}$$

In this equation, we have a sum over $\omega, \omega' = \Omega_\pm$. If $\omega \neq \omega'$, there are terms with a factor $e^{\pm 2git}$. We can neglect them[2] if $2g$ is large compared to the inverse of the relaxation rate [54]. Equation (B.37) reads now

$$\begin{aligned}
\mathcal{L}_1[\rho(t)] = & - i\frac{\Delta_L(\Omega_+)}{2}[a_+^\dagger a_+ \rho(t)] - i\frac{\Delta_L(\Omega_-)}{2}[a_-^\dagger a_- \rho(t)] \\
& + \gamma_L(\Omega_+)[n_L(\omega_+) + 1] \left(a_+ \rho(t) a_+^\dagger - \frac{1}{2}\{a_+^\dagger a_+, \rho(t)\} \right) \\
& + \gamma_L(\Omega_+) n_L(\omega_+) \left(a_+^\dagger \rho(t) a_+ - \frac{1}{2}\{a_+ a_+^\dagger, \rho(t)\} \right) \\
& + \gamma_L(\Omega_-)[n_L(\Omega_-) + 1] \left(a_- \rho(t) a_+^\dagger - \frac{1}{2}\{a_+^\dagger a_-, \rho(t)\} \right) \\
& + \gamma_L(\Omega_-) n_L(\Omega_-) \left(a_-^\dagger \rho(t) a_- - \frac{1}{2}\{a_- a_-^\dagger, \rho(t)\} \right).
\end{aligned}$$

The same process can be effectuate to the second term of equation (B.30). The only difference is the minus sign in a_+ for $H_{int,R}$. This modifies the cross terms, which we neglect anyway when performing the secular approximation. We obtain an expression of the same form as for $\mathcal{L}_1$ with the replacements $L \to R$ in γ, n and Δ, referring to the right bath.

Turning back to Schrödinger picture and neglecting the H_{Ls} as in the previous case, one finds for the time evolution of the system

$$\begin{aligned}
\dot{\rho}(t) = & - i[H_S, \rho(t)] \\
& + \{\gamma_L(\Omega_+)[n_L(\Omega_+) + 1] + \gamma_R(\Omega_+)[n_2(\Omega_+) + 1]\} \left(a_+ \rho_{\mathrm{S}}(t) a_+^\dagger - \frac{1}{2}\left\{a_+^\dagger a_+, \rho_{\mathrm{S}}(t)\right\} \right) \\
& + [\gamma_L(\Omega_+) n_L(\Omega_+) + \gamma_R(\Omega_+) n_2(\Omega_+)] \left(a_+^\dagger \rho_{\mathrm{S}}(t) a_+ - \frac{1}{2}\left\{a_+ a_+^\dagger, \rho_{\mathrm{S}}(t)\right\} \right) \\
& + \{\gamma_L(\Omega_-)[n_L(\Omega_-) + 1] + \gamma_R(\Omega_-)[n_2(\Omega_-) + 1]\} \left(a_- \rho_{\mathrm{S}}(t) a_-^\dagger - \frac{1}{2}\left\{a_-^\dagger a_-, \rho_{\mathrm{S}}(t)\right\} \right) \\
& + [\gamma_L(\Omega_-) n_L(\Omega_-) + \gamma_R(\Omega_-) n_2(\Omega_-)] \left(a_-^\dagger \rho_{\mathrm{S}}(t) a_- - \frac{1}{2}\left\{a_- a_-^\dagger, \rho_{\mathrm{S}}(t)\right\} \right),
\end{aligned} \tag{B.38}$$

[2]If we do not perform this approximation, we obtain the Redfield master equation presented in Sec. 5.4.

where H_S should be taken in the diagonal form.

Appendix C

Application of the third quantization

This chapter contains the detailed derivations of the results found in chapter 5.

C.1 Local approach

Using the methods of third quantization, we define successively

$$\mathbf{H} = \begin{pmatrix} \omega_1 & g \\ g & \omega_2 \end{pmatrix}, \quad \mathbf{K} = \begin{pmatrix} 0 & 0 \\ 0 & 0 \end{pmatrix},$$
$$\mathbf{M} = \frac{1}{2}\begin{pmatrix} \bar{\gamma}_L(\omega_1) & 0 \\ 0 & \bar{\gamma}_R(\omega_2) \end{pmatrix}, \quad \mathbf{N} = \frac{1}{2}\begin{pmatrix} \gamma_L(\omega_1) & 0 \\ 0 & \gamma_R(\omega_2) \end{pmatrix},$$
$$\mathbf{L} = \begin{pmatrix} 0 & 0 \\ 0 & 0 \end{pmatrix}.$$

For the $\mathbf{X}$ and $\mathbf{Y}$ matrices, we find

$$\mathbf{X} = \frac{1}{2}\begin{pmatrix} i\omega_1 - \frac{\gamma_L(\omega_1)-\bar{\gamma}_L(\omega_1)}{2} & ig & 0 & 0 \\ ig & i\omega_2 - \frac{\gamma_R(\omega_2)-\bar{\gamma}_R(\omega_2)}{2} & 0 & 0 \\ 0 & 0 & -i\omega_1 - \frac{\gamma_L(\omega_1)-\bar{\gamma}_L(\omega_1)}{2} & -ig \\ 0 & 0 & -ig & -i\omega_2 - \frac{\gamma_R(\omega_2)-\bar{\gamma}_R(\omega_2)}{2} \end{pmatrix}$$

and

$$\mathbf{Y} = \begin{pmatrix} 0 & 0 & \frac{\gamma_L(\omega_1)}{2} & 0 \\ 0 & 0 & 0 & \frac{\gamma_R(\omega_2)}{2} \\ \frac{\gamma_L(\omega_1)}{2} & 0 & 0 & 0 \\ 0 & \frac{\gamma_R(\omega_2)}{2} & 0 & 0 \end{pmatrix}.$$

The $\mathbf{P}$ matrix, which contains the eigenvectors of $\mathbf{X}$ is

$$\mathbf{P} = \begin{pmatrix} 0 & 0 & \frac{-i}{4g}\left(\sqrt{\lambda_+ + 16g^2} + \sqrt{\lambda_+}\right) & 1 \\ 0 & 0 & \frac{-i}{4g}\left(\sqrt{\lambda_+ + 16g^2} - \sqrt{\lambda_+}\right) & 1 \\ \frac{i}{4g}\left(\sqrt{\lambda_- + 16g^2} + \sqrt{\lambda_-}\right) & 1 & 0 & 0 \\ \frac{i}{4g}\left(\sqrt{\lambda_- + 16g^2} - \sqrt{\lambda_-}\right) & 1 & 0 & 0 \end{pmatrix}, \tag{C.1}$$

where we omitted on purpose the dependence in ω_1, ω_2 for $\lambda_\pm$ to lighten the notations. With the solution of the Lyapunov equation, (5.8) and equation (3.29), we can express the NMM:

$$\begin{aligned}
\xi_1 =& a_1^{\dagger L}(-P_{3,1}A_{11} - P_{4,1}A_{12}) + a_1^{\dagger R}(P_{3,1} + P_{3,1}A_{11} + P_{4,1}A_{12}) \\
&+ a_2^{\dagger L}(-P_{3,1}A_{12}^* - P_{4,1}A_{22}) + a_2^{\dagger R}(P_{3,1}A_{12}^* + P_{4,1} + P_{4,1}A_{22}), \\
\xi_2 =& a_1^{\dagger L}(-A_{11} - A_{12}) + a_1^{\dagger R}(1 + A_{11} + A_{12}) + a_2^{\dagger L}(-A_{12}^* - A_{22}) + a_2^{\dagger R}(A_{12}^* + 1 + A_{22}), \\
\xi_3 =& a_1^{L}(P_{1,3} + P_{1,3}A_{11} + P_{1,4}A_{12}^*) + a_1^{R}(-P_{1,3}A_{11} - P_{1,4}A_{12}^*) \\
&+ a_2^{L}(P_{1,3}A_{12} + P_{1,4} + P_{1,4}A_{22}) + a_2^{R}(-P_{1,3}A_{12} - P_{1,4}A_{22}), \\
\xi_4 =& a_1^{L}(1 + A_{11} + A_{12}^*) + a_1^{R}(-A_{11} - A_{12}^*) + a_2^{L}(A_{12} + 1 + A_{22}) + a_2^{R}(-A_{12} - A_{22}).
\end{aligned} \tag{C.2}$$

Rewriting the matrix $\mathbf{P}$ with general coefficients b, c, d, e, we have

$$\mathbf{P} = \begin{pmatrix} 0 & 0 & d & 1 \\ 0 & 0 & e & 1 \\ b & 1 & 0 & 0 \\ c & 1 & 0 & 0 \end{pmatrix}.$$

The purpose of this rewriting is to lighten the notations. Similarly, for the matrix $\mathbf{Z}$ we have

$$\mathbf{Z} = \begin{pmatrix} 0 & 0 & z_1 & z_2 \\ 0 & 0 & z_2^* & z_3 \\ z_1 & z_2^* & 0 & 0 \\ z_2 & z_3 & 0 & 0 \end{pmatrix}.$$

Following (3.29) for $\underline{\xi} = (\xi_1, \xi_2, \xi_3, \xi_4)^T$, we derive successively

$$\mathbf{Z}\underline{a}' = \begin{pmatrix} z_1(a_1^R - a_1^L) + z_2(a_2^R - a_2^L) \\ z_2^*(a_1^R - a_1^L) + z_3(a_2^R - a_2^L) \\ z_1(a_1^{\dagger L} - a_1^{\dagger R}) + z_2^*(a_2^{\dagger L} - a_2^{\dagger R}) \\ z_2(a_1^{\dagger L} - a_1^{\dagger R}) + z_3(a_2^{\dagger L} - a_2^{\dagger R}) \end{pmatrix},$$

and

$$\underline{a} - \mathbf{Z}\underline{a}' = \begin{pmatrix} a_1^L(1 + z_1) - a_1^R z_1 + a_2^L z_2 - a_2^R z_2 \\ a_1^L z_2^* - a_1^R z_2^* + a_2^L(1 + z_3) - a_2^R z_3 \\ -a_1^{\dagger L} z_1 + a_1^{\dagger R}(1 + z_1) - a_2^{\dagger L} z_2^* + a_2^{\dagger R} z_2^* \\ -a_1^{\dagger L} z_2 + a_1^{\dagger R} z_2 - a_2^{\dagger L} z_3 + a_2^{\dagger R}(1 + z_3) \end{pmatrix}. \tag{C.3}$$

Using L_i, $i \in \{1, ..., 4\}$ to label the elements of the vector computed in (C.3), we find

$$\underline{\xi} = \mathbf{P}^T\left(\underline{a} - \mathbf{Z}\underline{a}'\right) = \begin{pmatrix} bL_3 + cL_4 \\ L_3 + L_4 \\ dL_1 + eL_2 \\ L_1 + L_2 \end{pmatrix}, \tag{C.4}$$

with

$$\begin{aligned}
\xi_1 &= a_1^{\dagger L}(-bz_1 - cz_2) + a_1^{\dagger R}(b + bz_1 + cz_2) + a_2^{\dagger L}(-bz_2^* - cz_3) + a_2^{\dagger R}(bz_2^* + c + cz_3), \\
\xi_2 &= a_1^{\dagger L}(-z_1 - z_2) + a_1^{\dagger R}(1 + z_1 + z_2) + a_2^{\dagger L}(-z_2^* - z_3) + a_2^{\dagger R}(z_2^* + 1 + z_3), \\
\xi_3 &= a_1^{L}(d + dz_1 + ez_2^*) + a_1^{R}(-dz_1 - ez_2^*) + a_2^{L}(dz_2 + e + ez_3) + a_2^{R}(-dz_2 - ez_3), \\
\xi_4 &= a_1^{L}(1 + z_1 + z_2^*) + a_1^{R}(-z_1 - z_2^*) + a_2^{L}(z_2 + 1 + z_3) + a_2^{R}(-z_2 - z_3).
\end{aligned} \tag{C.5}$$

Unfortunately, replacing the coefficients b, c, d, e and Z_1, z_2, z_3 does not leads to an easily readable expression. Thus, we must keep these coefficients for the following.

To derive the steady state, we use the same ansatz as in Subsec. 4.1.1, i.e., the steady state is Gaussian and so it is diagonal in the Fock basis. Using property (3.32) with ξ_2, we have successively

$$\xi_2 \left|\rho_{NESS}\right\rangle = 0$$

$$\begin{aligned}\Leftrightarrow \sum_{n,n'} C_{n,n'}[a_1^\dagger \left|n,n'\right\rangle \left\langle n,n'\right| (-A_{11}-A_{12}) + \left|n,n'\right\rangle \left\langle n,n'\right| a_1^\dagger (1+A_{11}+A_{12}) \\ + a_2^\dagger \left|n,n'\right\rangle \left\langle n,n'\right| (-A_{12}^*-A_{22}) + \left|n,n'\right\rangle \left\langle n,n'\right| a_2^\dagger (A_{12}^*+1+A_{22})] = 0.\end{aligned}$$

Separating the sum and reindexing the first one, we find

$$\begin{aligned}\sum_{n,n'} \sqrt{n+1}\left|n+1,n'\right\rangle \left\langle n,n'\right| \left[C_{n,n'}(-A_{11}-A_{12}) + C_{n+1,n'}(1+A_{11}+A_{12})\right] \\ + \sqrt{n'+1}\left|n,n'+1\right\rangle \left\langle n,n'\right| \left[C_{n,n'}(-A_{12}^*-A_{22}) + C_{n,n'+1}(A_{12}^*+1+A_{22})\right] = 0\end{aligned}$$

The relations between the coefficients are found by equating each term to 0

$$\begin{aligned}C_{n+1,n'} &= C_{n,n'} \frac{A_{11}+A_{12}}{1+A_{11}+A_{12}}, \\ C_{n,n'+1} &= C_{n,n'} \frac{A_{12}^*+A_{22}}{1+A_{12}^*+A_{22}}.\end{aligned} \tag{C.6}$$

And thus,

$$C_{n,n'} = C_{0,0} \left(\frac{A_{11}+A_{12}}{1+A_{11}+A_{12}}\right)^n \left(\frac{A_{12}^*+A_{22}}{1+A_{12}^*+A_{22}}\right)^{n'} \tag{C.7}$$

We find the value of $C_{0,0}$ using the unitary of the trace of the state.

$$\mathrm{Tr}[|\rho_{NESS}\rangle] = 1$$

$$\begin{aligned}&\Leftrightarrow \sum_{l,m} \langle l,m| \sum_{n,n'} C_{0,0} \left(\frac{A_{11}+A_{12}}{1+A_{11}+A_{12}}\right)^n \left(\frac{A_{12}^*+A_{22}}{1+A_{12}^*+A_{22}}\right)^{n'} \left|n,n'\right\rangle \left\langle n,n'|l,m\right\rangle = 1 \\ &\Leftrightarrow \sum_{n,n'} \left\langle n,n'|n,n'\right\rangle \left(\frac{A_{11}+A_{12}}{1+A_{11}+A_{12}}\right)^n \left(\frac{A_{12}^*+A_{22}}{1+A_{12}^*+A_{22}}\right)^{n'} = \frac{1}{C_{0,0}} \\ &\Leftrightarrow \left(\sum_n \left(\frac{A_{11}+A_{12}}{1+A_{11}+A_{12}}\right)^n\right) \left(\sum_{n'} \left(\frac{A_{12}^*+A_{22}}{1+A_{12}^*+A_{22}}\right)^{n'}\right) = \frac{1}{C_{0,0}}\end{aligned}$$

The geometric series converges respectively when

$$\begin{aligned}|A_{11}+A_{12}| &< |1+A_{11}+A_{12}|, \\ |A_{22}+A_{12}^*| &< |1+A_{22}+A_{12}^*|.\end{aligned} \tag{C.8}$$

If one of these two conditions are not fulfilled, the existence of a unique steady state is not guaranteed. These conditions corresponds to the case when all rapidities β_i defined in (5.6 have their reel part positive. Considering that these geometric series converges, we find

$$\frac{1}{C_{0,0}} = (1+A_{11}+A_{12})(1+A_{22}+A_{12}^*). \tag{C.9}$$

We can finally express the steady state of the two-site junction

$$|\rho_{NESS}\rangle = \frac{\sum_{n,n'} \left(\frac{A_{11}+A_{12}}{1+A_{11}+A_{12}}\right)^n \left(\frac{A_{12}^*+A_{22}}{1+A_{12}^*+A_{22}}\right)^{n'} |n,n'\rangle\,|n,n'\rangle}{(1+A_{11}+A_{12})(1+A_{22}+A_{12}^*)}. \tag{C.10}$$

Bibliography

[1] J. Bardeen, L. N. Cooper, and J. R. Schrieffer, "Theory of superconductivity," *Phys. Rev.*, vol. 108, pp. 1175–1204, Dec 1957.

[2] W. E. Lamb and R. C. Retherford, "Fine structure of the hydrogen atom by a microwave method," *Phys. Rev.*, vol. 72, pp. 241–243, Aug 1947.

[3] T. Prosen, "Third quantization: A general method to solve master equations for quadratic open Fermi systems," *New Journal of Physics*, vol. 10, p. 043026, Apr. 2008.

[4] T. Prosen and T. H. Seligman, "Quantization over boson operator spaces," *Journal of Physics A: Mathematical and Theoretical*, vol. 43, p. 392004, Sept. 2010.

[5] T. Prosen and B. Žunkovič, "Exact solution of markovian master equations for quadratic fermi systems: thermal baths, open xy spin chains and non-equilibrium phase transition," *New Journal of Physics*, vol. 12, p. 025016, feb 2010.

[6] B. Žunkovič and T. Prosen, "Heat transport in quantum harmonic chains with Redfield baths," *AIP Conference Proceedings*, vol. 1468, no. 1, pp. 350–366, 2012.

[7] N. Gisin, G. Ribordy, W. Tittel, and H. Zbinden, "Quantum cryptography," *Rev. Mod. Phys.*, vol. 74, pp. 145–195, Mar 2002.

[8] M. A. Nielsen and I. L. Chuang, *Quantum Computation and Quantum Information: 10th Anniversary Edition*. Cambridge University Press, 2010.

[9] H. M. Wiseman and G. J. Milburn, *Quantum Measurement and Control*. Cambridge University Press, 2009.

[10] D. S. Kosov, T. Prosen, and B. Žunkovič, "Lindblad master equation approach to superconductivity in open quantum systems," *Journal of Physics A: Mathematical and Theoretical*, vol. 44, p. 462001, oct 2011.

[11] J. Fan and S. Jia, "Collective dynamics of the unbalanced three-level dicke model," *Phys. Rev. A*, vol. 107, p. 033711, Mar 2023.

[12] Y. Nakanishi and T. Sasamoto, "PT phase transition in open quantum systems with Lindblad dynamics," *Physical Review A*, vol. 105, p. 022219, Feb. 2022.

[13] R. Kosloff and A. Levy, "Quantum heat engines and refrigerators: Continuous devices," *Annual Review of Physical Chemistry*, vol. 65, no. Volume 65, 2014, pp. 365–393, 2014.

[14] J. Goold, M. Huber, A. Riera, L. del Rio, and P. Skrzypczyk, "The role of quantum information in thermodynamics—a topical review," *Journal of Physics A: Mathematical and Theoretical*, vol. 49, p. 143001, feb 2016.

[15] K. Joulain, J. Drevillon, Y. Ezzahri, and J. Ordonez-Miranda, "Quantum thermal transistor," *Phys. Rev. Lett.*, vol. 116, p. 200601, May 2016.

[16] M. Li, H. Wu, E. M. Avery, Z. Qin, D. P. Goronzy, H. D. Nguyen, T. Liu, P. S. Weiss, and Y. Hu, "Electrically gated molecular thermal switch," *Science*, vol. 382, no. 6670, pp. 585–589, 2023.

[17] P. Schlagheck, "Advanced quantum mechanics, partim ii." Univeristé de Liège, 2023.

[18] N. N. Bogoljubov, V. V. Tolmachov, and D. V. Širkov, "A new method in the theory of superconductivity," *Fortschritte der Physik*, vol. 6, no. 11-12, pp. 605–682, 1958.

[19] C. Timm, *Theory of Super Conductivity: Winter Semester 2011/2012 TU Dresden Institute of Theoretical Physics*. Independently Published, 2021.

[20] D. Manzano, "A short introduction to the Lindblad master equation," *AIP Advances*, vol. 10, p. 025106, Feb. 2020.

[21] G. Lindblad, "On the generators of quantum dynamical semigroups," *Commun.Math. Phys.*, vol. 48, no. 2, pp. 119–130, 1976.

[22] V. Gorini, A. Kossakowski, and E. C. G. Sudarshan, "Completely positive dynamical semigroups of N-level systems," *Journal of Mathematical Physics*, vol. 17, no. 5, pp. 821–825, 1976.

[23] V. Gorini, A. Frigerio, M. Verri, A. Kossakowski, and E. C. G. Sudarshan, "Properties of quantum Markovian master equations," *Reports on Mathematical Physics*, vol. 13, no. 2, pp. 149–173, 1978.

[24] P. Cappellaro, "Quantum theory of radiation interactions." Massachusetts Institute of Technology, 2013.

[25] A. G. Redfield, "On the theory of relaxation processes," *IBM Journal of Research and Development*, vol. 1, no. 1, pp. 19–31, 1957.

[26] H.-P. Breuer and F. Petruccione, *The Theory of Open Quantum Systems*. Oxford University Press, 2007.

[27] M.-D. Choi, "Completely positive linear maps on complex matrices," *Linear Algebra and its Applications*, vol. 10, no. 3, pp. 285–290, 1975.

[28] A. Jamiołkowski, "Linear transformations which preserve trace and positive semidefiniteness of operators," *Reports on Mathematical Physics*, vol. 3, no. 4, pp. 275–278, 1972.

[29] D. E. Evans, "Irreducible quantum dynamical semigroups," *Commun.Math. Phys.*, vol. 54, no. 3, pp. 293–297, 1977.

[30] D. E. Evans and H. Hanche-Olsen, "The generators of positive semigroups," *Journal of Functional Analysis*, vol. 32, no. 2, pp. 207–212, 1979.

[31] B. Buča and T. Prosen, "A note on symmetry reductions of the lindblad equation: transport in constrained open spin chains," *New Journal of Physics*, vol. 14, p. 073007, July 2012.

[32] F. Minganti, A. Biella, N. Bartolo, and C. Ciuti, "Spectral theory of Liouvillians for dissipative phase transitions," *Physical Review A*, vol. 98, p. 042118, Oct. 2018.

[33] V. V. Albert and L. Jiang, "Symmetries and conserved quantities in Lindblad master equations," *Physical Review A*, vol. 89, p. 022118, Feb. 2014.

[34] B. Debecker, J. Martin, and F. Damanet, "Spectral Theory of Non-Markovian Dissipative Phase Transitions," Sept. 2023.

[35] F. Minganti, V. Savona, and A. Biella, "Dissipative phase transitions in photon driven quantum nonlinear resonators," *Quantum*, vol. 7, p. 1170, Nov. 2023.

[36] G. Beaulieu, F. Minganti, S. Frasca, V. Savona, S. Felicetti, R. D. Candia, and P. Scarlino, "Observation of first- and second-order dissipative phase transitions in a two-photon driven kerr resonator," 2023.

[37] M. Riesch and C. Jirauschek, "Analyzing the positivity preservation of numerical methods for the liouville-von neumann equation," *Journal of Computational Physics*, vol. 390, pp. 290–296, 2019.

[38] A. M. Lyapunov, "The general problem of the stability of motion," *International Journal of Control*, vol. 55, no. 3, pp. 531–534, 1992.

[39] Wikipedia, "Normal order." https://en.wikipedia.org/wiki/Normal_order, 2024. Accessed: 2024-05-18.

[40] "Winter College on Optics: Quantum Photonics and Information | (smr 3424) (10-21 February 2020)."

[41] G. C. Wick, "The evaluation of the collision matrix," *Phys. Rev.*, vol. 80, pp. 268–272, Oct 1950.

[42] A. McDonald and A. A. Clerk, "Exact Solutions of Interacting Dissipative Systems via Weak Symmetries," *Phys. Rev. Lett.*, vol. 128, no. 3, p. 033602, 2022.

[43] P. P. Hofer, M. Perarnau-Llobet, L. D. M. Miranda, G. Haack, R. Silva, J. B. Brask, and N. Brunner, "Markovian master equations for quantum thermal machines: Local versus global approach," *New Journal of Physics*, vol. 19, p. 123037, Dec. 2017.

[44] M. Cattaneo, G. L. Giorgi, S. Maniscalco, and R. Zambrini, "Local versus global master equation with common and separate baths: superiority of the global approach in partial secular approximation," *New Journal of Physics*, vol. 21, p. 113045, nov 2019.

[45] S. Kim and F. Hassler, "Third quantization for bosons: symplectic diagonalization, non-hermitian hamiltonian, and symmetries," *Journal of Physics A: Mathematical and Theoretical*, vol. 56, p. 385303, sep 2023.

[46] A. McDonald and A. A. Clerk, "Exact solutions of interacting dissipative systems via weak symmetries," *Phys. Rev. Lett.*, vol. 128, p. 033602, Jan 2022.

[47] A. McDonald and A. A. Clerk, "Third quantization of open quantum systems: Dissipative symmetries and connections to phase-space and keldysh field-theory formulations," *Phys. Rev. Res.*, vol. 5, p. 033107, Aug 2023.

[48] Y. Nakanishi and T. Sasamoto, "$\mathcal{PT}$ phase transition in open quantum systems with lindblad dynamics," *Phys. Rev. A*, vol. 105, p. 022219, Feb 2022.

[49] A. Purkayastha, A. Dhar, and M. Kulkarni, "Out-of-equilibrium open quantum systems: A comparison of approximate quantum master equation approaches with exact results," *Phys. Rev. A*, vol. 93, p. 062114, Jun 2016.

[50] D. Gelbwaser-Klimovsky and A. Aspuru-Guzik, "Strongly coupled quantum heat machines," *The Journal of Physical Chemistry Letters*, vol. 6, no. 17, pp. 3477–3482, 2015. PMID: 26291720.

[51] P. Strasberg, G. Schaller, N. Lambert, and T. Brandes, "Nonequilibrium thermodynamics in the strong coupling and non-markovian regime based on a reaction coordinate mapping," *New Journal of Physics*, vol. 18, p. 073007, jul 2016.

[52] D. Newman, F. Mintert, and A. Nazir, "Performance of a quantum heat engine at strong reservoir coupling," *Phys. Rev. E*, vol. 95, p. 032139, Mar 2017.

[53] M. Perarnau-Llobet, H. Wilming, A. Riera, R. Gallego, and J. Eisert, "Strong coupling corrections in quantum thermodynamics," *Phys. Rev. Lett.*, vol. 120, p. 120602, Mar 2018.

[54] A. Rivas, A. D. K. Plato, S. F. Huelga, and M. B. Plenio, "Markovian master equations: A critical study," *New J. Phys.*, vol. 12, no. 11, p. 113032, 2010.